

Sending Video Over WiMAX for Inter-Vehicle Communications

Funmilayo Lawal

A thesis submitted to the
Faculty of Graduate and Postdoctoral Studies
In partial fulfillment of the requirements
For the MASc degree in Electrical and Computer Engineering

Ottawa-Carleton Institute for Electrical and Computer Engineering
School of Information Technology and Engineering
University of Ottawa

© Funmilayo Lawal, Ottawa, Canada, 2011

Abstract

We present an OPNET model that uses WiMAX technology to send video packets in an advanced inter-vehicle VANET environment. Our work focuses on real-time video streaming. A video model was created based on live traffics trace and then integrated into a WIMAX OPNET model. VANET mobility was modeled with a real world road map and VANET mobility simulators. We integrate an implementable controller over RTP to handle congestion control by setting a framework fit for future road safety development. Different mobility cases are studied and the performance measures such as end-to-end delay, jitter and visual experience are evaluated. Different design considerations are presented to enable designers to effectively build on and develop a realistic video VANET simulation model.

Acknowledgements

I would like to thank my supervisors Prof. Oliver Yang and Prof. Jun Huang for their unrelenting efforts and guardians throughout my degree. Special thanks to the members of CCNR lab at the University of Ottawa for all their support.

My sincere and high gratitude goes to my family – my parents for their priceless support and my siblings for their immeasurable help. You are all a true blessing to me. To the Fadirans, thank you for all your prayers and support. To my fiancé – Tosin Morolari, who always stood by me through the ups and downs of this degree, I say a heart-felt thanks to you. To all my friends - Wale, Anu, Tolu, Ore, Ak, Dele - to mention just a few, thank you.

To the author of all wisdom, who has helped through this degree, to Him my highest gratitude is ascribed. Thank you God.

Table of Contents

Title	i
Abstract	ii
Acknowledgements	iii
Table of Contents	iv
List of Figures	vii
List of Tables	ix
List of Acronyms	x
Chapter 1 Introduction	1
1.1 VANET	1
1.2 Video Traffic modelling	3
1.3 Real-time Transport protocol	4
1.4 Dedicated Short Range Communication vs. WiMAX for VANET	5
1.5 WiMAX for VANET	6
1.6 Congestion Control	7
1.7 Motivation	8
1.8 Thesis Objectives	9
1.9 Methodology	10
1.10 Thesis contribution	11
1.11 Thesis Organization	12
1.12 Publications	12
Chapter 2 Network Operation, Models and Assumptions	13
2.1 Network Protocols	13
2.1.1 General Network Layout of VANET	13
2.2 Network Models & Assumptions	17
2.2.1 VANET Model	18
2.2.1.1 VANET Mobility Model	18
2.2.1.2 RSU and Car Communication Model	20
2.2.2 Video Model	20
2.2.3 Traffic Controller Model	21
2.2.4 Simulation Model	22
2.3 Assumptions	26
Chapter 3 Experimental Setup	27
3.1 Trace Collection	27
3.2 Initial Analysis	28
3.3 Simulation Environment	32
3.4 Simulation Scenarios	33
3.4.1 Downtown Scenario	33
3.4.2 Residential Scenario	33
3.4.3 Highway Scenario	34

3.4.4 School Zone Scenario	35
3.5 Performance Measures	36
Chapter 4 Performance Evaluation of Downtown and School zone Scenarios	38
4.1 Small Network	38
4.1.1 Downtown Scenario	38
4.1.1.1 Time Evolution Performance	38
4.1.1.2 Mean End-to-End Delay	41
4.1.1.3 Buffer Overflow Percentage	42
4.1.2 School Zone Scenario	42
4.1.2.1 Time Evolution Performance	43
4.1.2.2 Mean End-to-End Delay	44
4.1.2.3 Buffer Overflow Percentage	45
4.2 Large Network	46
4.2.1 Downtown Scenario	46
4.2.1.1 Time Evolution Performance	46
4.2.1.2 Mean End-to-End Delay	48
4.2.1.3 Buffer Overflow Percentage	49
4.2.2 School Zone Scenario	49
4.2.2.1 Time Evolution Performance	50
4.2.2.2 Mean End-to-End Delay	52
4.2.2.3 Buffer Overflow Percentage	52
Chapter 5 -Performance Evaluation of Highway and Residential Area Scenario	53
5.1 Small Network	53
5.1.1 Highway Scenario	53
5.1.1.1 Time Evolution Performance	53
5.1.1.2 Mean End-to-End Delay	56
5.1.1.3 Buffer Overflow Percentage	56
5.1.2 Residential Scenario	56
5.1.2.1 Time Evolution Performance	56
5.1.2.2 Mean End-to-End Delay	59
5.1.2.3 Buffer Overflow Percentage	59
5.2 Large Network	60
5.2.1 Highway Scenario	60
5.2.1.1 Time Evolution Performance	60
5.2.1.2 Mean End-to-End Delay	62
5.2.1.3 Buffer Overflow Percentage	63
5.1.2 Residential Scenario	63
5.2.2.1 Time Evolution Performance	63
5.2.2.2 Mean End-to-End Delay	65
5.2.2.3 Buffer Overflow Percentage	66
5.3 Scenario Comparison	66
Chapter 6-Design Guidelines	68

Chapter 7-Conclusion	70
7.1 Future Work	71
References	73
Appendix A	77

List of Figures

Fig.1.1:	WiMAX Architecture	6
Fig.1.2:	Overall Architecture	11
Fig: 2.1:	Network Model Topology	13
Fig. 2.2:	Channel Allocation for DSRC	15
Fig. 2.3:	WiMAX Frame Structure	16
Fig. 2.4:	Video VANET OPNET Model Structure	17
Fig. 2.5:	Mobility Topologies	19
Fig. 2.6:	Mobile Node Architecture	22
Fig. 2.7:	Video Calling Part Manager	24
Fig. 2.8:	Video Called Party Manager	24
Fig. 2.9:	Video Called Part Flow Diagram with RTCP Implementation	25
Fig. 2.10:	Video Calling Party Flow Diagram with Traffic Controller Implementation	26
Fig. 3.1:	Setup for taking video Traces	27
Fig. 3.2:	Model Description for Video Traffic Generation	28
Fig. 3.3:	pdf of Video Trace	29
Fig. 3.4:	Correlation Length	29
Fig. 3.5:	Entire Trace IDC curve	30
Fig. 3.6:	Live Video Trace	31
Fig. 3.7:	Mini Pareto Video Traffic	31
Fig. 3.8:	Downtown Scenario	33
Fig. 3.9:	Residential Scenario	34
Fig. 3.10:	Highway Scenario	34
Fig. 3.11:	School zone Scenario	35
Fig. 3.12:	MOS and R-Factor Scale	37
Fig. 4.1:	End-to-end Delay for Downtown Scenario	40
Fig. 4.2:	MOS value curve for Downtown Scenario	41
Fig. 4.3:	Instantaneous Queue Size for Downtown Scenario	41
Fig. 4.4:	Mean End-to-End Delay for Downtown Scenario	42
Fig. 4.5:	Percentage of Buffer Saturation Curve for Downtown Scenario	43
Fig. 4.6:	End-to-End Delay for School Zone Scenario	44
Fig. 4.7:	MOS value for School Zone Scenario	45
Fig. 4.8:	Instantaneous Queue Size for School Zone Scenario	45
Fig. 4.9:	Mean End-to-End Delay Performance for School Zone Scenario	46
Fig. 4.10:	Percentage of Buffer Saturation Curve for School Zone Scenario	46
Fig. 4.11:	End-to-end Delay for Downtown Scenario (Large Network)	47
Fig. 4.12:	MOS value curve for Downtown Scenario (Large Network)	48
Fig. 4.13:	Instantaneous Queue Size for Downtown Scenario (Large Network)	49
Fig. 4.14:	Mean End-to-End Delay for Downtown Scenario (Large Network)	49
Fig. 4.15:	Percentage of Buffer Saturation Curve Downtown Scenario (Large Network)	50
Fig. 4.16:	End-to-End Delay for School Zone Scenario (Large Network)	51
Fig. 4.17:	MOS value for School Zone Scenario (Large Network)	51

Fig. 4.18: Instantaneous Queue Size for School Zone Scenario (Large Network)	52
Fig. 4.19: Mean End-to-End Delay Performance School Zone Scenario (Large Network)	52
Fig. 4.20: Percentage of Buffer Saturation Curve School Zone Scenario (Large Network)	53
Fig. 5.1: End-to-end Delay for Highway Scenario	55
Fig. 5.2: MOS value curve for Highway Scenario	55
Fig. 5.3: Instantaneous Queue Size for Highway Scenario	56
Fig. 5.4: Mean End-to-End Delay for Highway scenario	56
Fig. 5.5: Percentage of Buffer Saturation Curve for Highway Scenario	57
Fig. 5.6: End-to-End Delay for Residential Scenario	58
Fig. 5.7: MOS value for Residential Scenario	58
Fig. 5.8: Instantaneous Queue Size for Residential Scenario	59
Fig. 5.9: Mean End-to-End Delay Performance for Residential Scenario	59
Fig. 5.10: Percentage of Buffer Saturation Curve for Residential Scenario	60
Fig. 5.11: End-to-end Delay for Highway Scenario (Large Network)	61
Fig. 5.12: MOS value curve for Highway Scenario (Large Network)	62
Fig. 5.13: Instantaneous Queue Size for Highway Scenario (Large Network)	62
Fig. 5.14: Mean End-to-End Delay for Highway Scenario (Large Network)	63
Fig. 5.15: Percentage of Buffer Saturation Curve Highway Scenario (Large Network)	63
Fig. 5.16: End-to-End Delay for Residential Scenario (Large Network)	64
Fig. 5.17: MOS value for Residential Scenario (Large Network)	65
Fig. 5.18: Instantaneous Queue Size for Residential Scenario (Large Network)	65
Fig. 5.19: Mean End-to-End Delay Performance Residential Scenario (Large Network)	66
Fig. 5.20: Percentage of Buffer Saturation Curve Residential Scenario (Large Network)	66
Fig. A1: Processing Delay for Downtown Scenario	78
Fig. A2: Processing Delay for Highway Scenario	78

List of Tables

Table 1.1: Comparison of Some Wireless Technologies	7
Table 2.1: IEEE 802.16e Characteristics	15
Table 2.2: Mobility Model Summary	18
Table 2.3: RSU Parameters	19
Table 2.4: Traffic Model Comparison	20
Table 3.1: Mini Sources with Characterisation Values	32
Table 3.2: Simulation Parameters	33
Table 3.3: Scenario Summary	36
Table 5.1: Performance Summary of Small Networks	67
Table 5.2: Performance Summary of Large Networks	67

List of Acronyms

		Section of 1 st Appearance
AIMD	Additive Increase and Multiplicative Decrease	1.6
API-RCP	Adaptive Proportional Integration Rate Control Protocol	1.6
ARQ	Automatic Repeat reQuest	2.2.4
AU	Action Unit	3.2
BS	Base Station	2.1.1
CDMA	Code Division Multiple Access	1.5
CPU	Central Processing Unit	1.6
DSRC	Dedicated Short Range Communications	1.1
FCC	Federal Communication Commission	1.4
FM	Frequency Modulation	1.5
GDF	Geographic Data Files	2.2.1.1
GSM	Global System for Mobile Communications	1.5
HDTV	High Definition Television	1.2
IDC	Index of Dispersion for Count	3.0
IPv4	Internet Protocol version 4	2.1.1
LRD	Long Range Dependence	1.2
MAC	Medium Access Control	2.1.1
MIMO	Multiple-Input and Multiple-Output	1.5
MOS	Mean Opinion Score	3.3
OBU	On-Board Unit	1.4
OFDM	Orthogonal Frequency-Division Multiplexing	1.4
OSPF	Open Shortest Path First	3.1
pdf	probability density function	3.0
QoS	Quality of Service	1.2
RED	Random Early Detection	1.6
RFC	Request for Comments	3.1
RIP	Routing Information Protocol	3.1
RSU	Road Side Unit	1.9
RTCP	Real-Time Transport Control Protocol	1.3
RTP	Real-time Transport Protocol	1.3
SRD	Short Range Dependence	1.2
SS	Subscriber Station	1.9
TCP	Transport Control Protocol	1.3
TFRC	TCP Friendly Rate Control	1.6
TIGER	Topologically Integrated Geographic Encoding and Referencing system	2.2.1.1
UDP	User Datagram Protocol	1.3
UTF	Universal Trace Format	2.2.1.1

V2I	Vehicle to Infrastructure	1.9
V2V	Vehicle to Vehicle	1.9
VANET	Vehicular Adhoc NETWORK	1.0
VBR	Variable Bite Rate	1.2
WiMAX	Worldwide Interoperability for Microwave Access	1.0

Chapter 1

Introduction

Mobile wireless communication, by virtue of its versatility and utility convenience has now become a necessity. Users have come to desire not only the basic voice functionality of mobile wireless devices, but also all forms of mobile multimedia and data communication. Over the years, with the improvement of technology, the bandwidth over the wireless network has been increasing, at a measured pace. Over the past few decades, different modulation schemes have been developed to increase the data rate supported in wireless networks thus supporting a higher data rate. Technologies like WiMAX and other 3G technologies can theoretically support up to 74Mbps per channel [IEEE04]. This has created room for different types of applications in different specialities. Vehicular Adhoc NETWORK (VANET) is one such application.

The increase in road traffic volume over the years has led to a concern among researchers to create an effective, efficient and safe automotive environment. Safety and environmental issues have become one of the greatest concerns of both the automotive industry and governmental bodies. In USA alone, every 13 minutes a person dies due to motor vehicle accident, (this equates to about 110 people everyday [Ledg01]). Since physical road expansion might be impractical in some cases, the need to effectively manage the available road network cannot be overemphasized. VANET which consist of clusters of vehicles communicating wirelessly with each other and also with road side infrastructure endeavours to provide a solution to this problem. Telematics, which involves the use of telecommunications and informatics, is one of the major tools used in this area. In our field of research, our informatics is the real-time video traffic shared among vehicles and in turn road side infrastructures.

1.1 VANET

VANET is a unique area of wireless communication due to its peculiar characteristics. As a form of vehicular communication, VANET focuses on providing efficient solutions to environmental and comfort issues in the automotive industry, assisting road users and enhancing their decision making process while driving. Video technology will enhance these solutions. Video in VANET will aid navigation safety and give road users and relevant authority a precise and clear image of

the traffic conditions when necessary. For fast response from individuals and various traffic monitoring corporations, visual images will help in dispatching quick and relevant aid when required.

Cellular communication provides effective voice and data communication and could provide a platform for other multimedia communications among vehicles. However, vehicle to vehicle communication needs a unique ad-hoc communication scheme which is self-organising, and it can function without a pre-existing cellular infrastructural network. This is an essential feature of VANET because when conventional communication towers are suffering outages or are non-existent, ad-hoc communication can provide an effective way to transmit information. One has to bear in mind that the devices produced for this purpose must have certain heterogeneous capabilities to connect with other devices and in turn connect to an ever-increasing heterogeneous backhaul network.

At present, in various cities around the world, vehicle to infrastructure communication using the DSRC (Dedicated Short Range Communications) has already been put in place. There are “smart” traffic lights which can reduce drivers waiting times and reduce fuel consumption, thereby impacting the environment positively. From various statistics and studies [Glas08], this has the potential of reducing the time drivers wait at traffic lights by 28% thereby yielding a drop of 6.8% in CO₂ emissions.

Due to the rapidly changing topology and the speed of the vehicles in vehicular ad-hoc network, a number of issues become increasingly important to ensure the efficiency and stability of this network. Routing, congestion control and medium access are a few of these issues. Intel Corporation has decided this year [Inte10], to lead the development of video system on board of a car, others such as CogniVue has also entered this market. In our study, the key issue here is not the routing or signalling, it is the amount of traffic the high definition camera has pumped into the network. Here we focus on the video traffic issue, which is the key to unlock the power of video applications. Like every other wireless environment, transmitting video signals in a VANET poses more difficult concerns. Handling congestion and packet loss becomes more delicate in a VANET (wireless) environment where interference is inevitable. Interference such as electromagnetic waves from starting car engines, engine electronics, from Additive White Gaussian Noise and critical weather conditions can affect the QoS as seen by the user in a wireless medium. Obstacles along the LOS (Line of Sight) could also pose a major difficulty in

VANET. As discussed earlier, the topology is constantly changing and vehicles could move out of sight from one another causing an outage in data transmission.

In addition, unlike every other network environment, VANET mobility has a peculiar and unique nature due to the randomness of human behaviour. In creating an effective mobility model, vehicle to vehicle interaction and vehicle to infrastructure interaction needs to be considered carefully and closely. According to the classification presented in [HoBo01], vehicular traffic models can be classified into four categories: Sub-microscopic, Microscopic, Mesoscopic and Macroscopic. Sub-microscopic models describe the individual behaviour of vehicles and the operation of the sub-units that make up the vehicle. This aspect models the interaction of various vehicular components. Microscopic models focus on the movement of each vehicle with respect to the behaviour of surrounding vehicles. On the other hand, mesoscopic models describe the movement of groups of vehicles/drivers with homogenous behavioural patterns. Finally, macroscopic models cooperate a great deal of details by considering motion constraints such as road topology, traffic lights, streets, crossroads etc[FiHa07].

One of the major research issues in VANET is the creation of an effective simulation platform that can integrate a network simulator with a realistic vehicular traffic simulation model. According to [SoDr08] the effect of having a realistic mobility model is evident. In integrating a network model with a VANET mobility model, two approaches are identified [BoBe09]: an open-loop integration approach and a closed-loop integration approach. The latter entails integrating traces generated from a mobility simulator to a network simulator while the former runs the two simulators concurrently. In other words, in the closed-loop approach, the traffic simulator and the external VANET mobility simulator are connected using HLA (High Level Architecture) designed for distributed computer simulation systems so that the two components feed the most recent information back to each other. The closed-loop approach is more effective as it allows the effect of the wireless signals to govern the mobility patterns of drivers. It also models driver reactions to certain wireless signals as detailed in [SoDr08].

1.2 Video Traffic Modelling

Unlike other forms of traffic (like data and voice), video traffic has a dynamic stochastic nature. Different statistical studies [BaSh95, GaWi94] have revealed that the inherent (not source or

codec specific) characteristics of Variable Bite Rate (VBR) video traffic is the Long Range Dependence (LRD), and several other studies have shown the modelling of video traffic with both LRD and SRD (Short Range Dependence) [HuDe95, MaJi98, WaDu04]. However, more studies have shown that LRD does have significant impact on the queuing performance and characterization of video traffic and SDR modelling could underestimate the correlation, consequently real time video traffic can be modelled using LRD [BeSh95, HoPa01]. Furthermore, continuous extensive work has been done on VBR video from various specific sources, (e.g., from video conferencing cameras, web cameras, broadcast TV or HDTV [HeLa96, RyEl96], and non real-time processing/storage of data taken from the cameras installed in real public safety law enforcement car system [LiHu09], however, we are not aware of any comprehensive study related to real-time video traffic.

1.3 Real-time Transport Protocol

Real-time data is considered to be data with an arrival deadline to reach its destination, or else the information is no longer valid thus no time for retransmission. At the first attempt to transmit the packet, the best effort is made to deliver the packet as effectively as possible. Therefore, packet loss is not an issue of great concern in most real-time systems. Instead, latency poses a greater concern. As long as packets can be delivered quickly to the upper layer at the destination, the video resolution is of minimal importance. So it would be desirable to optimize the delay through each of the OSI layers for real-time application.

In theory [Tane96], the transport layer protocols should be independent of the underlying protocols in the layer below. In other words, TCP (Transport Control Protocol) or UDP (User Datagram Protocol) should not be affected whether the physical layer is a fibre optic cable or even radio. However, in practice, when these protocols where designed, their implementations where carefully optimized based on assumptions that are true for wired networks and fail for wireless networks [Tane96]. In wireless media, the behaviour of these protocols are quite different as the wireless medium is prone to interference from forces of nature and manmade effects.

TCP [JaBr92] and UDP [Post80] are protocols that have been used. However, they are not effective. TCP is best used for lossless data transfer as it ensures packet delivery by its support of packet retransmission. This poses a problem for real-time traffic as there is no time for

retransmission [BaMa03]. UDP is better for video traffic, but unfortunately cannot guarantee real-time or loss performance. RTP (Real-time Transport Protocol) [ScCa03] is a protocol designed for end-to-end real-time transport of multimedia (video) traffic. However, it does not take many performance issues into account including channel outage, traffic congestion, the end to end delay in a mobile environment and the unicast/multicast overhead issues.

1.4 Dedicated Short Range Communications (DSRC)

DSRC [FCC04] is a medium range wireless communication service which is specifically designed for vehicle to vehicle and vehicle to infrastructure communication. DSRC is designed to provide high data rate to ensure safety on the roads with minimal latency in communication links. The band is free and now available for use.

The Federal Communication Commission (FCC) in 1999 allocated 75MHz of spectrum in the 5.9GHz for use by Intelligent Transportation Systems [FCC04]. Earlier versions of DSRC were at 915MHz which could only cover distances less than 30m and a data rate of 0.5Mbps [InDr10]. At the moment, the DSRC service can cover a range of 1000m with data rates ranging from 6 to 27Mbps depending of the distance of the transmitter from the receiver. The DSRC service are made up of two main units, On-Board Units (OBU), which are usually mounted on the car and the Roadside Units (RSUs) which are transceivers that are usually located along the roadside.

Presently, DSRC is mainly used in electronic toll collection in USA. Potential applications of DSRC are emergency warning systems for vehicles, adaptive cruise control, forward collision warning, electronic parking payments, approaching emergency vehicle warning, transit or emergency vehicle signal priority, and in-vehicle signing [TuKn96]. Vehicles equipped with DSRC can communicate directly with each other, making it possible to send warning messages over to neighboring vehicles. Using the ad-hoc networking concept, this information can further penetrate into the network. Each vehicle in a vehicular network can act as a sender, receiver or a router. DSRC can also be used to provide in-vehicle entertainment for drivers and passengers.

One of the short comings DSRC faces is that it is based on 802.11a which cannot handle high speed mobility while maintaining an acceptable data rate. Therefore, it can only be integrated with other technology for use in the VANET. It also does not have the ability to

handover connections at high speed which is essential for high speed motion and cannot support high data rates.

1.5 WiMAX for VANET

WiMAX (Worldwide Interoperability for Microwave Access) [WiMa09] is a 4G equivalent technology that enables the delivery of last mile wireless broadband access. The name WiMAX was created by the WiMAX forum which was formed in June of 2001 to promote conformity and interoperability of the standard [Brit10]. The WiMAX technology [GhGh07] as it is provides ease deployment as it eliminates the use of cables and can save cost when used in remote and rural areas. The technology is scalable and has a flexible frequency re-use scheme because it uses OFDM technology. Unlike DSRC, WiMAX was designed to handle high data rates. It implements full MIMO (Multiple-Input and Multiple-Output) which is good for mobile and car applications by enhancing timely information delivery to save lives and improve quality of life.

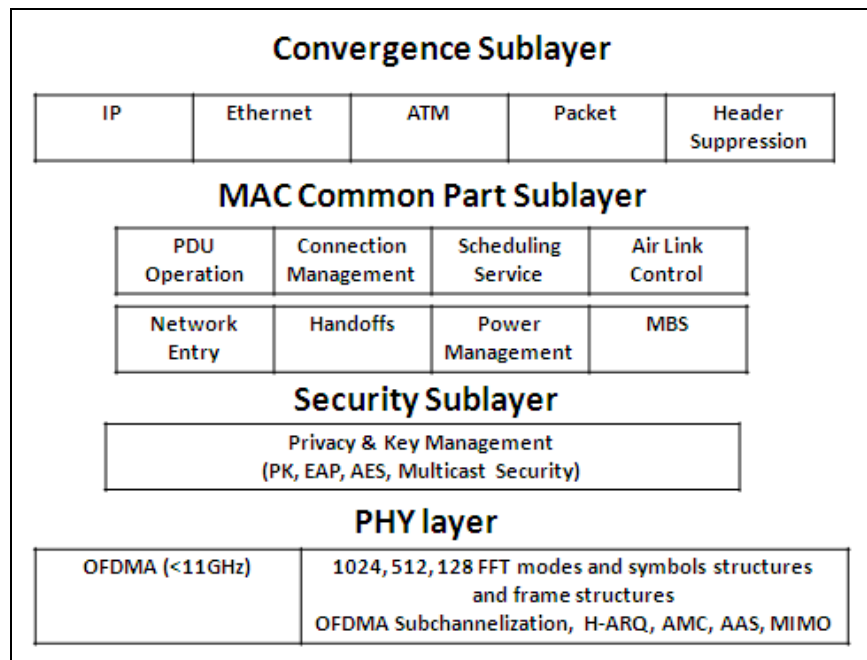


Fig. 1.1: WiMAX Architecture [Li06]

The architecture of this technology is shown in Fig. 1.1 [Li06]. At the physical layer, OFDMA is used. This allows for multiple accesses, high granularity bandwidth allocation, avoids subcarriers in deep fades and provides excellent signal isolation between subcarriers. [KuHu06]

Table 1.1: Comparison of Some Wireless Technologies

	DSRC	FM Radio	Cellular (GSM)	Cellular (CDMA)	WiMAX	Satellite
Max Range(Km)	< 1	hundreds	<10	<10	<50	thousands
Data Rate mbps	6-27	> 10 kbps	< 100 kbps	2-3	70	100-200
Coverage	LOS – duplex	Area – ½ duplex	Area - duplex	Area - duplex	Area - duplex	Area - duplex
Cost (per bit)	≈zero	≈zero	\$\$	\$\$	\$	\$\$\$
Average Latency	Very Lo	Hi	Lo	Lo	Lo	Lo
Mobile Connectivity	Lo	Lo	Hi	Very Hi	Hi	Very Hi
Sustainable connectivity speed (km/hr)	80	120	140	110	200	100

A comparison of these physical layer technologies that could be used for VANET is shown in Table 1.1[Morg10]. The ‘\$’ in the table was used to denote the cost per bit for each technology where ‘\$’ represents the least expensive and ‘\$\$\$’ represents the most expensive. DSRC which is the technology used for most VANET scenarios, requires Line of Sight (LOS) for duplex operation. Although DSRC cost very little, its sustainable connectivity speed is low for various applications and covers less than 1km radius.

Through comparison, one sees that WiMAX is the most cost effective approach by providing a data rate that can satisfy the needs of our mobile multimedia users (low latency and high coverage) at high speed and at an affordable cost.

1.6 Congestion Control

There are two main types of traffic congestion control in computer networking: explicit and implicit congestion control. Implicit congestion control usually controls the traffic from the end node (receiving) point. This method is usually not very effective as it is the router that knows the state of the network. Consequently, implicit congestion control does not provide smooth throughput for real-time and low link utilization. The end user congestion control can only control traffic when a packet is lost. However, for real time traffic, packet loss is not our concern, we concern ourselves more with delay, thus, implicit congestion control is more appropriate for our application.

Various works has been done on congestion control in wired environments [HoYa07], wireless environments [Hac99, RaSa10] and VANET [WiRo05]. Congestion control protocols

can also be classified into two main types [HoYa07]: window-based and rate-based. The window-based congestion control algorithms adjust the window-size according to the level of congestion detected in the network. Algorithms like RED (Random Early Detection) [FlJa93], its TCP variants (like Tahoe [JaKa88], NewReno [HaBr07]), and AIMD (Additive Increase and Multiplicative Decrease) [JaKa88] fall under this category. However, some of the approaches used in these algorithms can cause a fluctuation of the source sending rate; evidently not effective for real-time video streaming [HuXu03] in practice.

Rate-based congestion control algorithms on the other hand, allow each source in the network to directly adjust its sending rate based on the congestion notification received. TFRC (TCP Friendly Rate Control) [HaFl03] and API-RCP (Adaptive PI Rate Control Protocol) [HoYa07] falls under this category. API-RCP presents an effective way to calculate the source-sending rate based on the queue deviation.

Most of the algorithms mentioned above are built on top of TCP and have only been tested in wired networks. In wireless networks, delay is caused mostly by wireless interference rather than network congestion. Quite often packets are stored in a buffer waiting for proper bandwidth allocation before they can be delivered. As mentioned earlier, in real time traffic, buffering (incurring delay) is not wanted. We can tolerate a poorer quality, but delay is unacceptable. Explicit congestion control controls traffic at the router node, calculating the flow throughput more effectively. Smooth throughput for real-time and high link utilization. However, for practical purposes, explicit congestion control is more tedious to implement as for it to be effective, one has to load it on every router on the network, which will take time. This also consumes more CPU resources.

1.7 Motivations

From the review of various characteristics of VANET, one of the major challenges in VANET design is the development of an effective platform that can bring all issues described earlier under one umbrella – a simulation model. Since it is safer and more cost efficient to simulate possible solutions rather than field experimenting of driving at 140km/hr, creating an effective VANET simulation platform/model has become of pertinent importance in research and industry. One of the major challenges faced is integrating an effective mobility model that puts vehicle to vehicle interaction and vehicle to infrastructure interaction into consideration along with

possessing the full functionalities of a communication device with effective receiving, processing and transmitting capabilities, thus, emulating a real world situation. Human behavioural modelling are also some of the other issues to be modelled as close to reality as possible to produce conclusions that can be used in the real world. Although [SoDr08, WeHe08, LiKh09] have worked on creating a similar platform, no specific work have been done using OPNET as the network simulation tool. In addition, customizing the platform for real-time video traffic is a specific area we explored using different traffic congestion scenarios.

Our motivation also came from the statistics of road traffic fatalities. Statistics show that from 2000 through 2004, there were 44,192 accidental deaths in Canada. In the prime ages (15 to 24 age group), motor vehicle accidents accounted for 70% of the death course [Rama04]. In a city like California, with a population of 37million people, 1 million vehicle accident deaths are reported each year [Tran10]. Hence, developing a “smart car” that assists the driver without taking the control of the car from the driver will help reduce this drastically. This is the bigger picture of our research.

Furthermore, as mentioned in Section 1.6, implementing an explicit congestion control mechanism is more tedious to implement, we therefore sort to develop a simple congestion control algorithm designed to real-time video traffic over UDP.

Having examined the above issues, we seek to provide a head start in this direction, creating a platform where other VANET research concerns such as intelligent vehicular with sensing, communicating, information processing and analysis, learning and self-control capabilities can be effectively explored.

1.8 Thesis Objectives

The long term objectives of this research work are to provide a robust platform for effective VANET simulation, providing an environment to test, develop and deploy effective communication protocols that enhance real-time multimedia communication. Specifically, we would like to:

- i) Create a real-time Video OPNET model under VANET conditions.
- ii) Integrate a realistic VANET mobility model to test at various speeds.
- iii) Integrate a practical algorithm to survive network congestion.

- iv) Evaluate the performance of a practical controller through measurements of the end-to-end delay, jitter and visual MOS of the Video OPNET model using different buffer sizes and under different traffic congestion scenarios.

1.9 Methodology

We shall use a systematic approach to achieve the above objectives. The first step is to find a simulation tool that could allow the integration of the various part of our model. Of the few available network simulation languages such as Qualnet and NS-2, we shall use OPNET because it can present detailed models of network equipments and support a rich pool of communication protocols and standard. It also provides a good frame work which allows flexibility of design enabling us to integrate our mathematical video model effectively. We would like to develop an OPNET WiMAX model that can emulate the real world of cars on the road with each car acting as a WiMAX Subscriber Station (SS) capable of receiving, processing and forwarding data to the destination and consequently to the backhaul network via the a WiMAX Base Station. In our case, the WiMAX Base Station was a simpler form of a WiMAX enabled Base Station since it is being used as a RSU (Road Side Unit) in our application.

The next step is to collect a live video trace from a setup consisting of a car camera equipment. We play a series of videos from a monitor and have the camera capture the video with our system having a very high compression ratio We have chosen movies that range from action movies (which have more variation in frame sizes) to love stories (with less movement and therefore less variation in frame size). We characterized this life video trace using proven stochastic processes and integrated it into our model. We sought to develop a model that has as few parameters as possible to match the measurement and an implementable model. This model-based traffic generation method is used because our lab does not have the ACE [OPNE10] license to feed life data into our Opnet simulator.

We shall go further to integrate a realistic vehicular mobility model into our model. After careful research, we found that OPNET's trajectory models will not effectively simulate the V2V and V2I interaction. After searching, we have decided that VanetMobiSim [FiHa07] is the only VANET mobility model that can modify the output code generator in order to generate and output trace useable by other simulators. Hence, we choose VanetMobiSim as our mobility model tool and integrated its traces into our existing OPNET model using the open-loop

approach discussed in Section 1.1.

For our application, we do not intend to ‘cure’ congestion; we however want to ‘survive’ congestion. We thus propose an algorithm that reduces the compression rate of the video packets been sent once congestion is detected in the network. Before settling down with an approach, we shall explore other congestion control algorithms and try to understand the complexity of congestion control in real-time video streaming. Consequently, we shall design an effective feedback mechanism that informs the source of the current congestion state of the network, in order for the source to adjust its compression rate adequately providing a mechanism for the system to survive congestion.

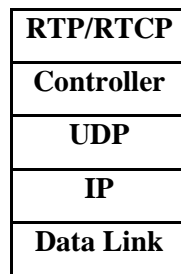


Fig.1.2 Overall Architecture

At this early stage, we make use of RTP/RTCP at the application layer, creating an effective feedback mechanism that can help systems survive congestion. In our research work, we focus on real-time video traffic where there is no time for retransmission. Fig.1.2 shows the overall architecture of our design.

In summary, this project sets the stage for a family of new application layer protocols that deal with channel outage due to position change, congestion due to traffic jam, and negative interaction between channel outage and congestion.

1.10 Thesis contribution

The contributions of this thesis are:

- i) The design and implementation of a theoretical video model.
- ii) The design and implementation of a practical traffic controller for video over RTP applications.
- iii) The integration of a VANET mobility model, communication tool and video model to provide a practical VANET simulation platform for the evaluation of video transport

1.11 Thesis Organization

The rest of the thesis is organized as follows. Chapter 2 discusses the network operations, models and assumptions used in this thesis. Chapter 3 presents the methodology used in this thesis by presenting the trace collection and stochastic analysis of the trace. We discuss the simulation platform, each scenario and present the simulation results in Chapters 4 and 5. Chapter 6 presents design guidelines and recommendations from the results presented in Chapters 4 and 5. We give our conclusion in Chapter 7, and discuss the future work.

1.12 Publications

The following publication covers part of the work in this thesis:

- i) F. Lawal, J. Huang and O. Yang, "Performance Tradeoff Study of Streaming Video among Vehicles", *Proceed. IEEE 72nd Vehicular Technology Conference*, Sept 2010, Ottawa.
- ii) J. Huang, F. Lawal, L. Jin and O. Yang, "Content-based blind compensation and shaping for streaming video," *Proceed. Canadian Conference on Electrical and Computer Engineering, 2009. CCECE '09*, pp.419-422, May 2009.

Chapter 2

Network Operation, Models and Assumptions

In this chapter, we discuss the general network operation of VANET and WiMAX as it related to our research. We then go further to explain the various components that make up our model. We shall discuss in details the sub-models and how they all contribute to a platform which is usable presently and in future development. Due to the difficulty and risk involves in creating and analysing the performance of the network described above, we sort to create a simulation model.

2.1 Network Operation

This section describes the network layout of VANET and WiMAX along with their operation that are of interest to this research.

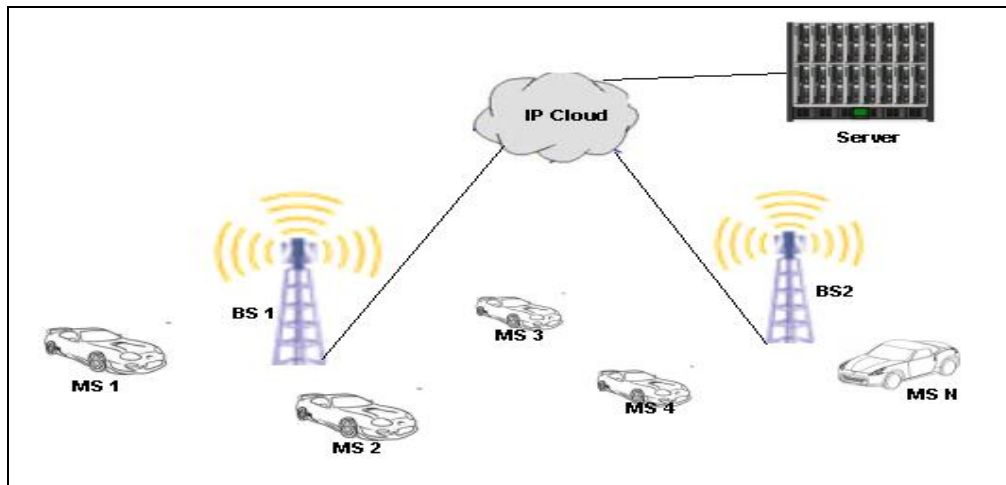


Fig 2.1: Network Model Topology

2.1.1 General Network Layout of VANET

In the VANET we envisioned, each vehicle has the ability to communicate with any neighbouring vehicles. Depending on the nature of the message, the information either remains within the VANET or venture out to the backhaul network via the RSU. For instance, brake-warning sent from preceding cars, tailgate and collision warnings are messages that can remain in the VANET network. On the other hand, detailed regional weather forecast, premonition of

traffic jams and collision notification are messages that are either transmitted from the backhaul network to the VANET via the RSU or vice versa. In our application, video messages are forwarded from the point of interest (which could be a traffic congestion area, road block, accident scene etc), to the backhaul network via the RSU to aid traffic personals, emergency agents or any other party to respond to such situations more effectively.

To study the traffics generated within the network, we consider a VANET consisting of N cars communicating with each other and with the internet via RSUs. The network topology is shown in Fig. 2.1. Each car is equipped with WiMAX transmitting and receiving capabilities at the Physical and the MAC layers.

The RSU (BS 1 or BS 2) has the capability to handle up to 100 cars simultaneously. Each car is associated with the RSU depending on their distance to one another. The video packets are routed and given priority due to the service class name associated with them and the scheduling type which handles the bandwidth request/grant mechanism. The *silver* service class and the rtPS (Real-time Polling Service) scheduling are used [OPNE10]. Maximum sustainable traffic and reserved traffic rates are set to 384kbps for this service class. At the SS station, the average SDU (Service Data Unit) size is 1500B. Each video arriving from the higher layer is expected to be within this size range. Any packet size greater than this must be segmented before encapsulated into a PDU (Protocol Data Unit) and transmitted with appropriate header information. When a SS wants to transmit video, the video is generated from the application layer using our traffic generation model, RTP/RTCP handles the traffic at the application layer. The packet goes through the UDP layer, IP layer before arriving at the MAC layer. At the MAC layer, the destination address is examined and the nearest RSU is assigned to handle the request. The packet is sent to the RSU and the RSU forwards the packet accordingly. The IP cloud is set to its default values and acts a router. The server is configured to accept packets generated by our model.

As discussed in our literature review, DSRC is a technology based on IEEE 802.11. Its spectrum has been allocated for the V2V and V2I communication in some parts of the world. Researchers are now exploring other physical layer technologies for this application. The detailed break down of the channel allocation in DSRC is shown in Fig 2.2.

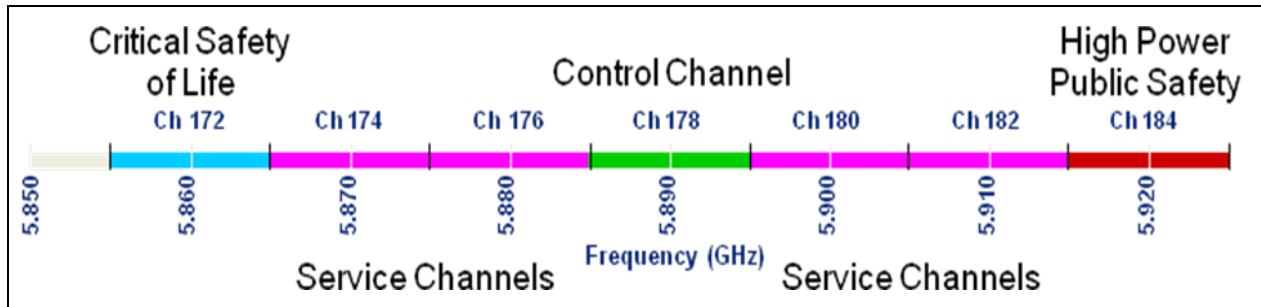


Fig 2.2 Channel Allocation for DSRC

In our work, we explore the possibility of using WiMAX technology as the physical and MAC layers for VANET. WiMAX (an IEEE 802.16 based technology), is a broadband wireless technology that can sustain voice, video and data services at high speed while maintaining high data rates. Mobile WiMAX is based of OFDMA physical layer of the 802.16e-2005 standard, which is a revision of the fixed WiMAX standard. IEEE 802.16e provides functionalities such as BS handoffs, MIMO (Multiple Input Multiple output) transmit/receive diversity, and scalable FFT (fast Fourier transform) sizes [Li06]. Table 2.1 shows these features at a glance. WiMAX is known for its high data rates providing up to 128Mbps downlink and 56Mbps uplink using its MIMO antenna techniques. In our case, we used SISO antenna technique which supports up to 1Mbps uplink and downlink. The fundamental premise of WiMAX MAC architecture is QoS. It defines service flows that can be mapped into gradual IP sessions to enable end-to-end IP based QoS. Scalability, Security and mobility management are some of the other major features of WiMAX technology.

Table 2.1: IEEE 802.16e Characteristics

Standard	IEEE 802.16e – 2005
Multiplexing	OFDMA
FFT size	Scalable (512, 1024, 2048, etc)
Duplexing mode	TDD
Modulation scheme	QPSK, 16-QAM, and 64-QAM
Subcarrier spacing	10.94kHz
Signal bandwidths	5, 7, 8.75, and 10MHz
Spectrum	2.3, 2.5, and 3.5 GHz

Note that mobile WiMAX allows for both TDD (Time Division Duplexing) and FDD (Frequency Division Duplexing). As shown in Table 2.1, we use the TDD mode as done in most deployments in order to accommodate the dominant asymmetric WiMAX traffic

The WiMAX technology uses OFDMA frames in order for multiple users to receive data

from the BS at the same time thereby increasing bandwidth utilization. The frames are structured into UL (Up-Link) and DL (Down-Link) sub-frame as shown in Fig. 2.3 [WiMa09]

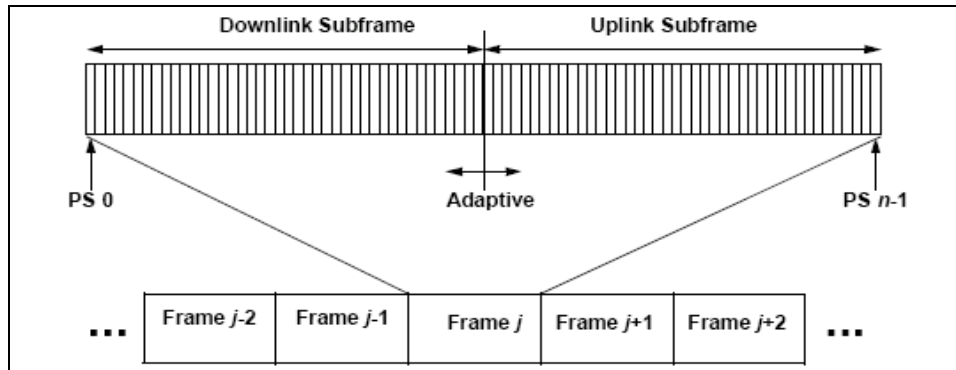


Fig. 2.3: WiMAX Frame Structure

All the MSs receive the frame control section of the DL sub-frame. The DL mapping field in the frame control section specifies the location and duration of DL data burst in the frame from a particular MS. Conversely, the UL mapping field specifies the location and number of time slots allotted in the frame for a particular MS to transmit its data on UL. All MSs listen to the frame control section in the DL frame, and receive or transmit data during the slots assigned to them by the BS [Ahma06]. As seen from Fig. 2.3, this structure enables dynamic allocation of DL and UL resources to efficiently support asymmetric DL/UL traffic.

In our OPNET model, WiMAX does not support network-assisted handover, base station-initiate periodic ranging and power management. A sub-channel is allocated to each user there by reducing the channel interference in the frequency domain. OFDMA (Orthogonal Frequency Division Multiple Access) is the scheme used allowing multiple access to every user on our network.

At the Network layer, IPv4 is used for addressing and RIP (Routing Information Protocol) [Malk98] is used as the routing protocol. We use UDP as the transport layer protocol to cater for the end-to-end delivery of packets. RTP is used at the application layer to combat the possible unreliability in UDP. RTP is a real-time streaming protocol designed for streaming audio and video. In conjunction, we use RTCP (Real-Time Transport Control Protocol) for controlling, signalling and quality service monitoring. Our congestion control mechanism builds on RTCP and thus reports the present condition of the network to the sender.

Note that although the network layer in VANET is also a unique area of study, this work does not focus on routing techniques and protocol optimization for this layer in VANET. Further up, our transport layer uses UDP and RTP in the application layer for streaming of live video. In real life, the video generated is VBR and the generation rate is random. A standard MPEG encoder generates three types of compressed frames. I, P and B frames. I-frames are compressed using intra frame information only. P-frames are coded similarly to I-frames but with the addition of motion compensation with respect to the previous I or P frame. B-frames are similar to P-frames except that the prediction is bi-directional. In general, I –frames are the largest followed by P and B frames respectively. After coding, the frames are arranged in deterministic order, which is called GOP (Group Of Pictures). This pattern is not specified hence different coders may use different patterns for subsequent GOPs.

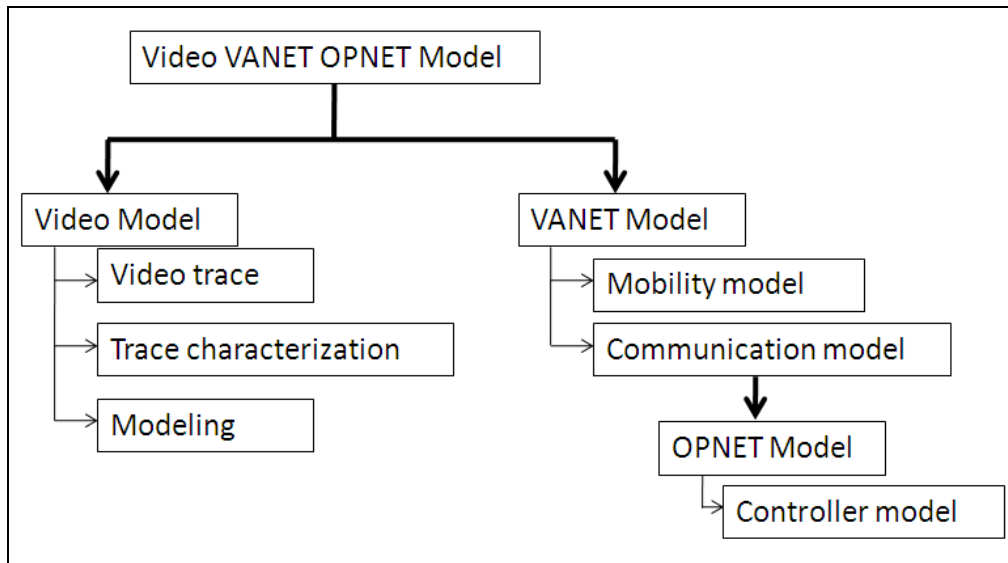


Fig: 2.4: Video VANET OPNET Model Structure

2.2 Network Models and Assumptions

Fig. 2.4 shows a diagram summarizing the various components of our model. The video VANET OPNET model, consist mainly of the Video model and the VANET model. Analysing a live video trace, characterising the trace and modelling the characterised trace to fix into our simulator obtained the Video model. On the other hand, the VANET model consists of the VANET mobility model and a communication model. OPNET modeller provided the platform for the communication model and allowed for the integration of the various components of the Video VANET OPNET model. Each component of the model will be examined in this chapter.

2.2.1 VANET Model

The following sections describe the VANET mobility model and the communication model used in our model.

2.2.1.1 VANET Mobility Model

Of the four categories of VANET mobility models described in Section 1.1, we adopted the macroscopic model. Among other factors in choosing the appropriate mobility model, we had to consider one that could be integrated into our OPNET platform. From our survey, Table 2.2 shows a summary of our findings.

Table 2.2: Mobility Model Summary

	ns2	qualNet	OPNET
MoVES	No	No	no
STRAW	No	No	no
VanetMobiSim	Yes	Yes	yes
SUMO	Yes	Yes	no
SHIFT	No	No	no
GMSF	Yes	yes	no

The result of this analysis presents VanetMobiSim [VaMob07] as the only mobility model found as of the time of development that could be integrated into OPNET consequently influencing our choice. VanetMobiSim's ability to integrate into OPNET comes with its flexible to manipulate its output file by coding its output generator file to produce a format desired by our simulator. It also generates traces in a special Universal Trace Format [FiHa07] in the form (*time node_id pos_X pos_Y velocity acceleration*) where *time* records the simulated time, *node_id* specifies the node in question, *pos_X* and *pos_Y* provides the X and Y coordinates of the specific node at the given time respectively and the *velocity* and *acceleration* shows the velocity at which the node moves and its acceleration at that time.

Besides its adaptable output abilities, VanetMobiSim incooperates both microscopic and macroscopic models to allow the modelling of vehicle-to-vehicle and vehicle-to-infrastructure interaction. Traffic light integration, stop signs, human mobility dynamics and safe inter-distance management is modelled in this tool. It allows the integration of road topology for GDF [Erti10] or TIGER [USCe10] to user-defined/ random topologies. The different forms of topology are shown in Fig. 2.5 [FiHa07]. VanetMobiSim provides a flexible platform in which the user can

configure the path used during a trip between Dijkstra shortest-path, road speed shortest path and a density –based shortest path. The trip generation could either by generated by random source-destination to activity-based [FiHa07].

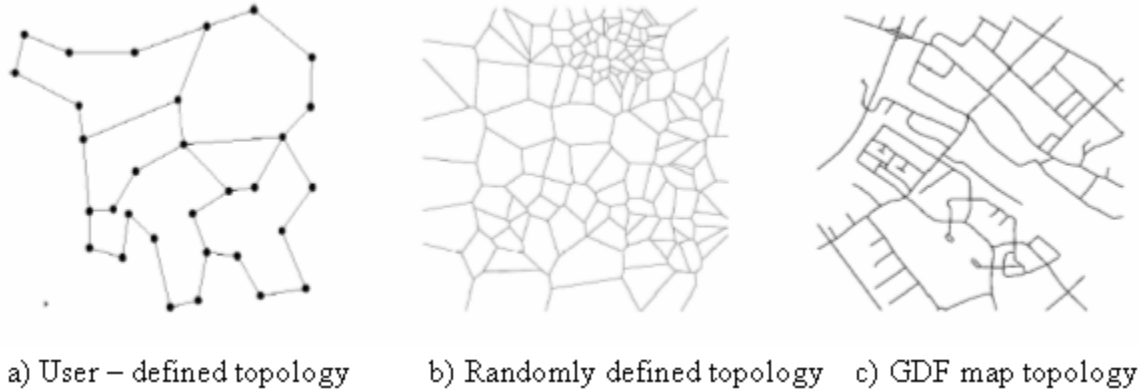


Fig. 2.5: Mobility Topologies

Table 2.3: RSU Parameters

Parameter	Value
Physical layer	IEEE 802.16e
BS TX power (W)	5
Number of TX	SISO
BS Antenna Gain (dBi)	15
Minimum Power Density	-80
Maximum Power Density	-30
Link bandwidth (MHz)	20
Base Frequency (GHz)	5.8
Physical layer Profile	OFDM

Besides its adaptable output abilities, VanetMobiSim incooperates both the microscopic and macroscopic models to allow the modelling of vehicle-to-vehicle and vehicle-to-infrastructure interaction. Traffic light integration, stop signs, human mobility dynamics and safe inter-distance management is modelled in this tool. It allows the integration of road topology for GDF [Erti10] or TIGER [USCe10] to user-defined/ random topologies. The different forms of topology are shown in Fig. 2.5 [FiHa07]. VanetMobiSim provides a flexible platform in which the user can configure the path used during a trip between Dijkstra shortest-path, road speed shortest path and a density –based shortest path. The trip generation could either by generated by random source-destination to activity-based [FiHa07].

2.2.1.2 RSU and Car Communication Model

The RSU and car communication are the major communication nodes in VANET. Our RSU is a simplified WiMAX BS. Each car is equipped with proper communication tools to enable car to car and car to infrastructure (RSU in our case) interaction. The design of each RSU is robust and non-application sensitive so that every car can send and receive a wide range of information. In our model, the car is equipped with WiMAX receiving and transmitting capabilities. Table 2.3 shows the basic essential characteristics of our model along with some typical settings in our work.

2.2.2 Video Model

The video model is one of the main components of our VANET OPNET model as our research focuses on real-time video communication in a VANET environment. In creating our video model, we put certain factors into consideration to measure the usefulness of the model. According to [Huan01] factors like parsimony, analytic correctness, flexibility, implementability and absolute accuracy were considered. As it is common knowledge, it is impractical to have all these factors in one model at high values. With respect to our application, we choose parsimony and implementability has our highest priorities.

Table 2.4: Traffic Model Comparison

Items	FBM	TCP	Mini Pareto
Parsimony	3	1	2
Analytical	1	1	2
Flexibility	1	1	1
Implemental	2	1	3
Accuracy	2	3	2

Using the factors mentioned above, on a scale of 1 to 3, 1 being the least and 3 the greatest, Table 2.5 shows other models and their rating with respect to the factors described above.

We have taken a systematic approach in developing our mini-Pareto model. Video traffic trace was collected using the same camera used for a road test. The traces were analyzed and stochastically represented and plugged into our simulation platform. Detailed discussion about these steps is presented in Chapter 3.

Pareto distribution which is a power law probability distribution function that has been used to model a number of everyday scenarios was used to model our video traffic. Pareto was originally used to describe the allocation of wealth among individuals [Reed01], it shows that “a larger proportion of the wealth in a nation is controlled by a small proportion of people” in that nation. This could be expressed in the “80-20 rule” [Reed01]. The Pareto distribution is a long tailed distribution which has two parameters, location and shape [ZhHe07]. This principle best describes video traffic due to the strong correlation between clusters of frames i.e. video slides inside an object representing an action unit in advanced video codec.

2.2.3 Traffic Controller Model

As discussed in Section 1.2, due to our application scenario (real-time safety-networking), we only seek to survive congestion. Our controller uses one byte to notify the source to reduce its sending rate. From our careful study, reducing the sending rate can be done in two ways: dropping packets or reducing quantization level.

In dropping packets, it could be done by discretion or dropped with a particular drop pattern being taken into consideration. For video traffic, the pattern of drop is a very key factor in the quality of service as seen by user. The frequency of drop becomes a more critical factor as compared to the percentage of drop. For instance, dropping 10 consecutive packets out of 100 packets is a 10% drop. Also, dropping 1 out of 10 packets in a packet fleet of 100 is a 10% drop. However, the latter is more tolerable than the former in our system. However, there is still an upper limit of approximately 25%, where more drops exceeding this threshold will render the video useless

According to our industrial partners, changing the quantization level will be the next practical and cost effective approach in terms of complexity and ease of deployment, to go over 25% bandwidth reduction. Hence, depending on the end-to-end delay, the destination is notified of the quantization level to use in encoding its preceding video frames. This method will bring down the total rate to 50% of original coding rate.

The choice of method is a trade off between frame rate and resolution. Dropping packets will lower the frame rate while reducing the quantization level will lower the resolution. The challenge in lowering the resolution is to do so in a way that the user experience is kept high.

2.2.4 Simulation Model

As described in Chapter 1, it is best and more cost-effective to create a simulation model as close to reality as possible on which tests and various design consideration can be performed before deployment. Our simulation model based on OPNET – a simulation tool, brings our Mini- Pareto model, VanetMobiSim (mobility model) and a traffic controller under the umbrella of one platform.

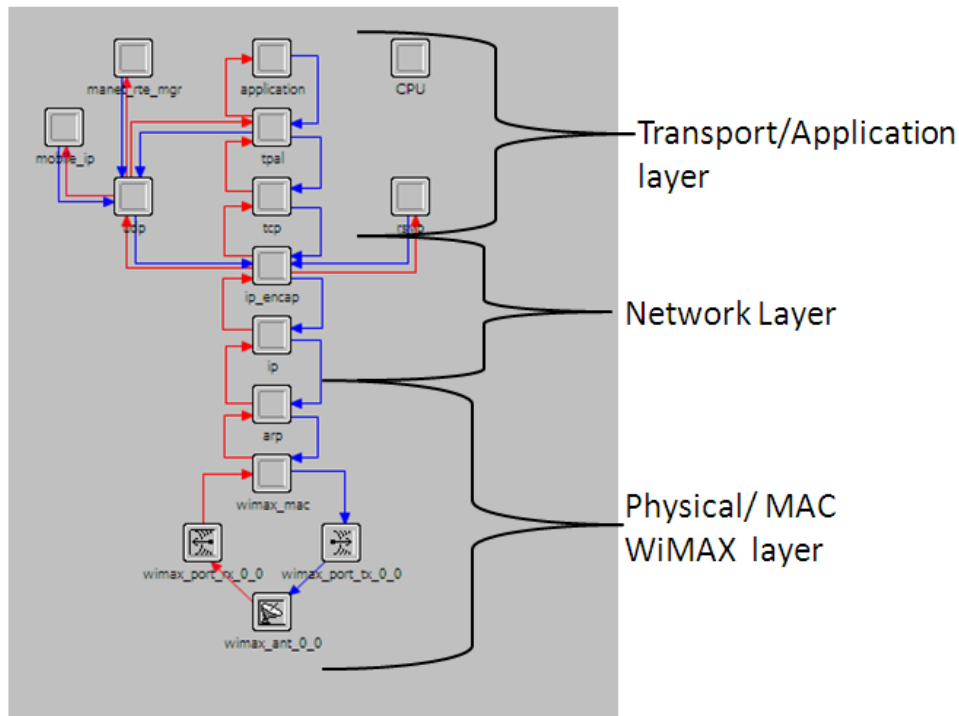


Fig. 2.6: Mobile Node Architecture

The Physical and MAC layers are those of the WiMAX 802.16e standard. The Transport layer uses the UDP protocol. RTCP was implemented at the Application layer to allow for feedback from the receiver to sender. This code was written in order to implement our controller which changes the quantization level at the source when congestion is detected as observed by the end-to-end delay at the receiver.

Fig. 2.6 shows a representation of each node (car) in our model. The model can be divided into three main layers – Physical/MAC WiMAX layer, Network Layer and Transport/Application Layer. The Physical/MAC WiMAX layer software processes models the WiMAX physical layer and MAC layer. This layer is responsible for data forwarding classifying higher-layer traffic to service flows, encapsulation /decapsulation of higher-layer packets in MAC frames, bandwidth request/grant mechanism, ARQ and packet delivery. It also handles

admission control initiation, activation of service flows, handover initiation, starting the scanning neighbour base stations, ranging (initial and periodic) and selecting the serving base station.

The network layer models the IP routing functions, fragmentation and reassembly. IP packets arriving on any interface are routed to the appropriate output interface based on their destination IP address. A dynamic routing protocol (e.g., Routing Information Protocol (RIP) or Open Shortest Path First (OSPF)) may be used to automatically and dynamically create IP routing tables and select routes in an adaptive manner. It also de-encapsulates packets arriving from the lower layer in order to forward the user data to the transport layer. This model serves as an interface between the higher layers and the IP layer.

The transport/application layer models the transport protocol and the application generation models. This process model implements RFC 768 for User Data Protocol (UDP) which we use for our model. As mentioned earlier, UDP provides connectionless transport service over IP. The main feature provided by this model is the mapping of port numbers to each UDP process. The process also assigns a local port, if unspecified, for any requests received from the application layer. The *tpal* node provides a basic, uniform interface between applications and different transport layer processes. The *tpal* process model is the root process which acts as an interface between the application layer and any transport layer.

All interaction with a remote application through *tpal* is organized into sessions. A session is a single conversation between two applications through a transport protocol. *Tpal* also provides a global registry of servers. Each server registers itself at the beginning of the simulation by providing the name of the service, the port index through which it can be accessed, and a popularity value that indicates how often clients use the service. Client applications can select servers from this registry.

RTCP and our controller model. The flow chart for the implementation is shown in Fig 2.9 and Fig. 2.10.

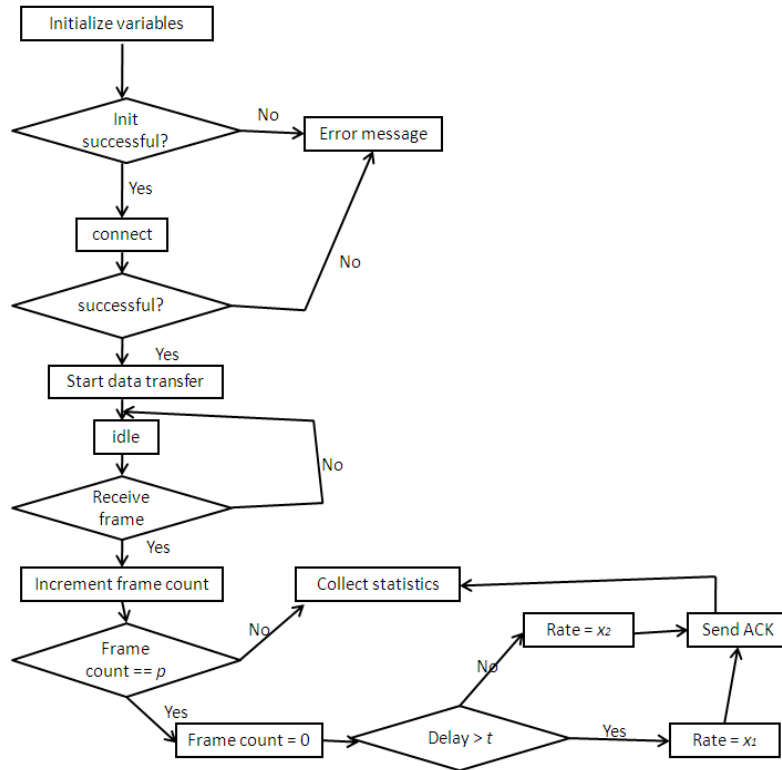


Fig. 2.9: Video Called Party Flow Diagram with RTCP Implementation.

Taking a closer look at Fig. 2.9, once the variables are initialized successfully, data transmission begins upon request. Once a frame is received, the frame count is incremented until it reaches a value p . Once p is reached, the frame count is set to zero and the end-to-end delay associated with the packet is checked. If the delay is greater than the threshold value t , (obtained from experience after running a series of simulations) a rate of x_1 is piggy-backed with the ACK packet and sent to the sender, else, a rate of x_2 is sent with the ACK packet.

Fig. 2.10 shows the implementation of the controller on the calling party manager using a flow diagram. Once the initialization process is successful, the video properties are collected and a connection is established with the receiver. For every packet received, the algorithm checks if it's an ACK packet, if it is not, the required statistics are collected and the packet is destroyed. If the packet is an ACK packet, the rate x_1 or x_2 is retrieved from the ACK packet and the parameters for call establishment are changed with respect to the new value obtained.

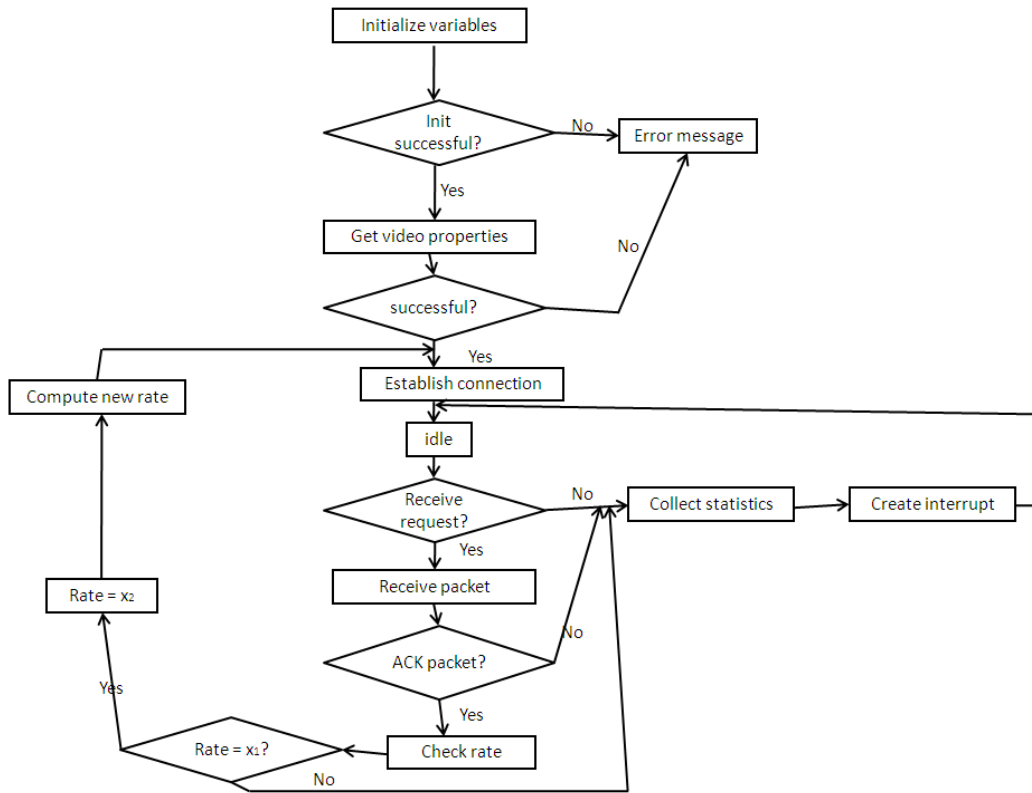


Fig. 2.10: Video Calling Party Flow Diagram with Traffic Controller Implementation.

2.3 Assumptions

Unless otherwise stated, the following are assumptions taken throughout the thesis:

- 1) Every vehicle in the network is equipped with necessary radio communication hardware. That is, every vehicle on the road has the WiMAX capability to receive from and send video data to other vehicles via the RSUs.
- 2) WiMAX BS is a “stationary” node. This is required due to the limitation of our Opnet model and we need it to act as an intermediate node for packet forwarding to the destination.
- 3) No disruption in a communication channel because one can use dedicated channel allocation once the node is in the communication range of a RSU.
- 4) There is no obstacle along the LOS between the RSU and the mobile cars. This would allow the simulation to monitor the vehicles so that it would not move out of range of the RSU.
- 5) Finite buffer size for each transmitter: this is a more realistic assumption which would also allow us to find the trade-off between buffer size and end-to-end delay.
- 6) The RSU use OFDMA for multiplexing and their is always a slot available for each SS sending video traffic.

Chapter 3

Experimental Setup

This chapter presents the experimental setup of our model. It discusses the trace collection process and the initial analysis done on the trace. The later sections then describe the simulation environment, scenarios and performance measures used in this work.

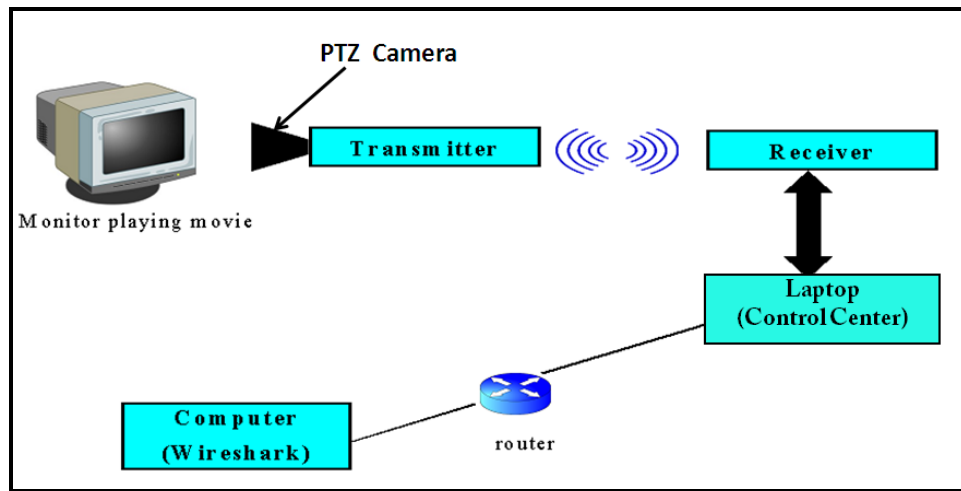


Fig. 3.1: Setup for taking video Traces

3.1 Trace Collection

We need to first collect video traces in order to model a video characteristic that is as close to reality as possible. Traces from a live camera were obtained using Wireshark™ software on a monitoring PC. The set-up is shown in Fig. 3.1. The monitor was used to play a series of video clips for 10 minutes each. The PTZ camera shown in Fig. 3.0 is used to capture the video being played by the monitor. The transmitter sends the compressed (in a ratio of 250:1) and encrypted video images to the control centre via a non-licensed 900MHz FHSS radio band. The receiver block decodes and decompresses the received video frames and plays the image at the control centre at about 20fps. The control centre laptop and the receiver are connected using a RS232 serial port. The control centre is then connected through a router to a computer hosting the packet trace capturing tool – Wireshark™. Once the system is turned on, the computer with the Wireshark™ software is set to access the ‘capture’ folder in the control centre then stream the video. The Wireshark™ software [Comb08] is then turned on and the trace capture begins. The video clips were chosen based on the activity rate in the clip. Three types of video clips are

chosen and described in the following.

- i) Action movies. This type of movies has a lot of movement and hence more variation in frame sizes. “The Prisoner” by Jackie Chan was chosen for study here.
- ii) Drama: This type of movies has an average movement and hence, it’s a mixture of frame sizes. “The Game Plan” with Dwayne Johnson was chosen for this study.
- iii) A romantic: This type of movies has very slow scenes hence, little or no variation in frame sizes. “28 Day: with Sandra Bullock was chosen for this study.

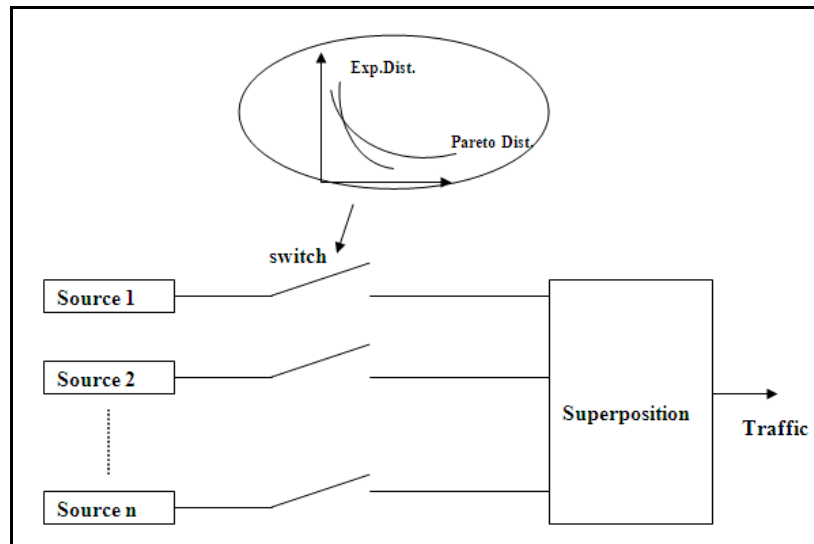


Fig 3.2: Model Description for Video Traffic Generation

3.2 Initial Analysis

The next challenge was to analyse the trace and create a video traffic model. Fig. 3.2 shows the schematics of our traffic model. The number of sources, n , was to be chosen bearing in mind the trade-off between parsimony and accuracy (Parsimony refers to the provision of the simplest and most frugal available solution to a certain problem.). Each source represents each set of video traffic stream with the switch being regulated. The switch is configured to form traffic with a long range dependency. We modelled the on-time switch by a Pareto distribution and the off-time by a Poisson process since we believe the memory between action sequences is negligible, but within the same AU (Action Unit), the sequences are strongly correlated [GuJi04].

We choose $n = 9$ for our model as this combination was the best trade-off we found between parsimony and accuracy. From our studies we realised that the more mini-sources created, the higher the accuracy and the more the parameters needed to match the trace. However, due to the computational complexity (and therefore the simulation time), we have decided on $n = 9$ to be

the reasonable value while providing an acceptable accuracy.

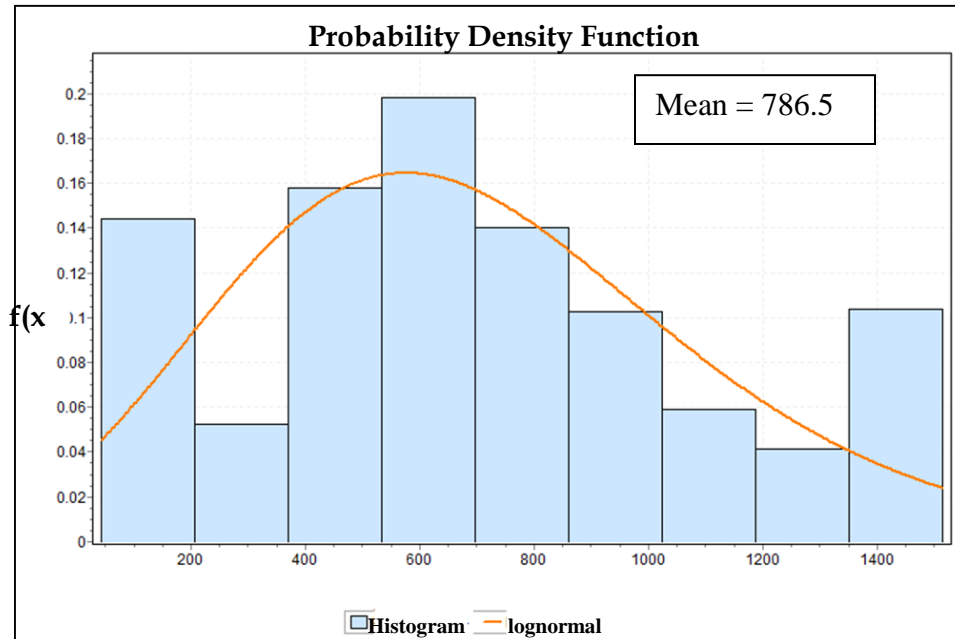


Fig. 3.3: pdf of Video Trace

Having obtained the pdf (Fig. 3.3) of the video trace collected using a tool called EasyFit™ [Easy09]. The program first decided that the lognormal distribution as the best distribution to fit the given data. The orange curve is the result automatically generated using the lognormal distribution.

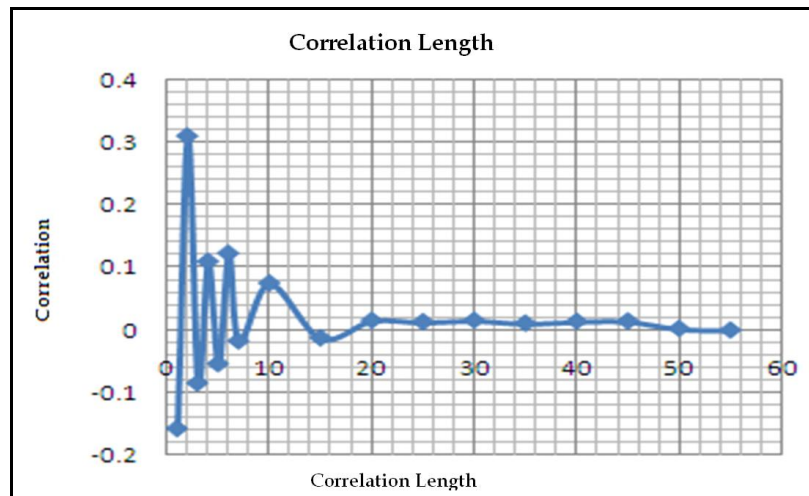


Fig. 3.4: Correlation Length

For our Pareto, the shape which is the mean value was obtained from the correlation length of the trace and the mean value of the interarrival time. The correlation curve is shown in Fig. 3.4. Correlations show a predictive relationship in a sequence of data [RyE196]. Figure 3.4 shows

that our frames are correlated since actions are correlated, however, as one can see, there is not much correlation beyond a length of 20 seconds, consequently, our correlation length is visually chosen for simplicity.

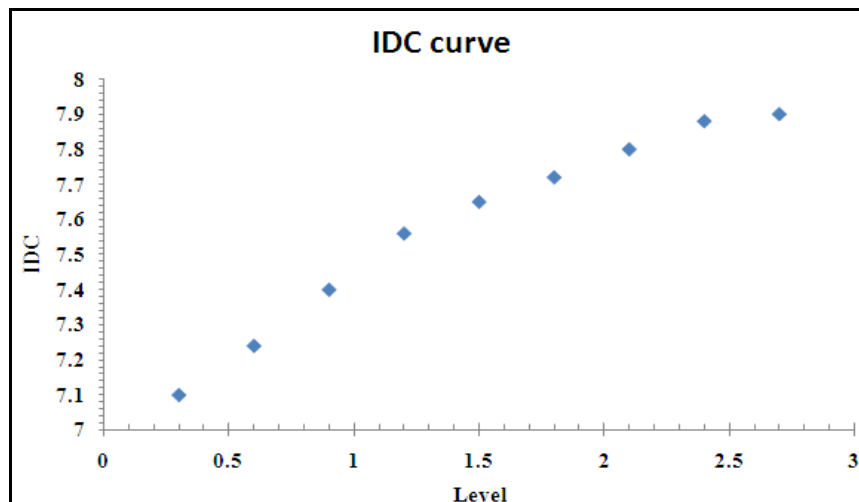


Fig 3.5: Entire Trace IDC curve

The location parameter, α , of the Pareto distribution is related to the Hurst parameter as shown in Equation 1 below. The slope of the IDC (Index of Dispersion for Count – ratio of variance for levels of time aggregation) curve (Fig. 3.5) gives the Hurst parameter from Equation 2. As shown from the curve, the Fractal effect calms down, but does not disappear, for this reason we call it persistent Hurst phenomenon [MeLe96].

$$H = \frac{1}{2} \left(\alpha - 1 \right) \quad (3.1)$$

$$H = \frac{1}{2} \left(+ slope \right) \quad (3.2)$$

When video is compressed with little loss of information, the peak to average ratio decreases, but the correlation increases, and the total uncertainty remains the constant. The Hurst parameter can be used to reflect this invariance phenomenon of entropy conservation property [HoPa01]. Since our video is highly compressed but still preserves the original entropy of the information, we use the Hurst parameter to accurately capture this invariance. On the other hand, an exponential distribution was used to model the mean off time, which represents the time between each action scene. This distribution was chosen with the observation that the action scene sequence is relatively memoryless. Table 3.1 shows a summary of each mini Pareto source and its characterization values.

Table 3.1: Mini Sources with Characterisation Values.

Bins	Mean Off-Time (ms)	Mean On-Time (ms)	Frame Duration (ms)	Packet Size (Bytes)
mini1	7531	195	8	125
mini2	20603	453	18	290
mini3	6911	702	28	450
mini4	5515	960	38	615
mini5	7800	1216	32	779
mini6	10400	1472	39	943
mini7	18200	1723	46	1104
mini8	27300	1984	53	1272
mini9	10400	2232	59	1430

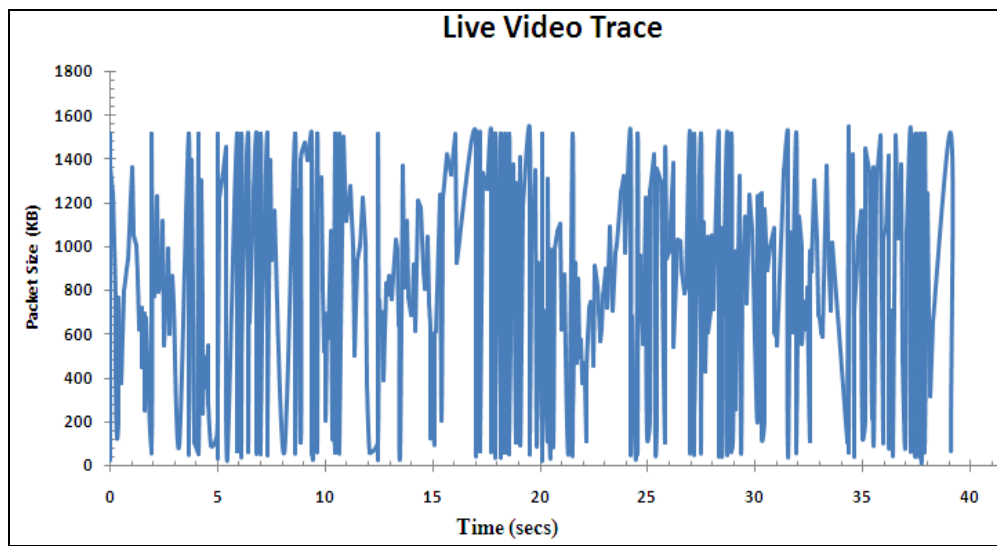


Fig. 3.6 Live Video Trace

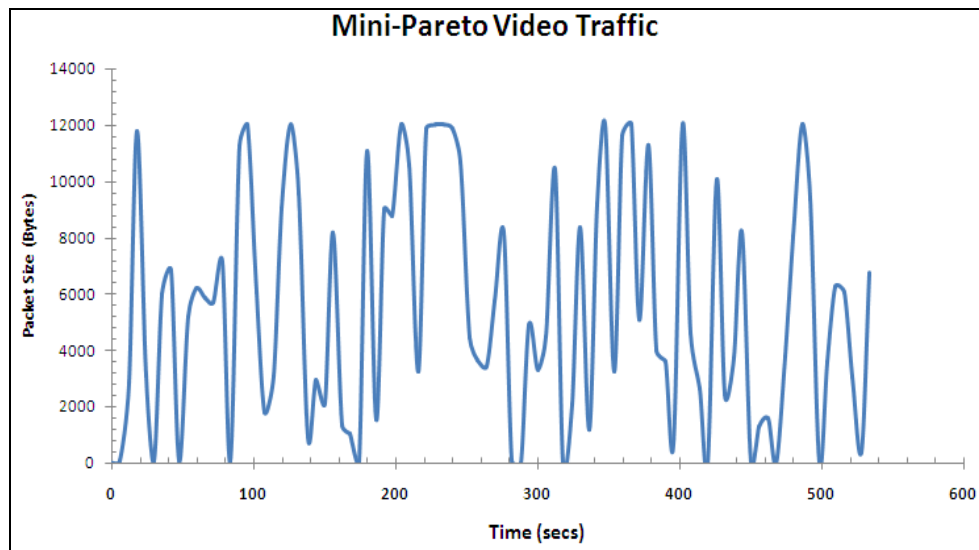


Fig 3.7 Mini- Pareto Video Traffic

Figures 3.6 and 3.7 show the live video trace and the generated mini-pareto video traffic respectively. Although not exactly the same, the simulated traffic appears to capture the randomness of the live video traffic.

3.3 Simulation Environment

As discussed earlier, OPNET was found to be a better platform that can help to integrate a complete communication tier node with a robust VANET mobility model. OPNET can provide a platform to create and test an analytic and practical video model and can also provide the ability to integrate the model into a VANET environment.

Table 3.2: Simulation Parameters

Parameter	Value
Physical layer	IEEE802.16e (WiMax)
Data rate	10Mbps
BS TX power	5 W
MS Tx power	1 W
Antenna type	Omni-directional
BS antenna gain	15dBi
MS antenna gain	9dBi
Link bandwidth	20MHz
Modulation scheme	16-QAM
Path loss parameter	vehicular environment
Number of vehicles	10
Mobility model	VanetMobiSim
Number of RSU's	2
Simulated time	3600secs
Seeds	127
Terrain dimensions	1300X1250m

The simulation parameters for each scenario is shown in Table 3.2, in places where parameters were changed for specific purposes, it will be indicated and discussed. Each simulation was simulated for a simulation time of 3600secs. The terrain dimensions vary slightly from scenario to scenario. They are an average of 1300 X 1250 m in area. The relative (x, y) position on the terrain is used to integrate the VANET mobility model trajectories and obtain the initial positions of the vehicles. Vehicular environment for the path loss parameter is modelled according to the description in the ‘Radio Tx Technologies for IMT2000’ white paper of the ITU [ITUR97]. The shadow fading standard deviation was set to 10dB. The mobility pattern (trajectory) during the simulation is predefined using the *VanetMobiSim* discussed in Section 2.2.1.1. The trajectories

vary from scenario to scenario and will be discussed accordingly.

3.4 Simulation Scenarios

We choose to simulate four scenarios: downtown scenario, highway scenario, residential area scenario and school zone scenario. Our goal was to study different geographic areas with varying traffic congestion (density), varying wireless interference and varying traffic speed limit.

We discuss below the specifications of model components in each scenario. In general, each scenario consists of N mobile nodes (vehicle - MS) and two Base Stations (BS) to cover the geographical area represented.



Fig. 3.8: Downtown Scenario

3.4.1 Downtown Scenario

Fig. 3.8 depicts the scenario used to simulate the city center with clusters of cars, a number of intersections with stop signs and traffic lights. The maximum speed in this scenario is 40km/hr. The trajectory (shown with the white lines in Fig. 3.8) for this scenario was generated from the *VanetMobiSim* with 9 traffic lights and stop signs at the other intersections.

3.4.2 Residential Scenario

This scenario was used to simulate residential areas where cars are sparsely populated. The maximum speed in this scenario is 40km/hr. A real residential map of Sulzbach in Germany was

used to generate the trajectory (shown by the white lines in Fig. 3.9) in this scenario due to its availability in the format required (GDF – Geographic Data Format) as shown in Fig. 3.9.

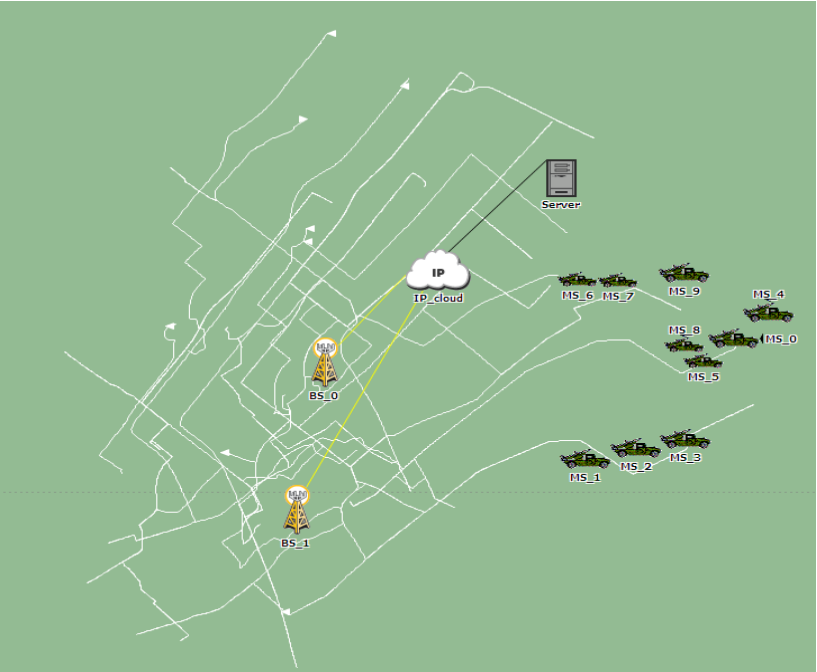


Fig. 3.9: Residential Scenario

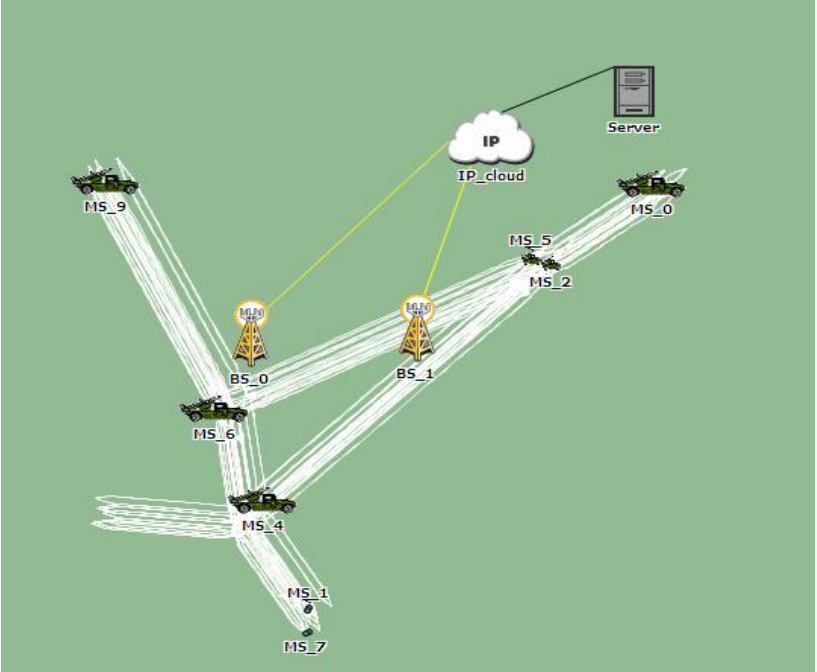


Fig. 3.10: Highway Scenario

3.4.3 Highway Scenario

This scenario was used to simulate the highway with a minimum speed of 60km/hr and a

maximum speed of 100km/hr. In the trajectory of this scenario, the maximum number of traffic lights is one, just before the cars enter the highway. Fig. 3.10 shows this scenario with the trajectory represented by the white lines shown.

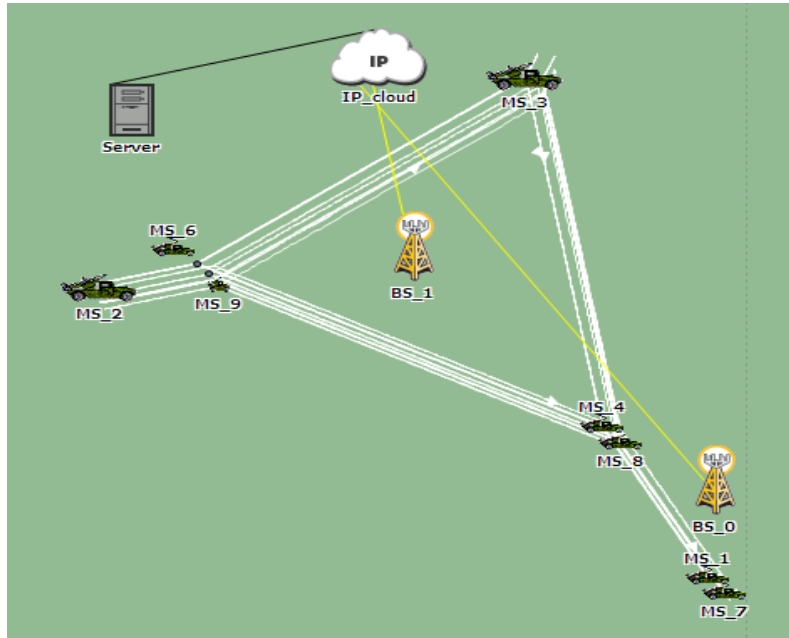


Fig. 3.11: School zone Scenario

3.4.4 School Zone Scenario

This scenario was used to simulate a school zone with lots of stop signs and obstructions that can let children safely cross the road. The maximum speed in this scenario is 30km/hr. The trajectory in this scenario was generated using specific formatting in *VanetMobiSim*. Fig. 3.11 show a screen shot of this scenario.

Table 3.3: Scenario Summary

	Pathloss	Traffic congestion	Speed Limit
Highway Scenario	Free space	Congested	100km/hr
School Zone Scenario	Type B	Sparsely congested	30km/hr
Residential Area Scenario	Type C	Very Sparsely congested	40km/hr
Downtown Scenario	Type A	Very congested	40km/hr

In summary, Table 3.3 shows the different scenarios and the major differences in terms of wireless interference configuration, traffic congestion density and speed limit. We use path loss

models already configured in OPNET to represent the different wireless interference configurations. The “Free Space” path loss refers to the classical free space path loss, “Type A” represents a hilly terrain with moderate-to-heavy tree densities, “Type C” represents mostly flat terrain with light tree densities and ‘Type B’ is a compromise between Types A and C [ErGr99].

3.5 Performance Measures

This section defines the performance measures used in the project to evaluate different behaviours in our simulation.

i) End to End Delay

We define end-to-end delay (in seconds) to be the time duration from the instant when a packet arrives at the source node (safety cameras on board car) until the time it is received at the destination node. This performance measure presents a wholistic view of the time components in video capture, encoding and network delay before an end user visualises the images received. In real-time traffic, this parameter is very critical as it shows how ‘current’ the information at the end user (e.g., a law enforcement officer) is. Since we track this at the application layer, the end-to-end delay also takes into account compression delay and all other delays incurred along the communication path and system.

ii) Jitter

Jitter is defined to be the variation of delay between consecutive packets. If two consecutive packets leave the source node with time stamps $t1$ and $t2$ and arrive at the destination at time $t3$ and $t4$ after reassembly and play back, then the jitter will be represented by equation 4.

$$\text{Jitter} = (t4 - t3) - (t2 - t1) \quad (3.3)$$

Negative jitter means that the packets were received in different time range i.e $(t4 - t3) < (t2 - t1)$

iii) Visual MOS Rating

This is a subjective parameter that measures the quality of video received by the server, judging the end-user experience. This measure was borrowed from the same parameter used to measure the MOS (Mean Opinion Score) in voice. The calculations follow the definition given by the ITU-T recommendation G.107 which is presented in Equation 3 [MeJa05].

$$R = R_o - I_s - I_d - I_e + A \quad , \quad (3.4)$$

where R represents a factor that has the value of between 0 to 100, with 100 representing the best quality and 0 the worst quality; R_o is the SNR (Signal to Noise Ratio), I_s is the simultaneous impairment factor, I_d represents impairment caused by delay, I_e is the equipment impairment factor as a result of low-bit codecs and packet loss and A is the advantage factor that compensates for the loss caused by other factors.

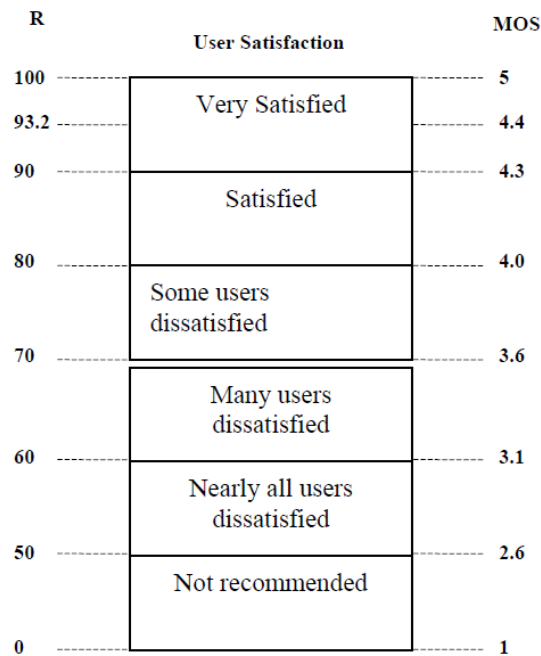


Fig. 3.12: MOS and R-Factor Scale [MeJa05]

R is then matched to the MOS value by the scale shown in Fig.3.12. In our simulation tool, MOS is calculated using the delay, packet loss and jitter, hence, we can relate this to our video traffic. To customize this parameter for video use however, we created a testbed case with all the ‘ideal’ conditions, that is, one car to one base-station implying more than sufficient bandwidth, hence keeping R as high as possible simulation wise. Having done this, our Visual MOS value was 3.6, invariably, 3.6 will represent our best visual experience and 1 the worst visual experience.

iv) Buffer Overflow Percentage

This measure shows the fraction of time for which arriving packets find the buffer at the SS station full. This measure implicitly reflects the percentage of time video packets are lost due to buffer overflow.

Chapter 4

Performance Evaluation of Downtown and School zone Scenarios

This chapter evaluates the performance of sending video over a WiMAX VANET under the Downtown and School zone scenarios (Ref: Section 3.4). Performance measures such as end-to-end delay, jitter and MOS Value will be evaluated and discussed for each scenario. Two network sizes are evaluated: a small network consisting of 10 cars and 2 RSU's and a larger network of 30 cars and 2 RSU's. This was done to evaluate the scalability of our explicit control algorithm. After 10 secs into the simulation, the WiMAX bandwidth is observed to vary from 125 kHz to 20MHz (due to the adaptive modulation used as specified in Table 3.2). At the same time, we observe the video bandwidth also varies randomly with a peak of about 200 kbps and with an average of about 50 kbps at the Subscriber Station. With this peak to average ratio of 6dB, we observe congestion occurs often in our simulation.

4.1 Small Network

We study a network of 10 cars and 2 RSU's. Each car in this network has a maximum sustainable traffic rate of 384Kbps except where otherwise stated. The link between the RSU and the backhaul network was a DS3 link with a capacity of 44.736Mbps as shown in Fig. 2.1. The buffer size at each SS was set to 256KB except where otherwise stated. The simulation was run for 60mins simulated time and the number of packets generated per node is about 10,000.

4.1.1 Downtown Scenario

The downtown scenario was used to simulate an area with a cluster of cars. In this scenario, a mobility model with high traffic density was used to simulate the typical downtown area of most cities. The maximum speed of cars in this scenario is 40km/hr to simulate a traffic congested area. The other specifics of this scenario is shown in Table 3.3 and discussed in Section 3.4. The end-to-end delay of packets, the jitter and the MOS value are evaluated.

4.1.1.1 Time Evolution Performance

We presented the instantaneous values of end-to-end delay, the visual MOS and the queue length as time evolves. These results can be used to evaluate the effectiveness of the controller

algorithm implemented. It is important to evaluate the time evolution performance as this shows instantaneous behaviour and caters for our real-time application and visual experience.

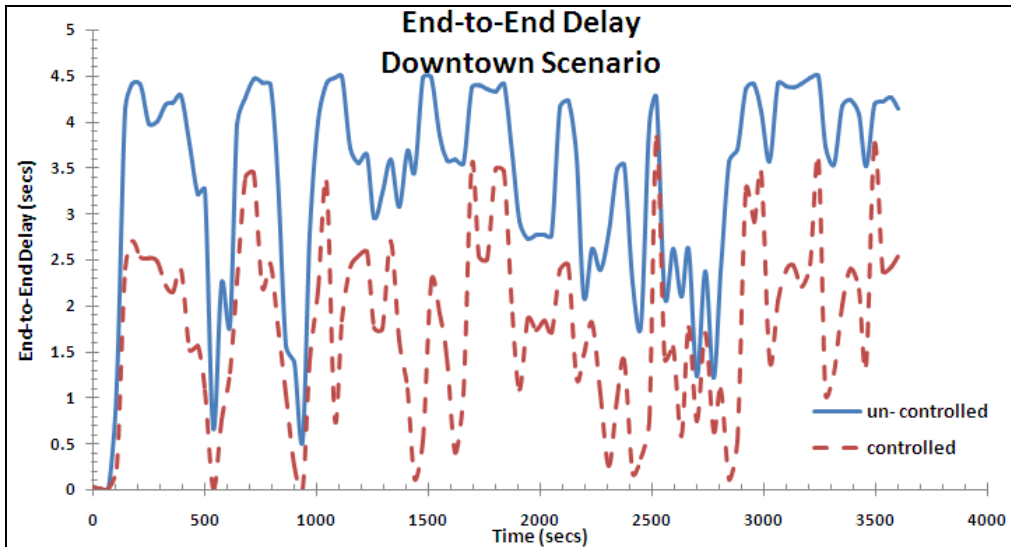


Fig 4.1: End-to-end Delay for Downtown Scenario

The curve shown in Fig. 4.1 shows the end-to-end delay of a node in the VANET network. There are two lines shown on the graph; the thick line represents the end-to-end delay of the video packets at a node without implementing the controller algorithm while the dotted line shows the end-to-end delay of the video packets running the controller algorithm. It can be seen that the end-to-end delay is reduced. For this scenario, the controller is triggered once the end-to-end delay is greater than 0.1secs. The threshold of 0.1secs was chosen from among many simulation runs of different threshold values. Taking a close look at Fig. 4.1, there are many fluctuations in the end-to-end delay which is not desirable by the user. The controller is seen to reduce the end-to-end delay but not regulate the fluctuations, as this was not the focus at this stage.

Fig. 4.2 shows the visual MOS value of the downtown scenario. In this case, we can see that the controller has a negative effect on the visual experience as seen by the user. “Negative” in this context is defined from our end-user survey experience.

It is known that the user would rather have a low quality video streaming as opposed to a fluctuation between low and high quality. Since the end-to-end delay is reduced as a result of the controller, the quality of the video received by the user increases, however, it does not maintain this increase. A fluctuation occurs between low quality and high quality which is undesirable.

We also see the importance of regulating (keeping at a constant value), the instantaneous end-to-end delay. This will keep the quality of video as seen by the user constant.

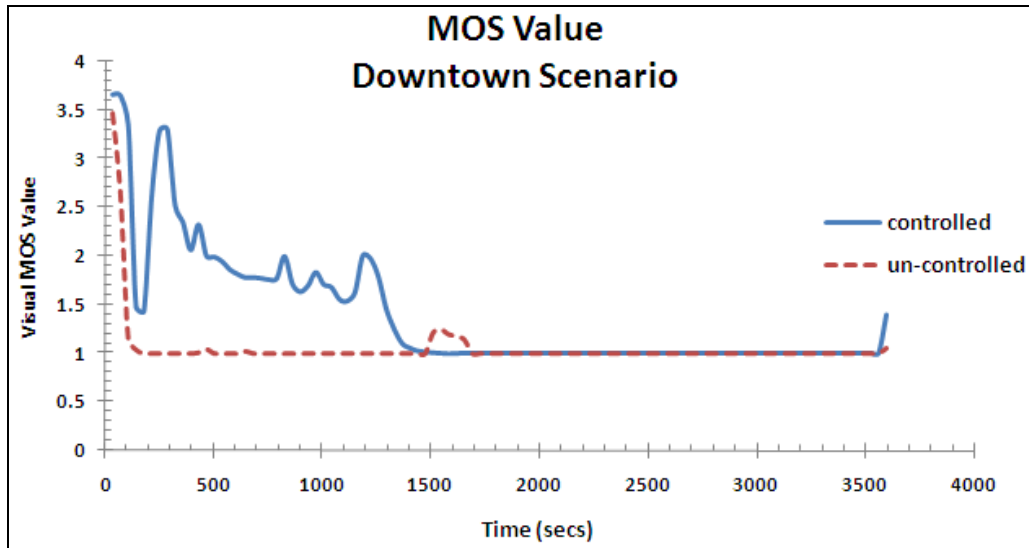


Fig 4.2: Visual MOS value curve for Downtown Scenario

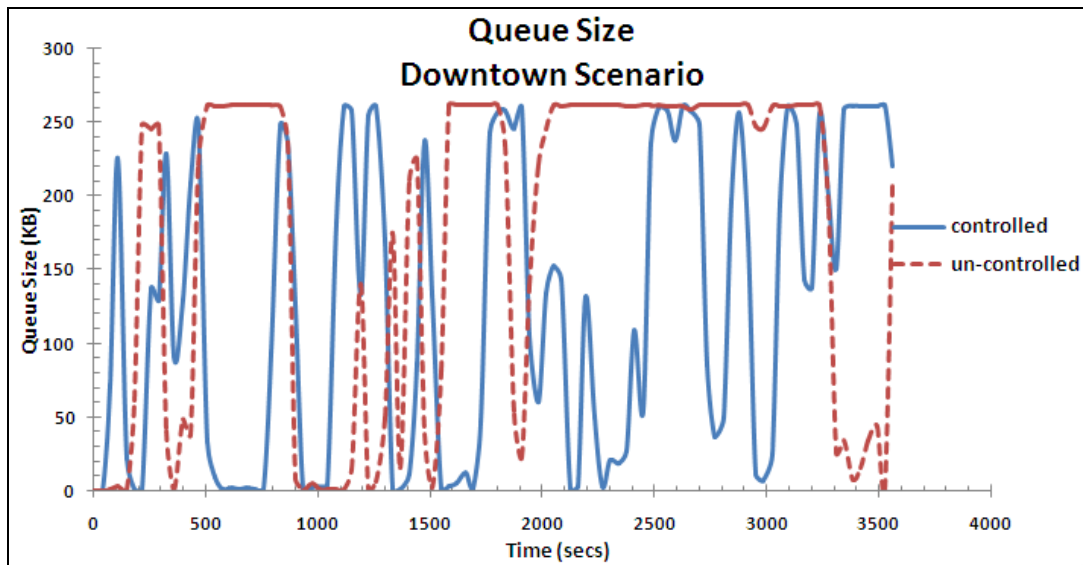


Fig 4.3: Instantaneous Queue Size for Downtown Scenario

The instantaneous queue size is shown in Fig. 4.3. The thick line represents the instantaneous queue size when the controller algorithm is implemented and the dotted line represents the instantaneous traffic when the algorithm is not implemented. The curves show a variation in queue size as the time elapse. It is shown that the thick line does not hit the maximum buffer size (256KB) as often as the dotted line hits the maximum buffer size. This

could be related to the percentage of time the buffer is full which in turn relates to the loss rate due to the buffer capacity. One can thus say that the controller reduces the loss rate due to buffer overflow from Fig. 4.3.

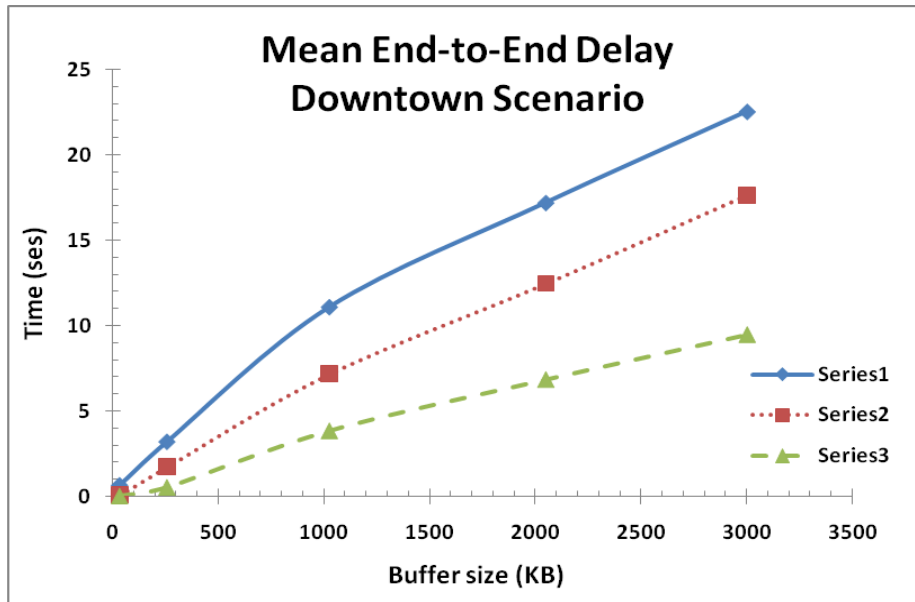


Fig 4.4: Mean End-to-End Delay for Downtown Scenario

4.1.1.2 Mean End-to-End Delay

Fig. 4.4 shows the mean end-to-end delay performance for the Downtown Scenario at different sustainable traffic rates as the buffer size at the SS increases. The curve shown is a linearly increasing function with a positive slope. At a data rate of 384kbps, the end-to-end delay increases averagely with a constant slope. As the buffer size increases, the slope of the curve decreases. A similar behaviour is seen for data rates of 0.5Mbps and 1Mbps except that mean end-to-end delay is reduced as a result of increase in the service rate. This is expected as the mean end-to-end delay is proportional to the buffer size for a traffic characterised by Pareto distribution. It is also important to note that since the protocol used is UDP/RTP, once the video packets find the buffer full, the packets are discarded and there is no re-transmission.

4.1.1.3 Buffer Overflow Percentage

Fig. 4.5 shows the percentage of buffer saturation measured over a period of time against the buffer size at different service rates. The curve shown is a linear curve with a negative slope. As expected, as the buffer size increases, keeping the service rate at a constant, the percentage of

time for which arriving video packets find the buffer full decreases. This in turn implies that as one increases the buffer size, the loss rate reduces and the end-to-end delay increases. The trade-off between these two parameters is discussed in Chapter 6.

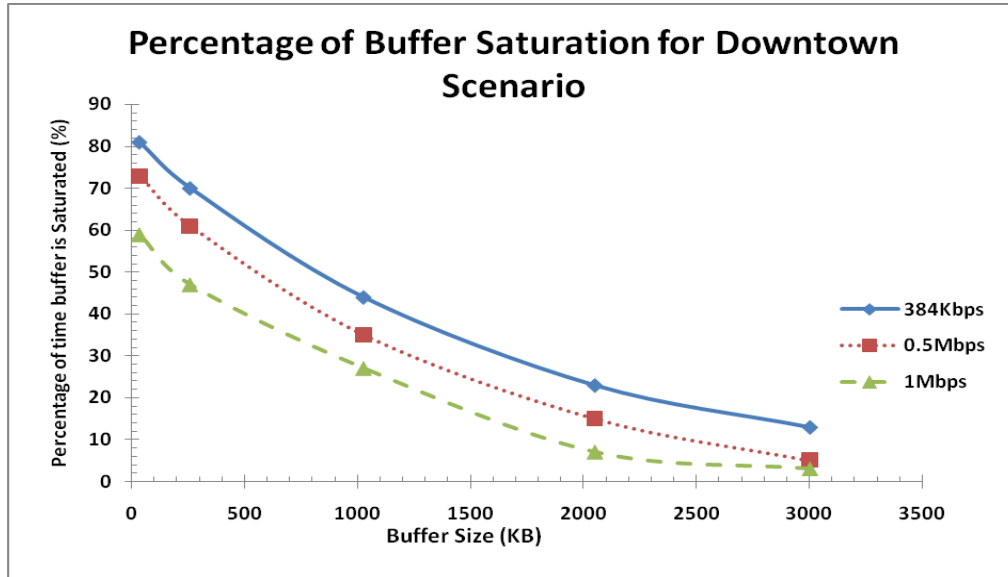


Fig 4.5: Percentage of Buffer Saturation Performance Curve for Downtown Scenario

4.1.2 School Zone Scenario

The School zone scenario was used to simulate a semi-populated area with stop-signs and a speed limit of 30km/hr. In this scenario, a mobility model with clusters was used to generate the trajectory for each node. The clusters are programmed to populate the scenario at random times during the simulation process to mimic the behaviour of a School zone environment. The path loss model to be applied to signals being received at the WiMAX MAC in this scenario was the "Vehicular Environment" model as described in the "Radio Tx Technologies for IMT2000" white paper of the ITU already developed by OPNET [ITUR97]. The shadow fading standard deviation is set to 10dB. The end-to-end delay of packets and the MOS value is examined after running the simulation for 60mins simulation time. Apart from the above parameter values, other common values can be found in Section 3.4 and Table 3.3

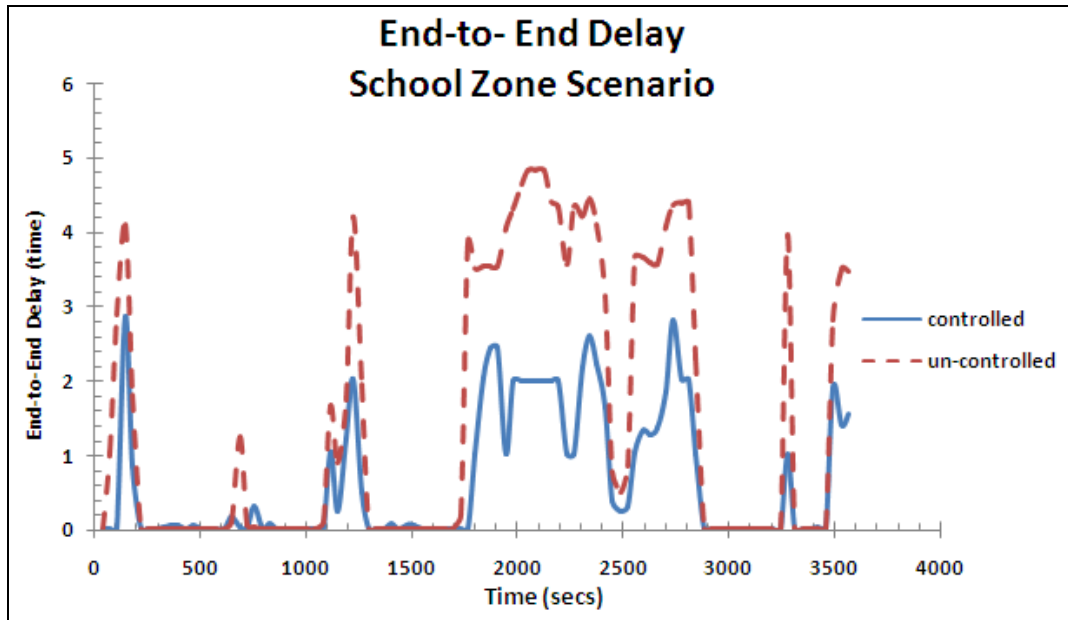


Fig. 4.6: End-to-End Delay for School Zone Scenario

4.1.2.1 Time Evolution Performance

The controller sensitivity for this scenario was set to 0.1secs i.e., once the end-to-end delay reaches a mark of 0.1secs, the controller is triggered. From Fig. 4.6, the controller is seen to come into effect once the threshold end-to-end delay is attained. The school zone scenario is not as busy in terms of traffic as the downtown scenario so the controller is not busy most of the time. It can be observed from the results that the speed is minimal in this case; only interference causes a greater portion of the delay unlike the Highway scenario where speed is a greater factor. The peaks in the curve occur as a result of high traffic volume during certain moments in this scenario. Unlike the downtown scenario where the traffic is highly populated most of the time, this scenario only have few highly populated areas. This explains the peaks in the end-to-end delay from time to time.

Fig. 4.7 shows the MOS value for the school zone scenario The MOS value is seen to increase at certain points which correspond to the points where the end to end delay reduces. This is a negative effect as discussed earlier as the user will rather have a constant quality of video (either high resolution or low resolution), than having the quality fluctuating between high and low resolution.

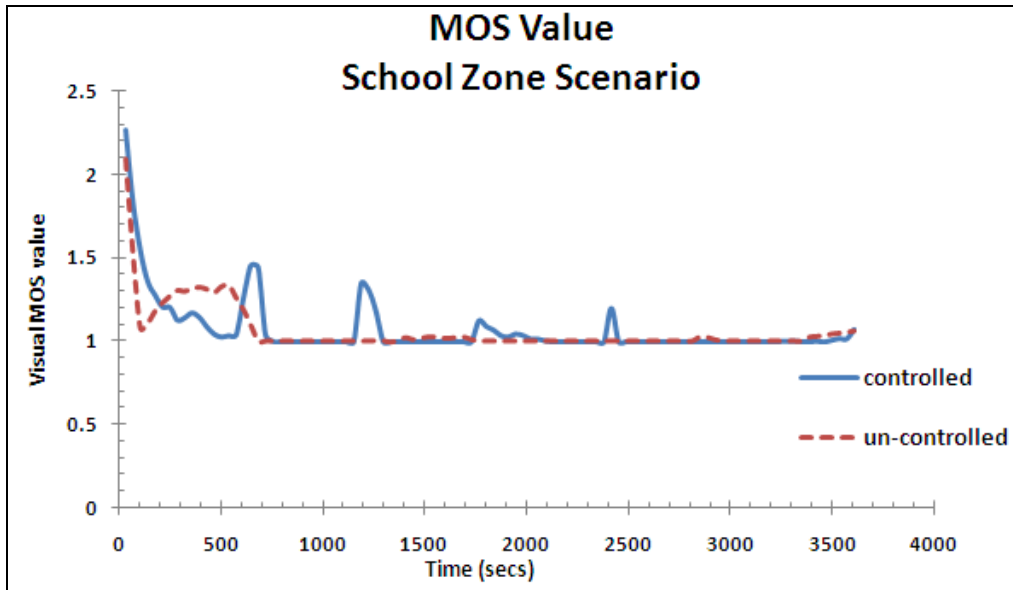


Fig. 4.7: MOS value for School Zone Scenario

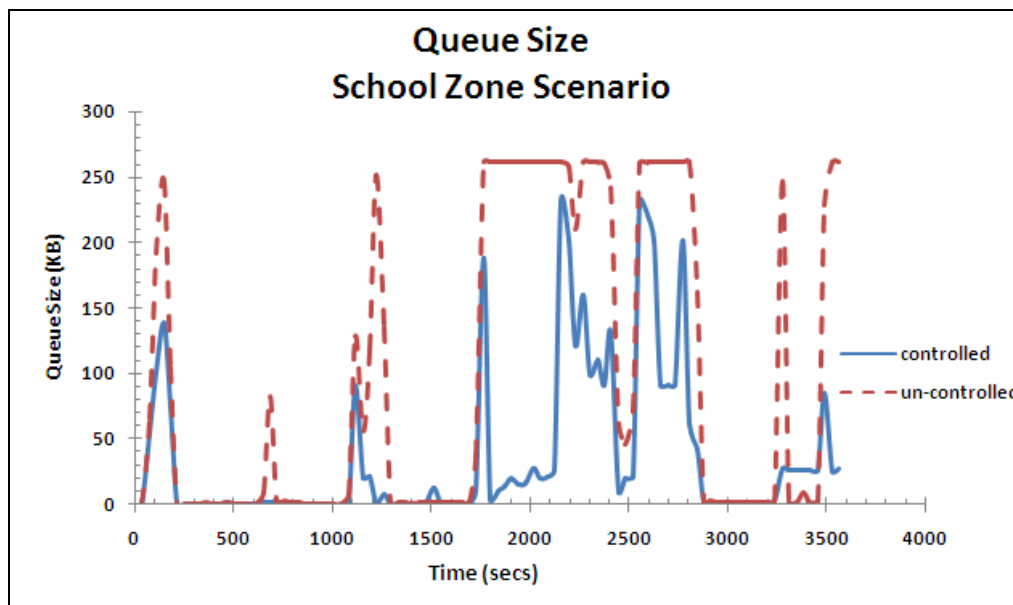


Fig. 4.8: Instantaneous Queue Size for School Zone Scenario

Fig. 4.8 shows the instantaneous queue size for the School Zone Scenario. The dotted line shows the queue size of the un-controlled traffic and the thick line shows the instantaneous queue size of the controlled traffic. The queue size is seen to fluctuate at certain peaks. This corresponds to the behaviour shown in Fig. 4.6. The controller is seen to reduce the instantaneous queue size and invariably, reduces the end to end delay.

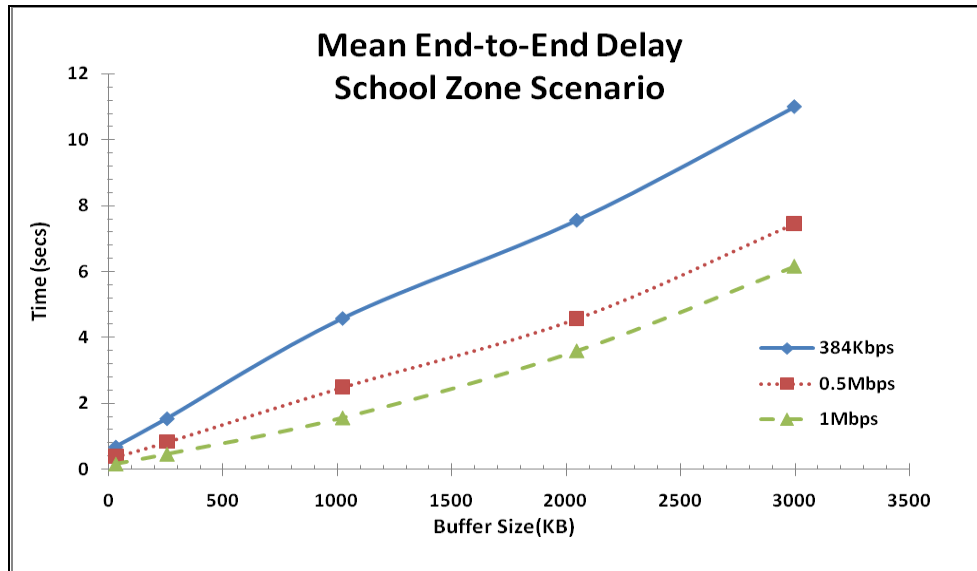


Fig. 4.9: Mean End-to-End Delay Performance for School Zone Scenario

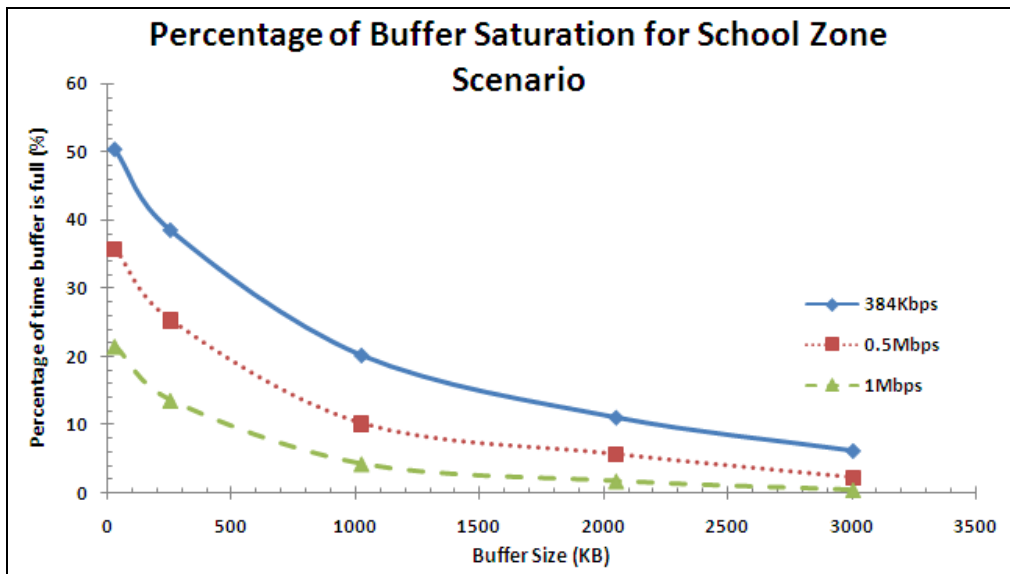


Fig. 4.10: Percentage of Buffer Saturation Performance for School Zone Scenario

4.1.2.2 Mean End-to-End Delay

Fig. 4.9 shows the mean end-to-end delay performance as it varies with different buffer sizes and service rates. The mean end-to-end delay is seen to increase as the buffer size increases and decrease as the service rate increases. The curve is a linearly increasing curve with a positive slope. This corresponds with the behaviour of a traffic that follows the Pareto distribution. The difference in the mean end-to-end delay for the service rates of 0.5Mbps and 1Mbps is not

substantial as compared with that of the Downtown Scenario. This is due to the fact that the school zone scenario has light traffic implying that the delay is caused by other factors different from the buffer capacity. These factors may include wireless interference from different sources or LOS.

4.1.2.3 Buffer Overflow Percentage

The percentage of buffer overflow is shown in Fig. 4.10. It is seen that at higher service rates the buffer does not saturate since the school zone scenario has lighter traffic as compared to the downtown scenario.

4.2 Large Network

In the large network, we study a network of 30 cars and 2 RSU's. Each car in this network has a maximum sustainable traffic rate of 384Kbps. The link between the RSU and the backhaul network was a DS3 link with a capacity of 44.736Mbps as shown in Fig. 2.1. As discussed earlier, this section studies the scalability of the controller algorithm implemented.

4.2.1 Downtown Scenario

The simulation conditions remain as explained in Section 4.1.1.

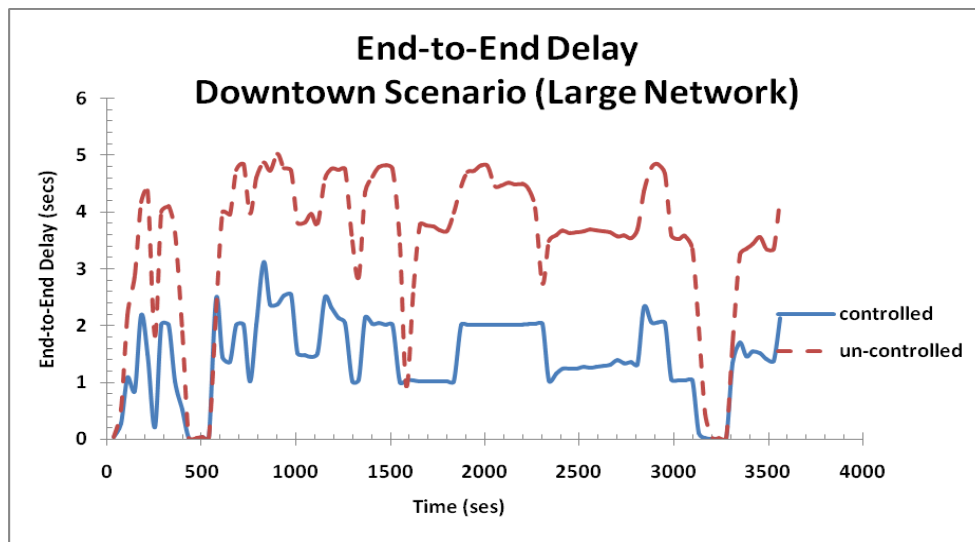


Fig. 4.11: End-to-end Delay for Downtown Scenario (Large Network)

4.2.1.1 Time Evolution Performance

The time evolution performance representation for the large network shows the same performance measures explained in Section 4.1.1.1.

The curve shown in Fig. 4.11 shows the time evolution of the end-to-end delay of a node in the large network. The thick line represents the controlled end-to-end delay while the dotted lines show the end to end-to-end delay without implementing the controller algorithm. The controller can be seen to be effective in this scenario. From the graph, the peaks in end-to-end delay could be accounted for by the traffic congestion that occurs in the downtown scenario as explained in the Section 4.1.1.1. The behaviour is also similar to Fig. 4.1 except that the end to end delay values are higher in this case due to the increase in network size. The controller sensitivity was set to 0.1secs and the controller is seen to be active majority of the time.

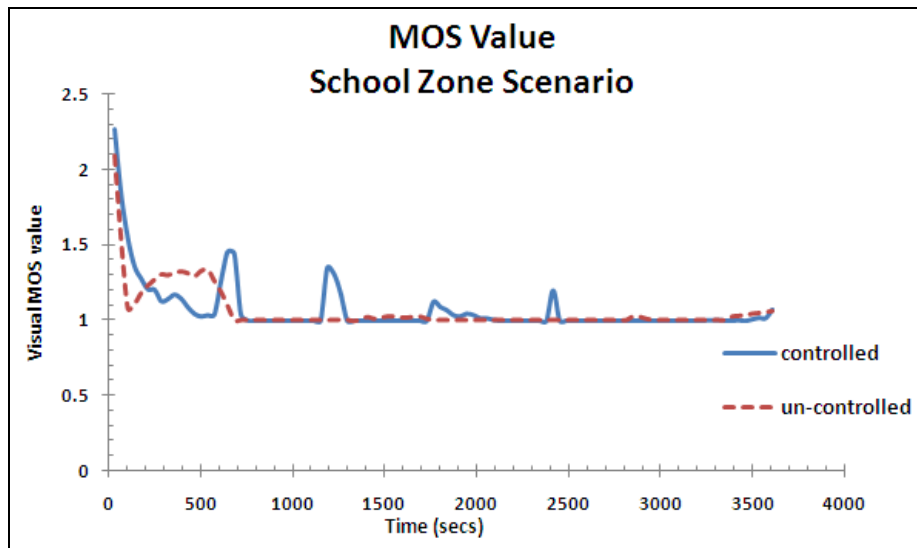


Fig 4.12: MOS value curve for Downtown Scenario (Large Network)

Fig 4.12 shows the MOS value for the downtown scenario in the large network. The effect of the controller is seen here to be negative, as it causes a fluctuation in the quality of video as seen by the user. This behaviour corresponds with the end-to-end delay results shown in Fig. 4.11.

Fig 4.13 shows the instantaneous Queue Size for the Downtown Scenario for the large network. The thick line shows the instantaneous queue size for the controlled traffic while the dotted line shows the instantaneous queue size for the un-controlled traffic. The buffer size is seen to reach its peak majority of the time in the un-controlled traffic. The controller is also seen

to reduce the times in which the queue size reaches its peak but does not eradicate it. This implies that the controller does not eradicate packet loss. As mentioned earlier, in real time traffic, packet loss is not of major concern; instead, packet delay poses greater concern.

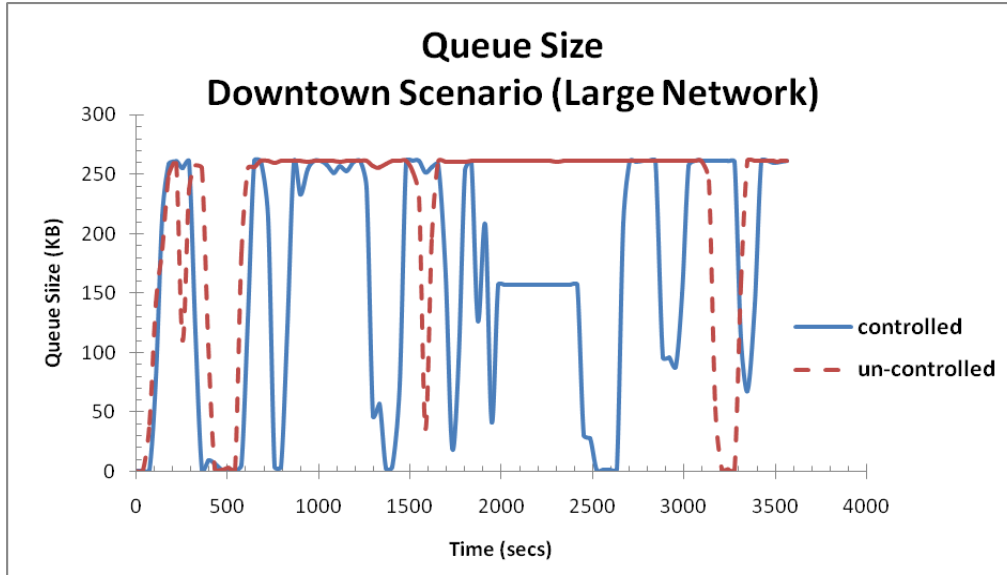


Fig 4.13: Instantaneous Queue Size for Downtown Scenario (Large Network)

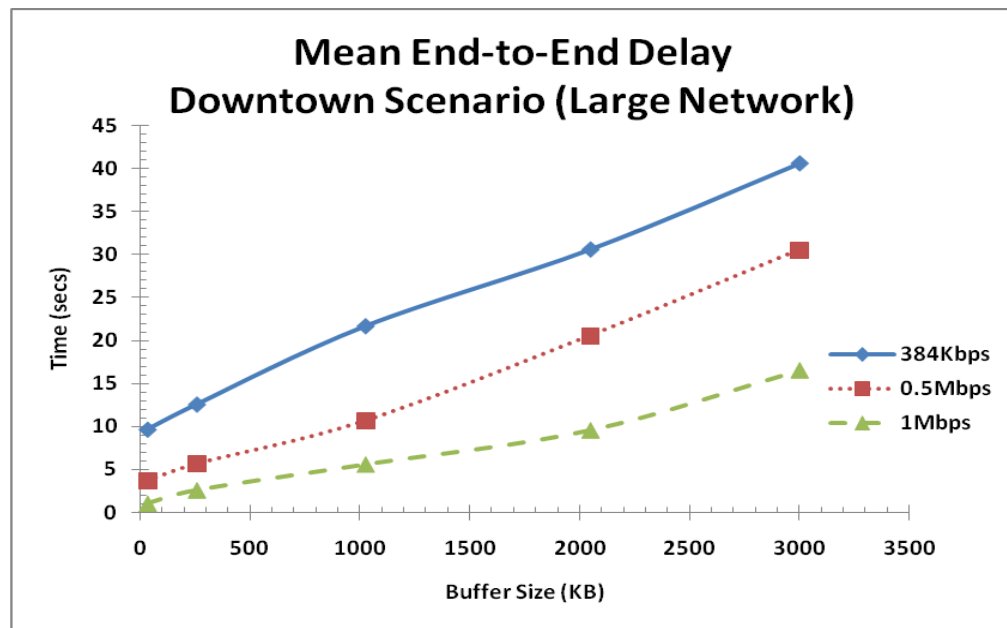


Fig. 4.14: Mean End-to-End Delay Performance Curve for Downtown Scenario (Large Network)

4.2.1.2 Mean End-to-End Delay

Fig 4.14 shows the mean end-to-end delay performance curve for downtown scenario in the large

network setup at different sustainable data rates. The buffer size is kept constant and the sustainable data rates are set to 384kbps, 0.5Mbps and 1Mbps. The behaviour is seen to be similar to what is shown in Fig. 4.4 except that the values are much higher in Fig 4.14 as expected since the traffic has increased in the larger network.

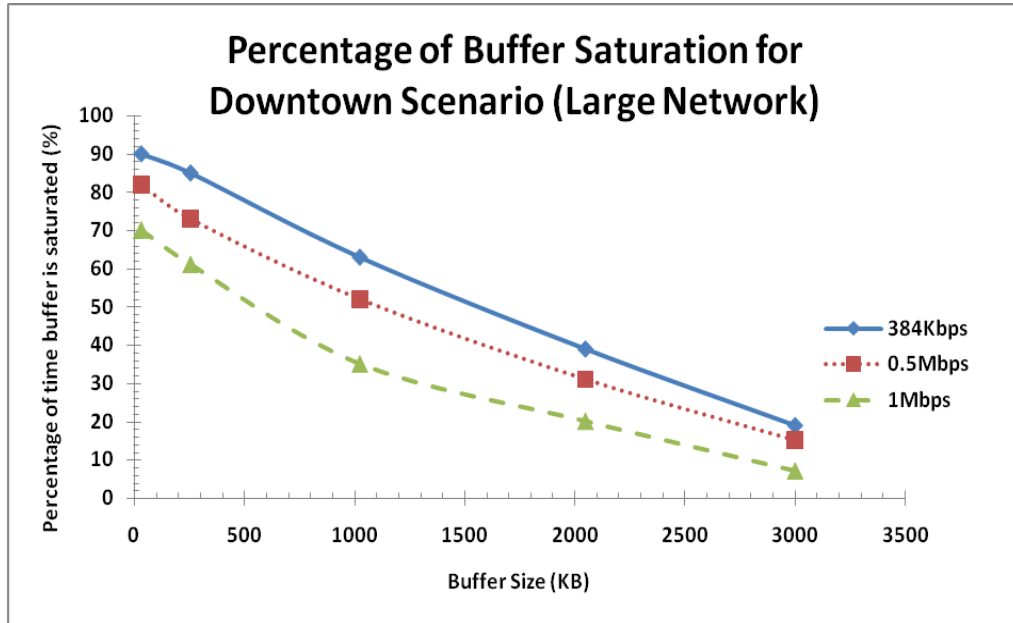


Fig. 4.15: Percentage of Buffer Saturation Performance Curve for Downtown Scenario (Large Network)

4.2.1.3 Buffer Overflow Percentage

Fig 4.15 shows the percentage of buffer saturation performance, which implicitly shows the loss due to buffer overflow. It is seen that as the buffer size and service rates increase, the percentage of time for which the buffer is full decreases. The loss rate gets larger as the scale of the network increases. More design guidelines will be discussed in Chapter 6.

4.2.2 School Zone Scenario

The simulation conditions remain as explained in Section 4.1.2.

4.2.2.1 Time Evolution Performance

Fig. 4.16 shows the end to end delay for the school zone scenario in the large network. The controller is seen to reduce the end to end delay. The behaviour is similar to what is seen in Fig 4.6 except that the end to end delay values are higher in this case. As discussed in Section

4.2.2.1, the cars in the School Zone Scenario has a maximum speed of 40km/hr, therefore, the speed is not a factor that affects end-to-end delay in this case – interference is more of a greater factor.

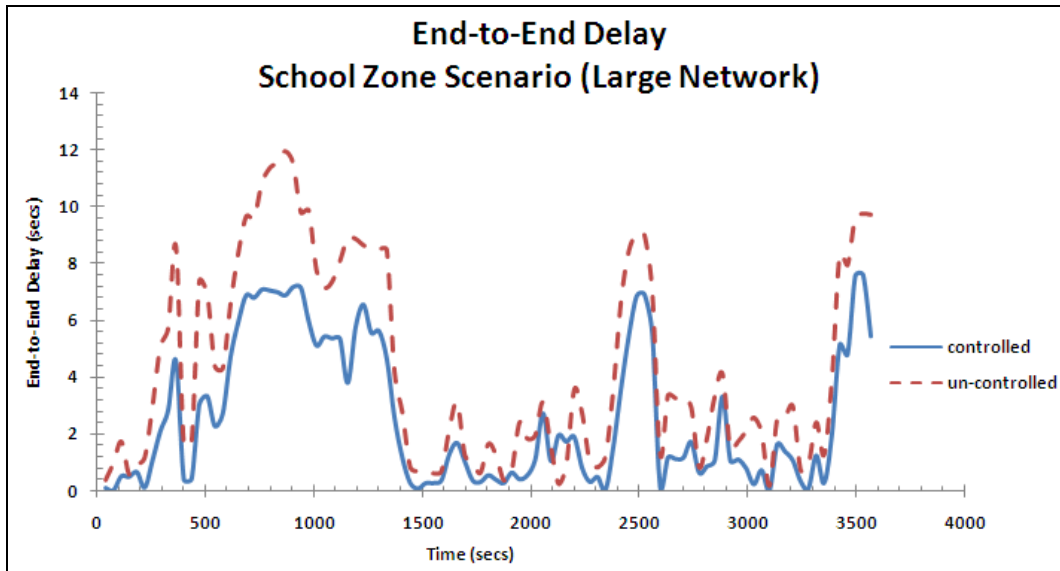


Fig. 4.16: End-to-End Delay for School Zone Scenario (Large Network)

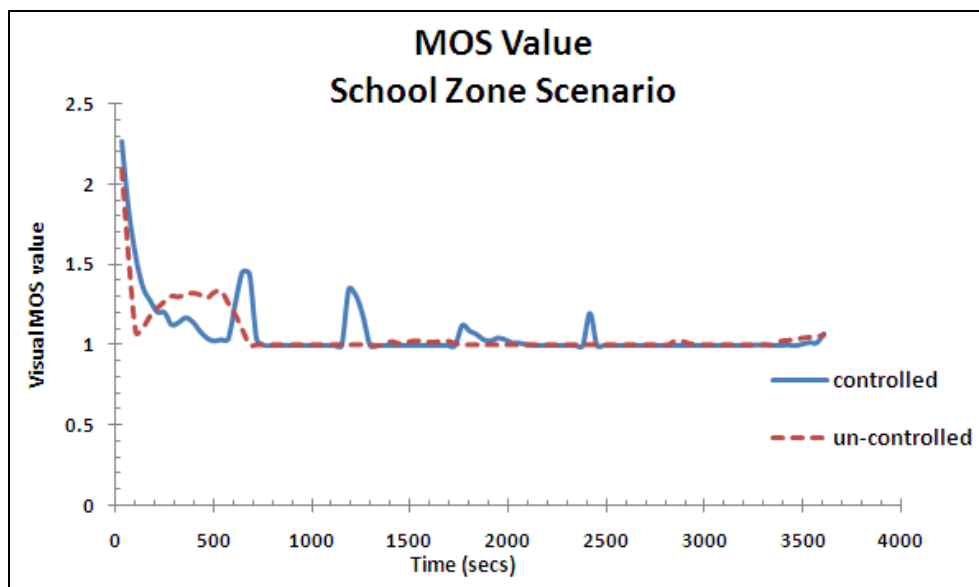


Fig. 4.17: MOS value for School Zone Scenario (Large Network)

Fig. 4.17 shows the MOS value for the School Zone Scenario for the large network. Although the MOS does not reach the peak value, the behaviour seen in Fig. 4.17 is more desirable since the MOS value remains at a constant value and does not keep fluctuating.

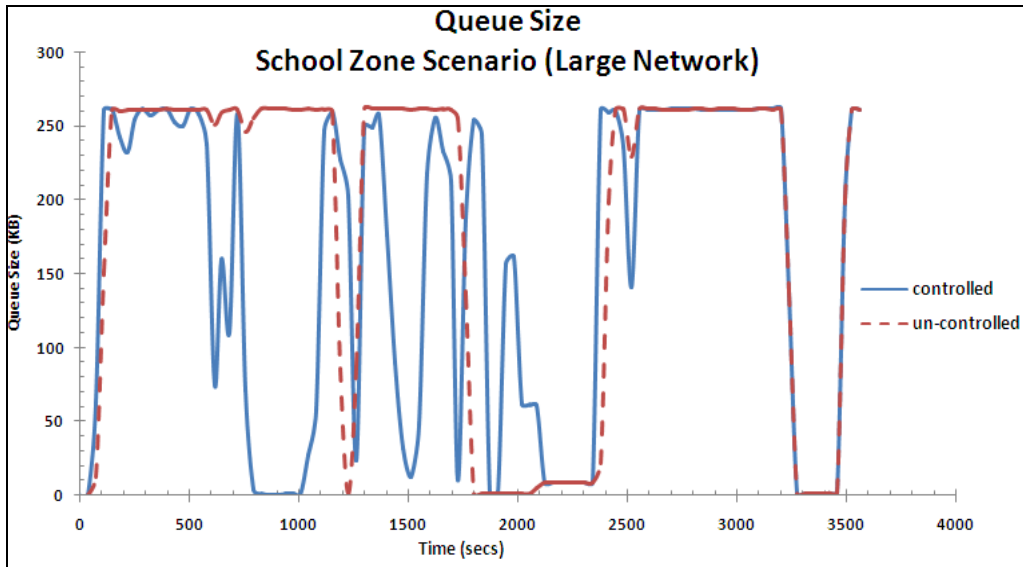


Fig. 4.18: Instantaneous Queue Size for School Zone Scenario (Large Network)

Fig. 4.18 shows the instantaneous queue size for the school zone scenario for the large network. The behaviour seen in this Figure is similar to what is found in Fig. 4.8 except that the queue is full most of the time in Fig. 4.18 due to the increase in the network size.

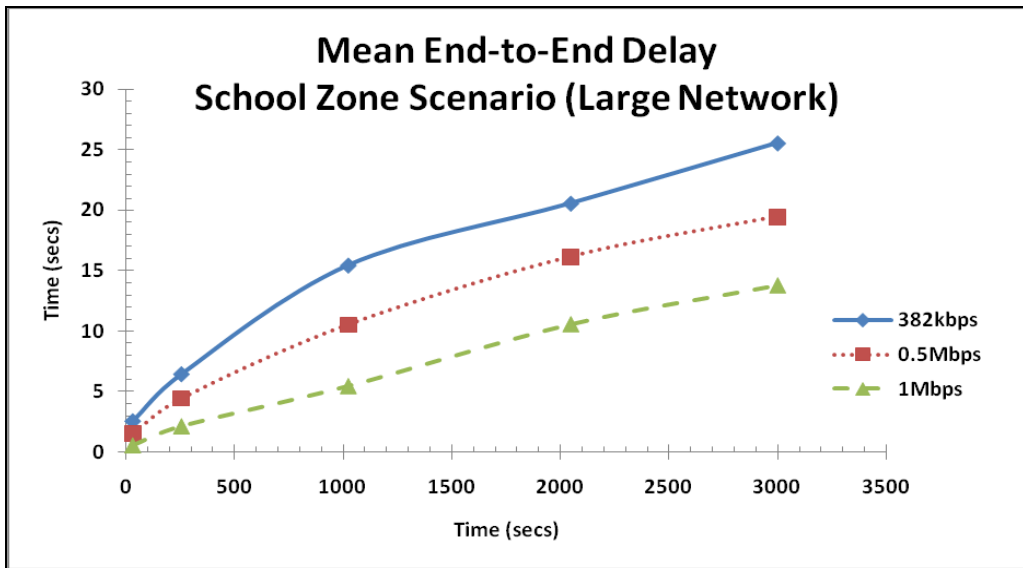


Fig. 4.19: Mean End-to-End Delay Performance for School Zone Scenario (Large Network)

4.2.2.2 Mean End-to-End Delay

Fig. 4.19 shows the mean end-to-end delay performance as it varies with different buffer sizes and service rates. The behaviour is as expected and similar to what was explained in Section 4.1.2.2. The end to end delay is however higher as there are more cars contending for the

available resources. Furthermore, as stated earlier, speed is not a factor in this scenario.

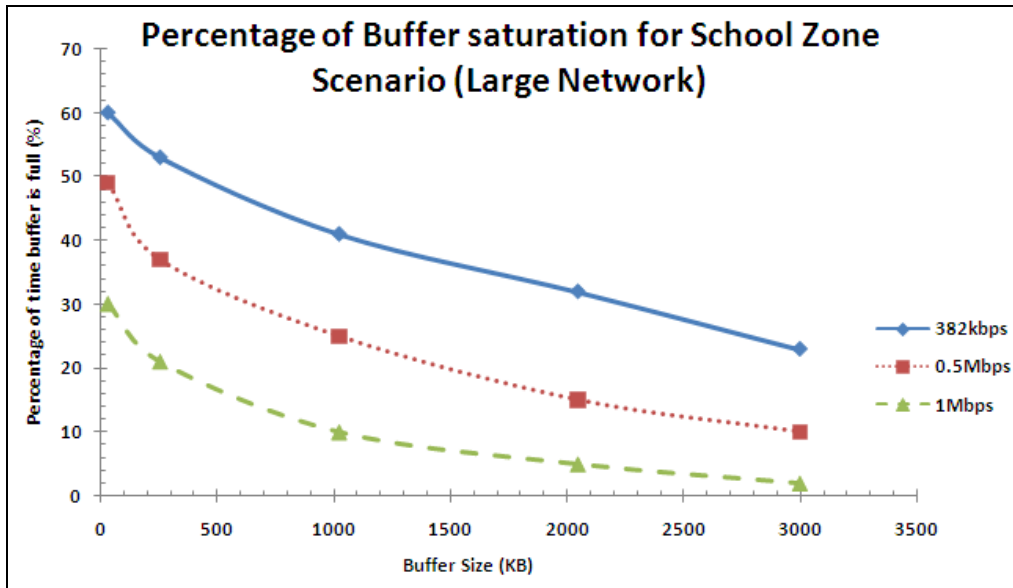


Fig 4.20: Percentage of Buffer Saturation Performance for School Zone Scenario (Large Network)

4.2.2.3 Buffer Overflow Percentage

The buffer overflow percentage for the School Zone Scenario is presented in Fig. 4.20. The behaviour is as expected – as the service rate increases, the percentage of times for which the buffer is saturated reduces.

Chapter 5

Performance Evaluation of Highway and Residential Area Scenario

This chapter evaluates the performance of sending video over a WiMax VANET under the Highway and Residential area scenarios (Ref: Section 3.4). Performance measures such as end-to-end delay, jitter and Visual MOS rating will be evaluated and discussed for each scenario. Two network sizes are evaluated: a small network consisting of 10 cars and 2 RSU's and a larger network of 30 cars and 2 RSU's. This was done to evaluate the scalability of our explicit congestion control algorithm. After 10 secs into the simulation, the WiMAX bandwidth is observed to vary from 125 kHz to 20MHz (due to the adaptive modulation used as specified in Table 3.2). At the same time, we observe the video bandwidth also varies randomly with a peak of about 200 kbps and with an average of about 50 kbps at the Subscriber Station. With this peak to average ratio of 6dB, we observe congestion occurs often in our simulation.

5.1 Small Network

This section discusses the highway and residential area scenario and the results obtained from simulating each scenario using a small network of 10 cars and 2 RSU's. Each car in this network has a maximum sustainable traffic rate of 384Kbps. The link between the RSU and the backhaul network was a DS3 link with a capacity of 44.736Mbps as shown in Fig. 2.1. The buffer size at each node was set to 258KB except where otherwise stated.

5.1.1 Highway Scenario

The Highway scenario simulates an area where cars move at high speed of 100km/hr. This scenario uses the parameters described in Section 3.3 and 3.4.3. Other specific conditions are shown in Table 3.3.

5.1.1.1 Time Evolution Performance

The highway scenario presents the most varying end-to-end delay results as seen in Fig. 5.1. This can be accounted for due to the speed of the vehicular nodes in this scenario and the wireless interference. The controller threshold was set to 0.1secs in order to keep the controller active

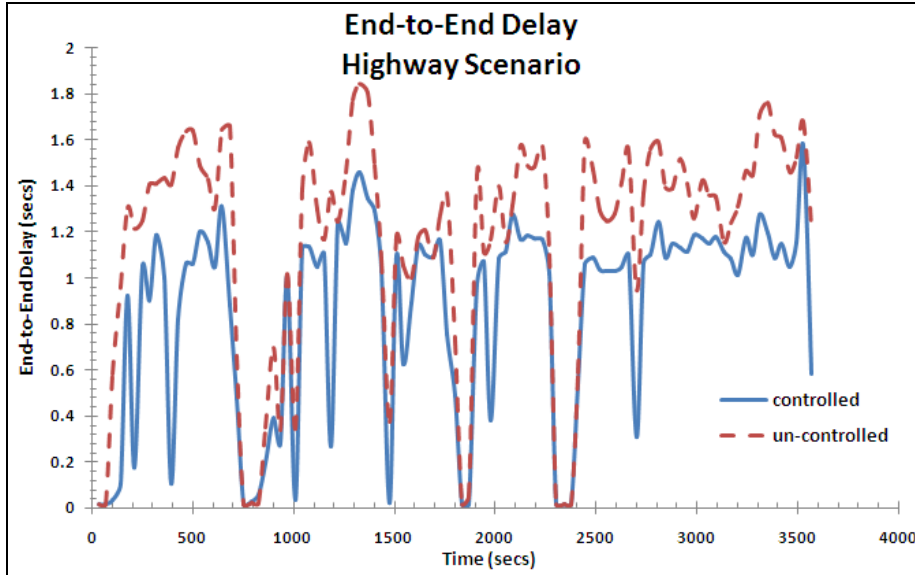


Fig. 5.1: End-to-end Delay for Highway Scenario.

majority of the time. From Fig. 5.1, one can see that the controller reduces the end to end delay but not to a substantially minimal point. This is due to the speed of the vehicles in this scenario; the controller is always active, there-by losing it effectiveness. One can also see the effect of the periodic feedback as some packets go ‘un-noticed.’

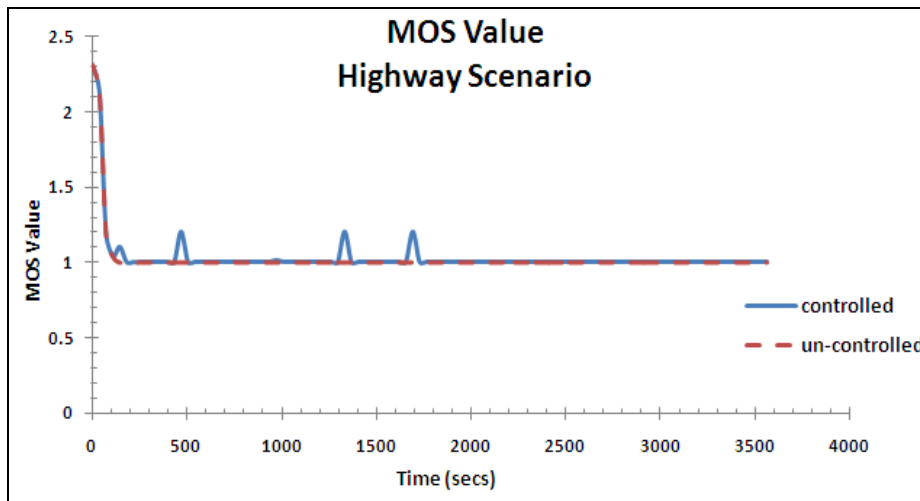


Fig. 5.2: MOS value for highway scenario.

MOS value for the highway scenario is shown in Fig. 5.2. The controller in this case tends to keep the visual experience at a constant rate. This can be explained by the range of variation in the end-to-end delay experienced in this scenario. Since the controller does not reduce the end to

end delay substantially, the effect is not seen on the users' visual experience in Fig 5.1. The fluctuations in end to end delay also contribute in lowering the quality of video seen by the user.

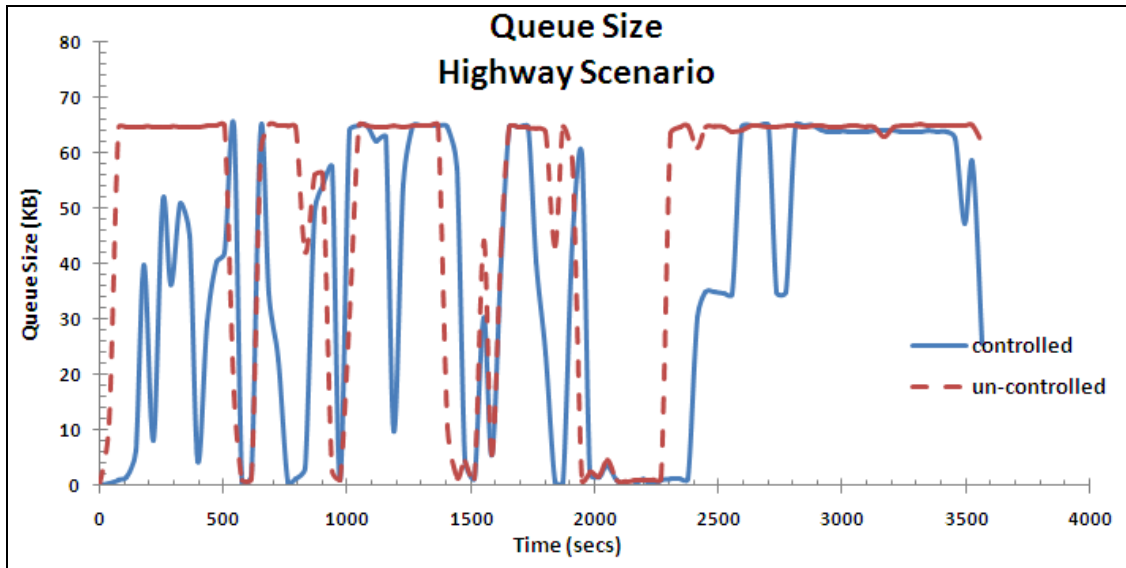


Fig 5.3: Instantaneous Queue Size for Highway Scenario

Fig. 5.3 shows the effect of the controller on the queue size. As opposed to being kept at a maximum of 64kB, once the controller detects congestion in the network, the queue size could drop to as low as 50kB.

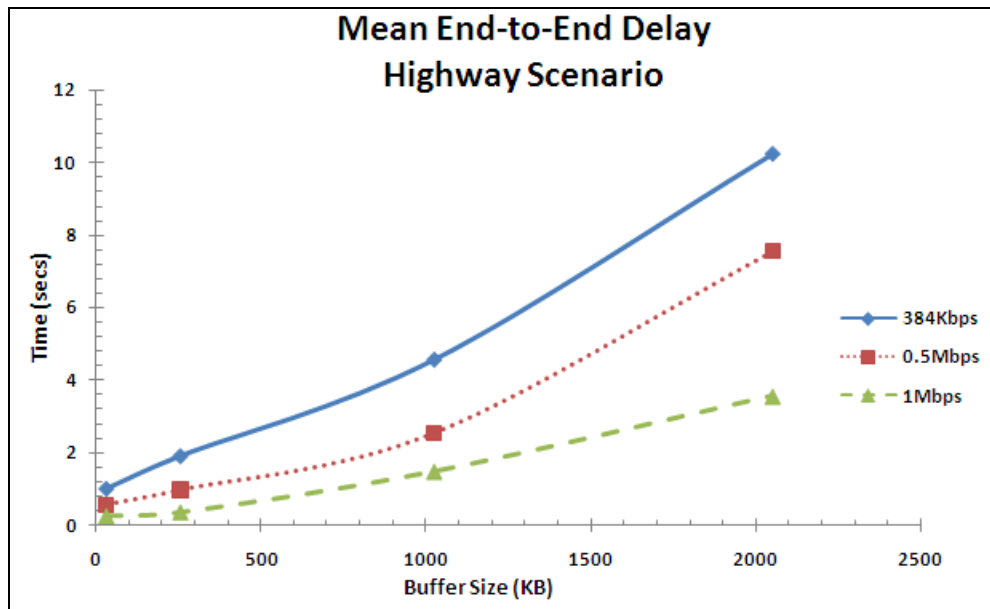


Fig. 5.4: Mean End-to-End Delay Performance for Highway Scenario.

5.1.1.2 Mean End-to-End Delay

The mean end-to-end delay performance for the highway scenario is shown in Fig. 5.4. As expected, as the service rate increases, the end-to-end delay reduces. However, one can see that the speed of the vehicles is a large factor here. Increasing the service rate reduces the end-to-end delay and increasing the buffer size increases the end-to-end delay.

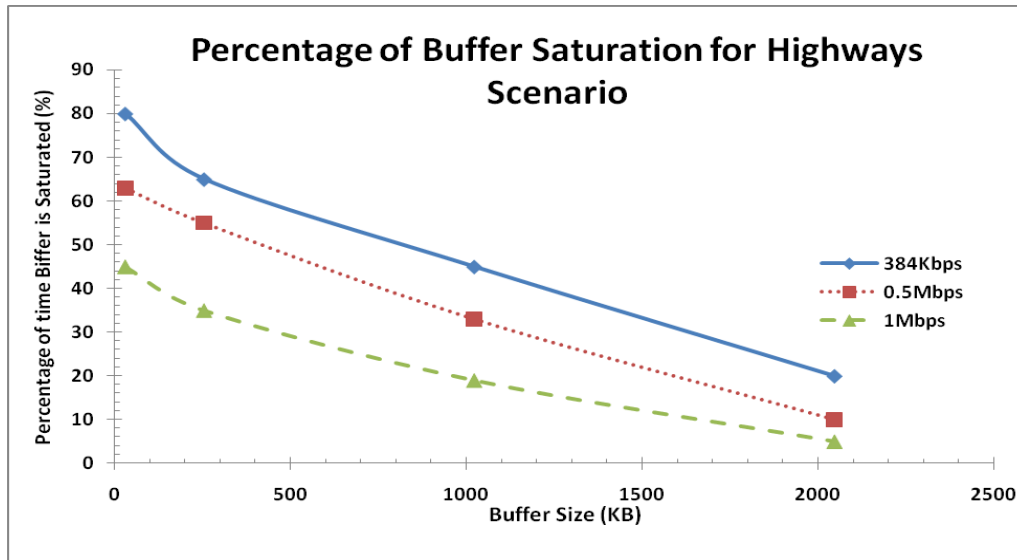


Fig. 5.5: Percentage of Buffer Saturation Performance for Highway Scenario.

5.1.1.3 Buffer Overflow Percentage

The percentage of buffer saturation of the Highway scenario is shown in Fig. 5.5. The normal trend is followed in this case, i.e., as the buffer size increases, the percentage of time for which the buffer is full decreases. It is important to note that the reduction in percentage of buffer saturation as the service rate increases in this scenario might be due to other factors such as, packet loss due to connection drops and reduced bandwidth.

5.1.2 Residential Scenario

This scenario uses the parameters described in Section 3.3 and 3.4.2. The environmental settings for this scenario can be found in Table 3.3.

5.1.2.1 Time Evolution Performance

Fig. 5.6 shows the end-to-end delay for the residential area scenario. The controller is seen to

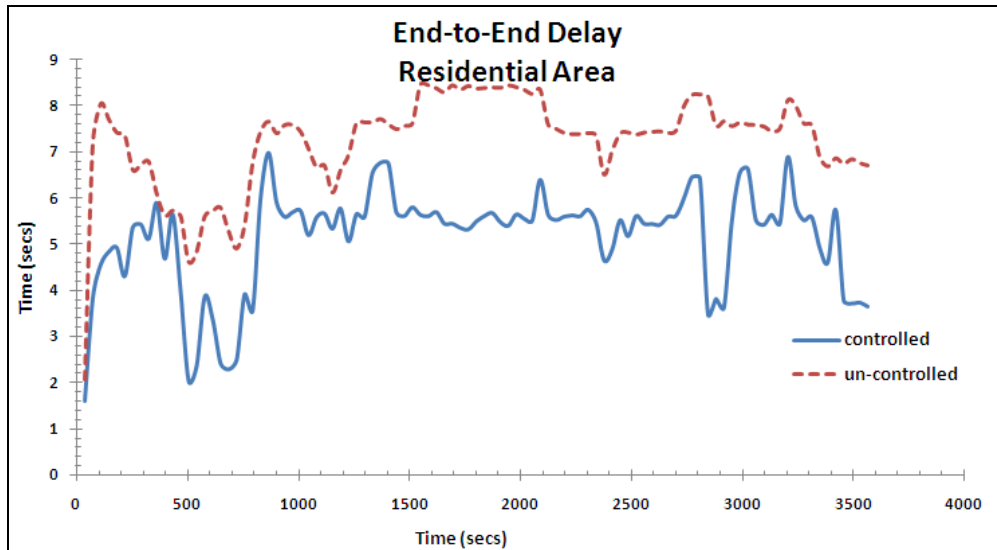


Fig. 5.6: End-to-end delay for the Residential Area Scenario.

reduce the end-to-end delay; however, the percentage of reduction is smaller than the previous scenarios. This can be explained by scarcity of cars (node/hops) in this scenario. Hence, one can conclude that fraction of delay caused by traffic congestion is minimal; a greater portion of the delay is caused by interference and trip time. Furthermore, the car speed and radio interference is higher in the scenario than the other scenarios, hence, limiting the bandwidth. The controller sensitivity was set to 0.1secs, hence, the controller is busy most of the time and its effectiveness is reduced.

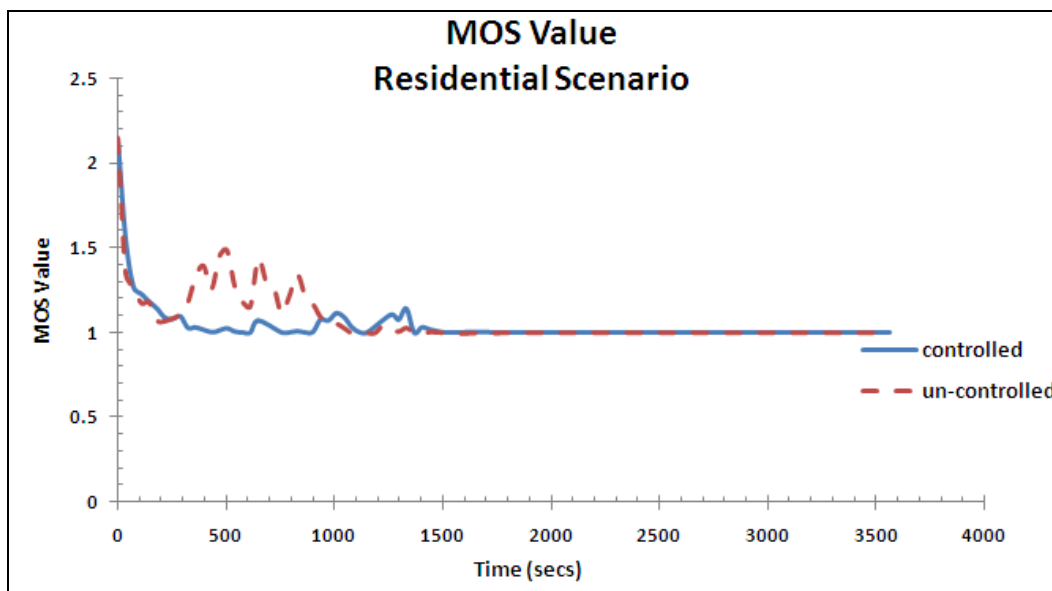


Fig. 5.7: MOS Value for Residential area scenario.

As observed earlier, the controller tends to increase the quality of video, however, causing a fluctuation in the process as shown in Fig. 5.7. The fluctuations seen at the early stages of the curve are due to the reduction in the end to end delay as seen in Fig. 5.6. In the latter part of the simulation, the reduction in end to end delay is no longer substantial accounting for the MOS value remaining at 1.

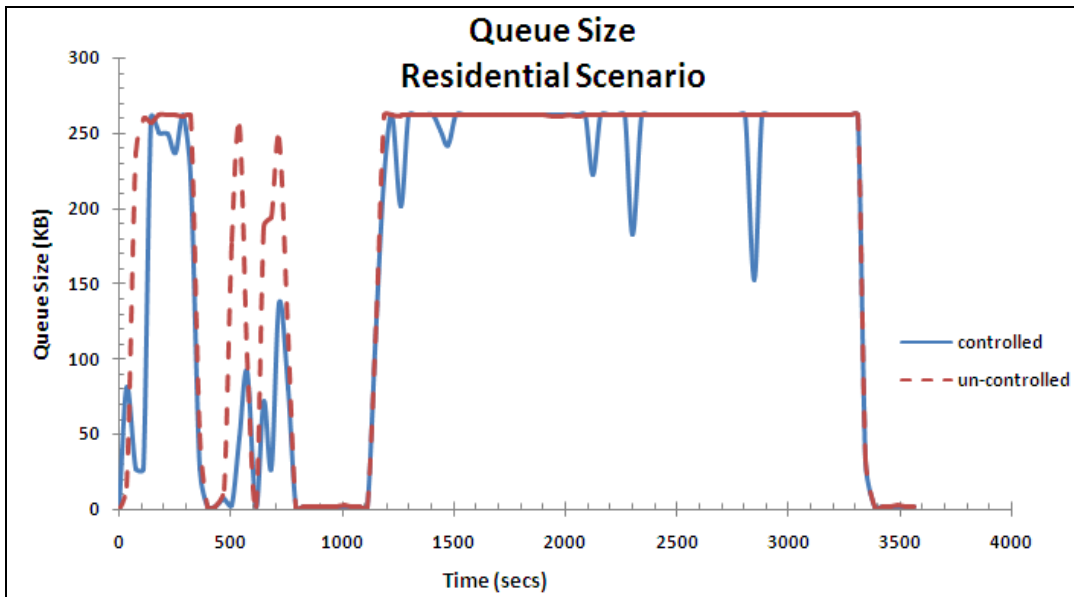


Fig 5.8: Instantaneous Queue Size for Residential Scenario

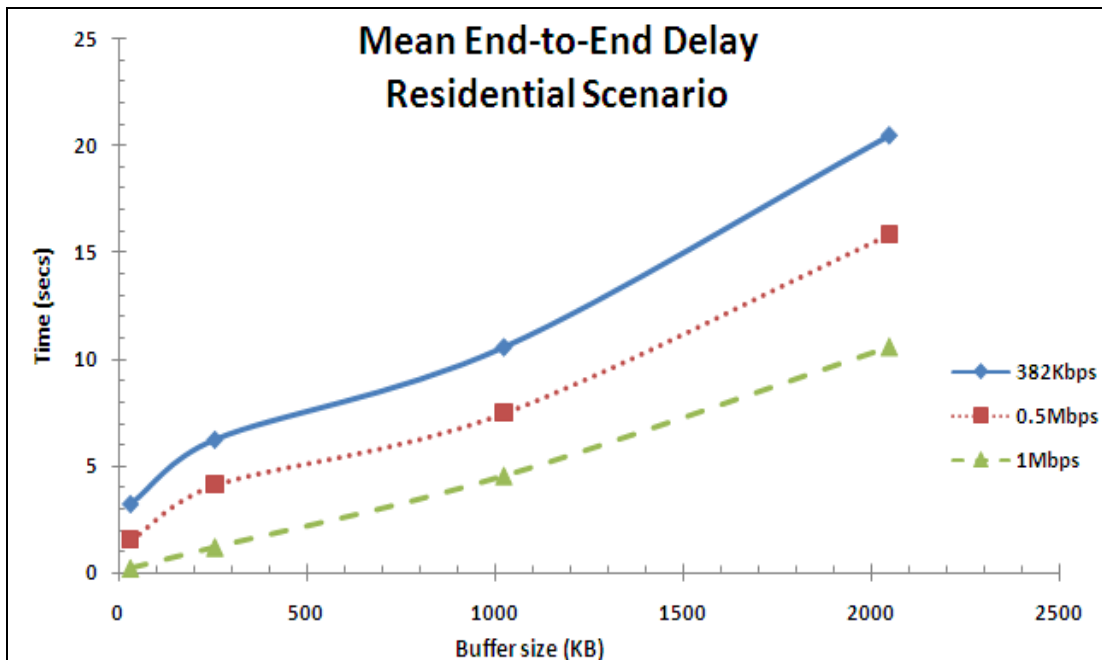


Fig. 5.9: Mean End-to-End Delay Performance Residential area scenario

Fig 5.8 shows the instantaneous queue size for the highway scenario. The dotted line shows the queue size when the controller algorithm is not implemented while the thick line shows the instantaneous queue size when the controller traffic is implemented. The queue is seen to full majority of the time in this scenario. This corresponds to the end to end delay behaviour shown in Fig. 5.6.

5.1.2.2 Mean End-to-End Delay

Fig. 5.9 shows the mean end-to-end delay performance for the residential area scenario. This performance curve follows the expected trend. The curve is a linearly increasing curve with a positive slope. The end-to-end delay increases as the buffer size increases. This is expected since our traffic is characterized using a Pareto distribution. The mean end-to-end delay is seen to high as seen in Fig. 5.6.

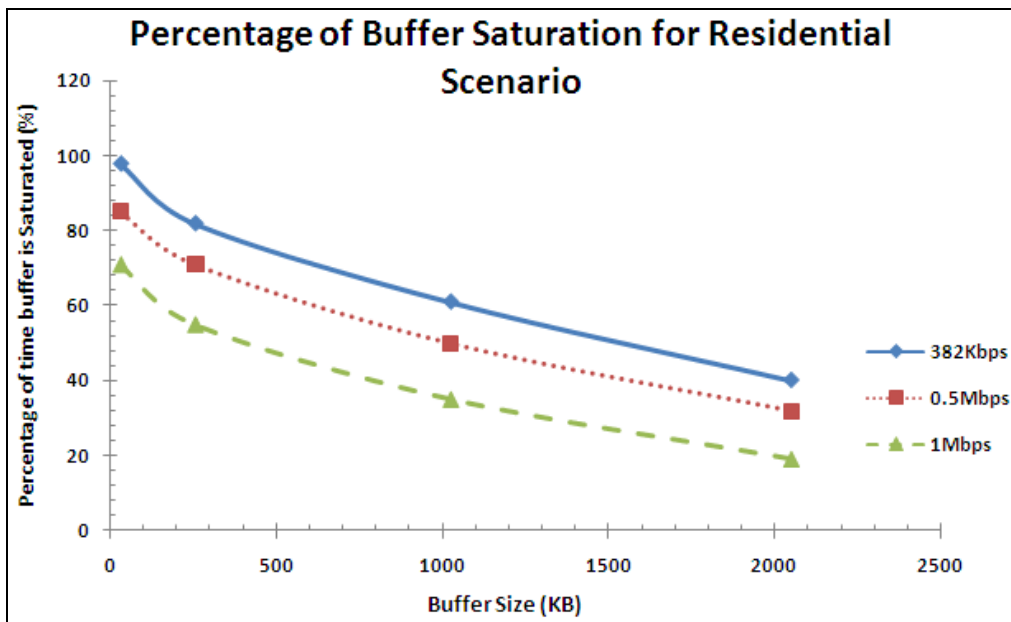


Fig. 5.10: Percentage of Buffer Saturation Performance for Residential area scenario.

5.1.2.3 Buffer Overflow Percentage

Fig. 5.10 shows the percentage of buffer saturation for the residential area scenario. This performance curve decreases linearly with respect to the buffer size for most of the buffer range. The percentage also reduces as the service rate increases. The buffer is seen to saturate often when the end-to-end delay becomes high in Fig. 5.6 (going as high as 8secs often). This suggests

there is much higher probability of the buffer overflow as seen in Fig. 5.10.

5.2 Large Network

In the large network, we study a network of 30 cars and 2 RSU's. Each car in this network has a maximum sustainable traffic rate of 384Kbps. The link between the RSU and the backhaul network was a DS3 link with a capacity of 44.736Mbps as shown in Fig. 2.1. As discussed earlier, this section evaluates the scalability of our explicit controller algorithm.

5.2.1 Highway Scenario

This scenario uses the parameters described in Section 3.3 and 3.4.3. Table 3.3 also shows the environmental parameters for this scenario.

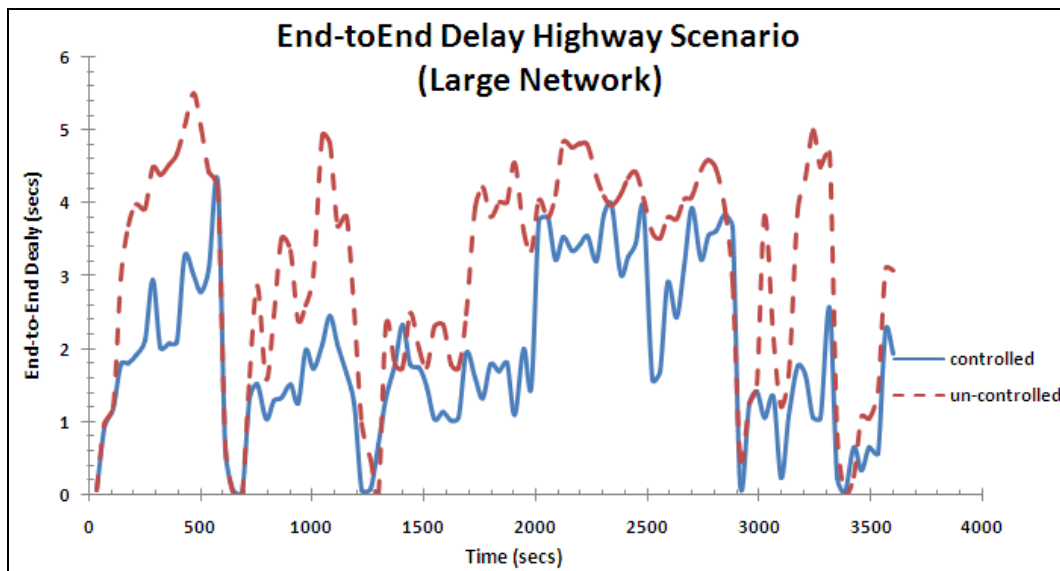


Fig. 5.11: End-to-end Delay for Highway Scenario (Large Network)

5.2.1.1 Time Evolution Performance

Fig. 5.11 shows the end-to-end delay for the highway scenario in the large network. The thick line shows the end to end delay when the controller is implemented and the dotted line shows the end to end delay when the controller algorithm is not implemented. The controller sensitivity was set to 0.1secs similar to what was set in Section 5.1 for proper comparison. The behaviour seen here is similar to what is seen in Fig. 5.1 except that the end to end values are much higher in this case due to increase in the network size. The controller is seen to reduce the end to end delay in this case, although, its effectiveness reduces at the latter part of the curve. The speed is

also a factor that could affect the controller algorithms effectiveness in this case.

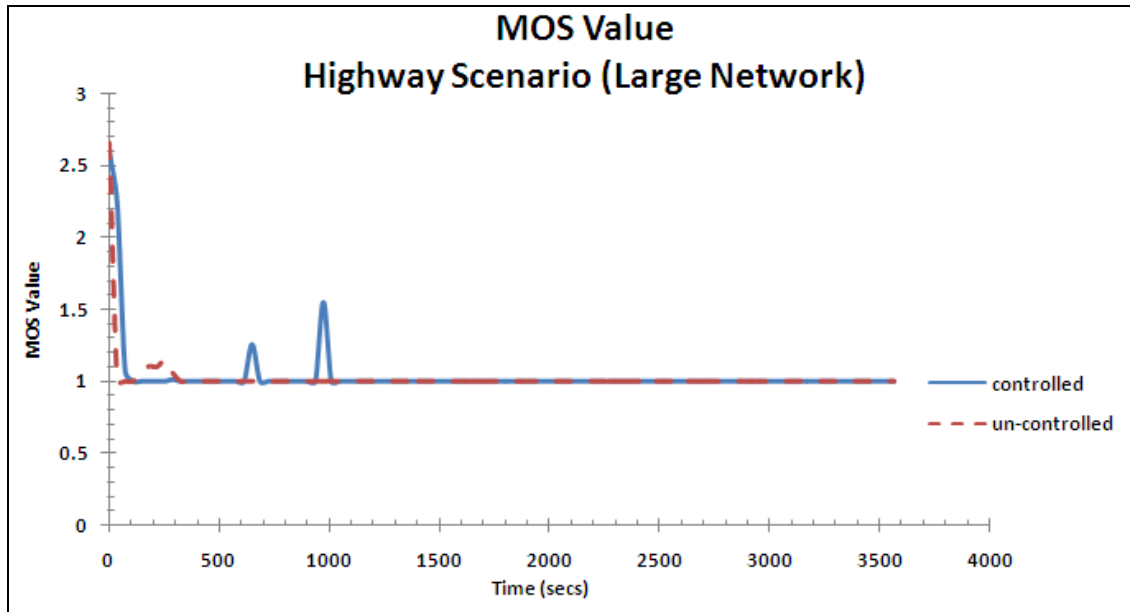


Fig. 5.12: MOS value for Highway Scenario (Large Network)

Fig. 5.12 shows the MOS value for the highway scenario for the large network. The effect of the controller is not seen in this scenario as the change in end-to-end delay is not significant enough to affect the quality of service as seen by the user. The end to end delay is also high in this scenario; this explains why the MOS value remains at a low value of 1 in most of the simulation.

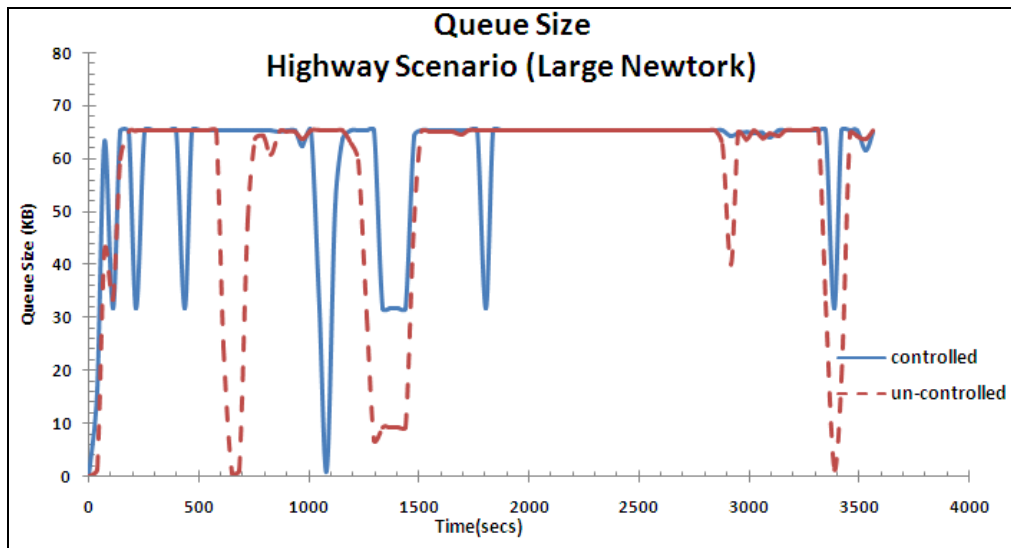


Fig. 5.13: Instantaneous Queue Size for Highway Scenario (Large Network)

Fig. 5.13 shows the effect of the controller on the queue size. Comparing this Figure with Fig. 5.3, the maximum queue size is reached more in this case due to the increase in network size. As discussed early in this Section, the effectiveness of the controller algorithm is reduced. This explains why we don't see much reduction on the queue size as compared with Fig. 5.3.

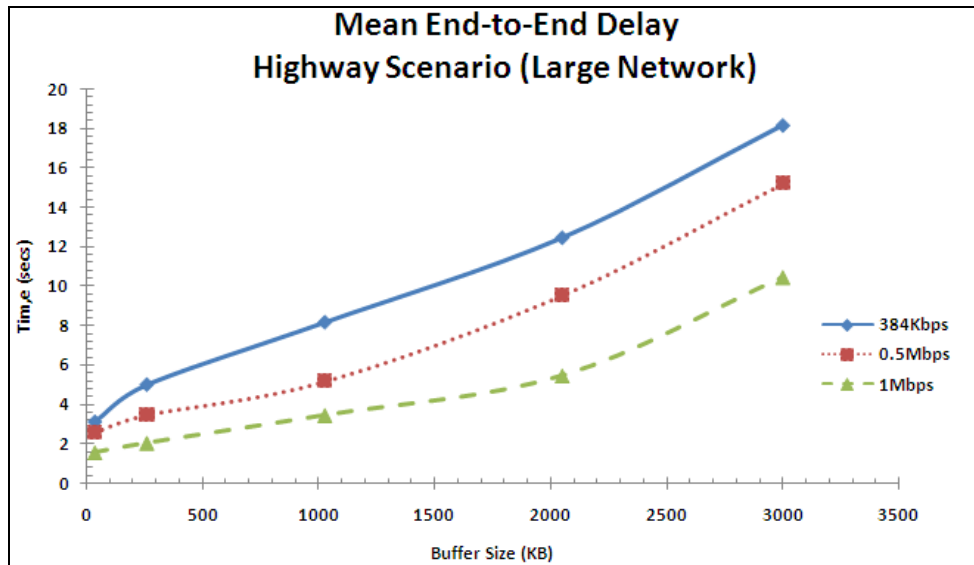


Fig. 5.14: Mean End-to-End Delay Performance for Highway Scenario (Large Network)

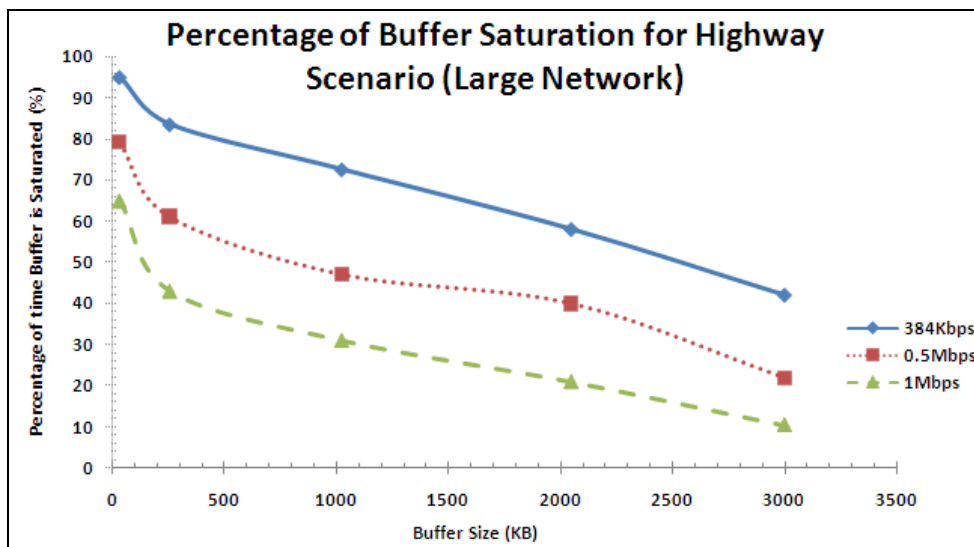


Fig. 5.15: Percentage of Buffer Saturation Performance for Highway Scenario (Large Network)

5.2.1.2 Mean End-to-End Delay

Fig. 5.14 shows the mean end-to-end delay performance for the highway scenario in the large network for varying buffer sizes and service rates. The behaviour is as expected, as the buffer

size increases the mean end-to-end delay increases as the packets have more room to queue. This is similar to what is shown in Fig. 5.4 except the mean end to end delay is higher in this case due to the increase in network size.

5.2.1.3 Buffer Overflow Percentage

The percentage of buffer saturation performance curve for the highway scenario is shown in Fig. 5.15 for the large network. It is seen that as the percentage of buffer overflow reduces as the buffer size increases and the service rate increases. This behaviour is consistent with what is presented in Fig. 5.5 except that the percentage of buffer saturation is higher in this case since the network size is increased.

5.2.2 Residential Scenario

This scenario uses the parameters described in Section 3.3 and 3.4.2. Other parameters for this scenario are also shown in Table 3.3.

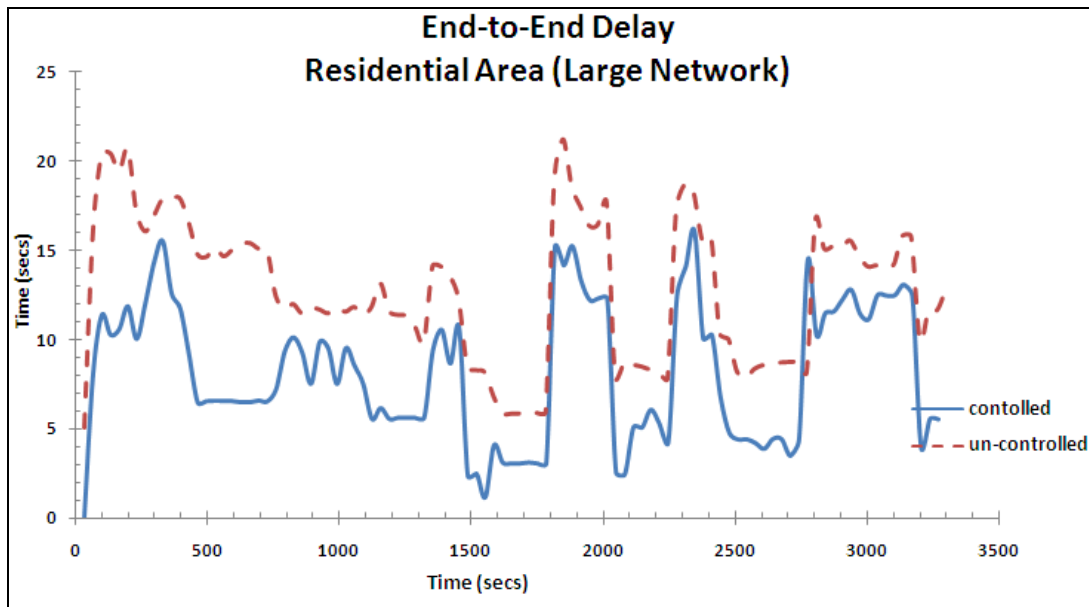


Fig. 5.16: End-to-end delay for Residential area Scenario (Large Network)

5.2.2.1 Time Evolution Performance

The end-to-end delay for residential area scenario for the large network is shown in Fig. 5.16. The controller sensitivity was set to 0.1secs for proper comparison with the Section 5.1. The behaviour seen here is similar to what is shown in Fig. 5.6 except that the end to end delay is much higher. The controller is seen to reduce the end-to-end delay; however, in the latter part of

the simulation, the reduction is not substantial. This could be explained by the higher constraint placed on the controller algorithm by expanding the network size.

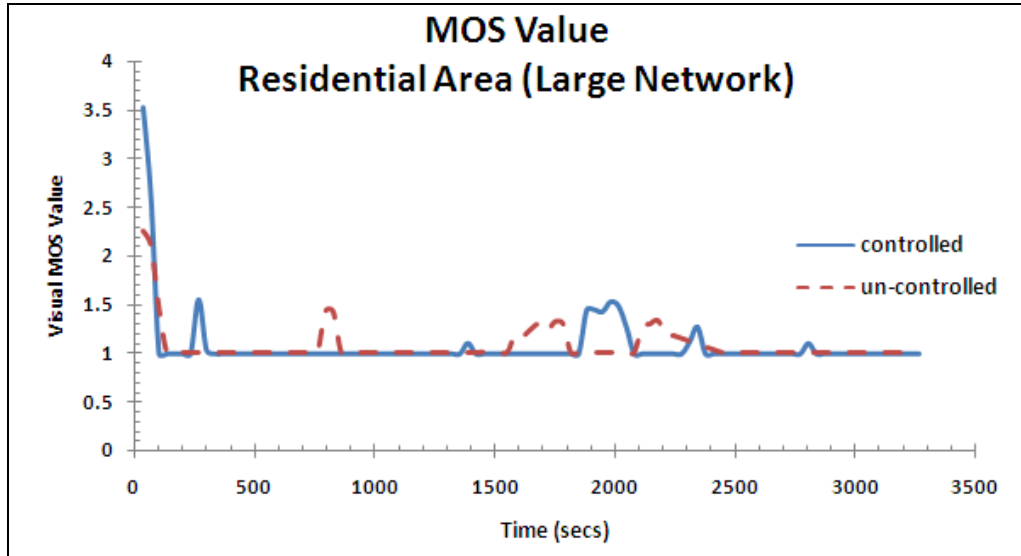


Fig. 5.17: MOS Value for Residential area Scenario (Large Network)

Fig. 5.17 shows the MOS value. This is seen to vary slightly from time to time. The fluctuations are seen when the end to end delay is reduced to a minimal point. As discussed earlier, the fluctuations distort the visual experience of the user.

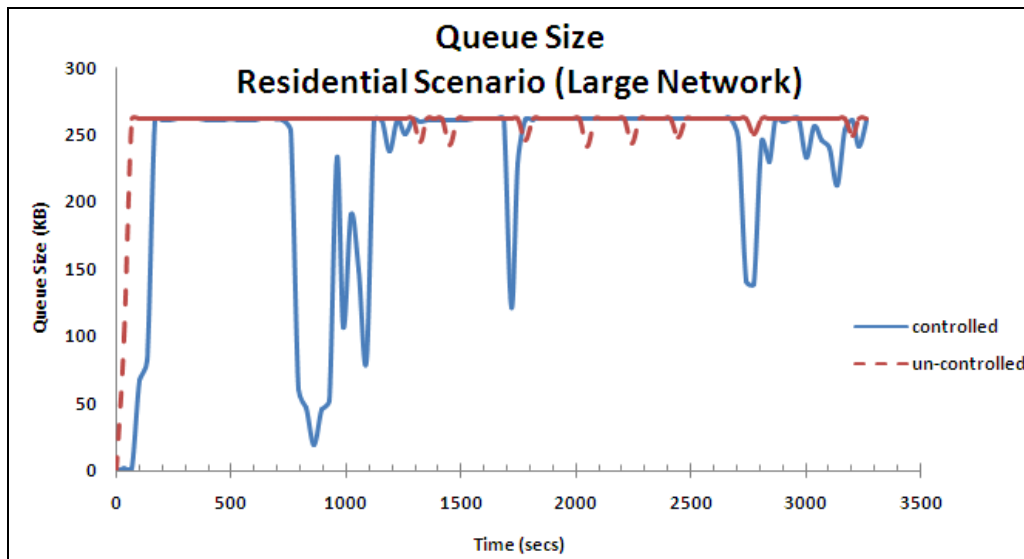


Fig. 5.18: Instantaneous Queue Size for Residential area Scenario (Large Network)

Fig. 5.18 shows the instantaneous queue size for the residential scenario for the large network. Comparing this Figure to Figure 5.8, one can see that the queue size is higher in this case since the network size as increased. The controller manages to reduce the queue size in

some instances in this case which is consistent with the behaviour seen in Fig. 5.16.

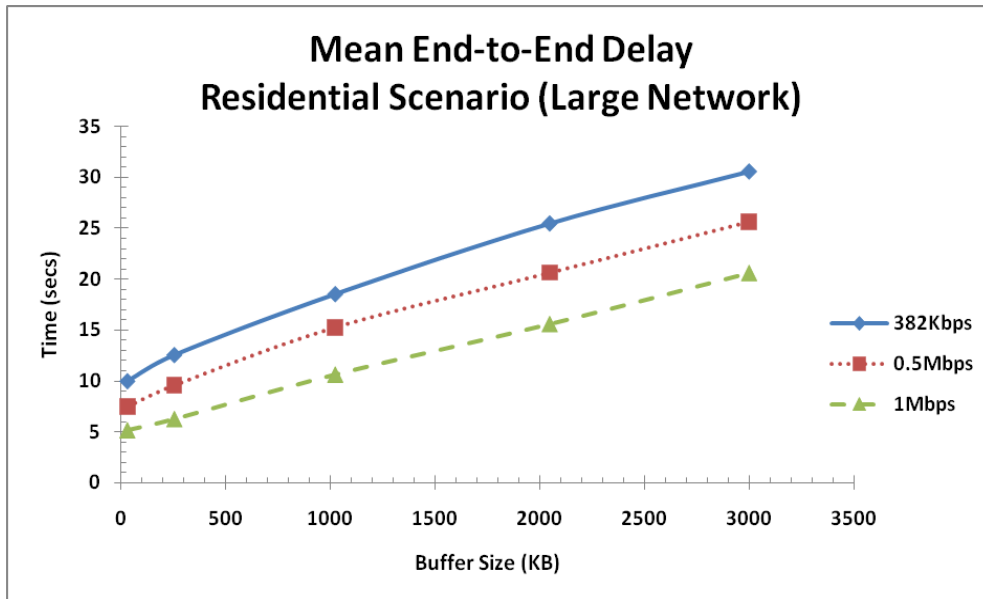


Fig. 5.19: Mean End-to-end Delay Performance for Residential area Scenario (Large Network)

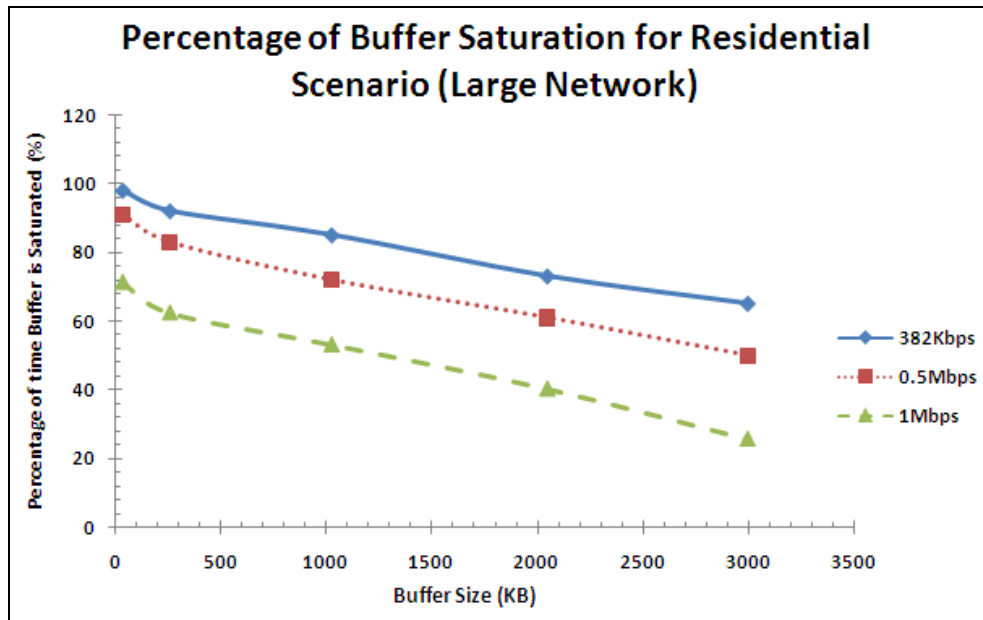


Fig. 5.20: Percentage of Buffer Saturation for Residential area Scenario (Large Network)

5.2.2.2 Mean End-to-End Delay

The behaviour of the mean end-to-end delay performance and the percentage of buffer saturation for the residential area scenarios are similar to what is discussed in Section 5.1.2.2 and 5.1.2.3 respectively except that the values are higher in this case due to the increase in network size. The

curves for the large scenario are shown in Fig. 5.19 and Fig. 5.20.

5.3 Scenario Comparison

This section compares the end-to-end delay and jitter for the highway and Residential area scenarios.

Table 5.1: Performance Summary of Small Network

Scenarios	Average End-to-end delay (secs)	Average End-to-end delay (secs) [controlled]	Jitter (ms) Standard deviation	Average Visual MOS
Highway	4.08069	2.932	2.986	1.034
Residential Area	7.2313	5.1463	1.897	1.07
Downtown	3.37165	1.76098	0.981	1.394
School zone	1.5241	0.66667	2.171	1.074
Benchmark	0.5	0.203	0.005	3.6

Table 5.2: Performance Summary of Large Networks

Scenarios	Average End-to-end delay (secs)	Average End-to-end delay (secs) [controlled]	Jitter (ms) Standard deviation	Average Visual MOS
Highway	0.958	0.429	3.986	1.081
Residential Area	12.84234	8.16463	1.997	1.081
Downtown	3.487	1.442	1.742	1.052
School zone	4.3764	2.627	3.091	1.2
Benchmark	0.7	0.32	0.005	3.6

Tables 5.1 and 5.2 show the summary of the end-to-end delay (controlled and non-controller), standard deviation of jitter and average visual MOS for each scenario in the small network and large network respectively. These tables are the mean value of the time evolution results shown in Sections 4.1.1.1, 4.1.2.1, 4.2.1.1, 4.2.2.1, 5.1.1.1, 5.1.2.1, 5.2.1.1 and 5.2.2.1. The tables contain Benchmark figures, which represent the ideal scenario of one vehicle and on RSU with ample bandwidth to transmit and minimal interference. For proper comparison it is important to refer to the Benchmark (the ideal case) for proper comparison. Residential scenerio presents the highest average delay. This can be explained from the fact that the cars are scanty on the road, hence, the location of the BS/RSU becomes a factor of great importance. At instances where the cars are far from the RSU, we see the delay increase due to decrease in available bandwidth. The

highway scenerio follows with a slightly reduced end-to-end delay. For highway, only the speed affects the bandwidth, while in the school zone scenerio, only interference affects the bandwidth.

Variation in the jitter leads to an unapealing visual experience. The highway scenerio has the worst jitter variation. This could be explained due to the speed of the cars, the constantly changing topology of the network and the Doppler shift. The combination of the Jitter and Delay leads to the worst Visual MOS rating.

Chapter 6

Design Guideline

From the results presented, it is obvious that we require a form of traffic shaper and controller to control the bandwidth and delay thus enhancing the visual experience of the user. In designing a traffic controller for this purpose, the frequency of the controller messages has to be taken into close account. From our study, sending the controller messages after receiving 10 packets was for smaller networks. For larger networks, it might be more efficient to send the ACK packets more frequently bearing in mind that this might also affect the bandwidth utilization. Also, in a more critical scenario with strict real-time deadlines, the controller messages should be sent out more frequently.

A general rule of thumb cannot be found at this point because the design of the controller will be dependent on the specific application in order to maximize the controller's efficiency. For instance, in applications where strict deadlines are required for the delivery of packets (e.g. surgical operations done remotely), the feedback is of greater importance than the bandwidth utilization.

The controller algorithm also has to regulate the fluctuation in end to end delay. The fluctuations increase the jitter affecting the quality of service as seen by the user. From an end users perspective, keeping the fluctuation as minimal as possible is more important than increasing the quality of the video (reducing the end to end delay). It is important to note that these recommendations are subjective and highly dependent on the specific application.

Similar to designing any other network, one has to consider the scenario of use. This is of great importance in VANET as seen from our experiments. Depending on the scenario, the behaviour is different and the factors that affect quality are different. Although there are generic factors such as interference that affect all scenarios, some scenarios such as the highway scenario will have to put the speed of the vehicles into consideration. Scenarios such as the residential scenario will have to consider the scarcity of cars.

The buffer size of each node is also of great importance as this has an impact on the end-to-end delay. Choosing the right buffer size is dependent on the application in question. Our suggestion is that applications with strict deadlines should choose a buffer size of between 64KB

and 256KB. This will reduce the queueing delay and in turn reduce the end to end delay for such applications. The loss rate also has to be considered bearing in mind that the higher the percentage of buffer saturation, the higher the loss rate due to buffer overflow.

The data rate is also an important factor that needs to be carefully chosen. This is mostly dependent on the scenario. For scenarios like the highway and downtown, one would suggest a high data rate of between 0.5Mbps and 1Mbps. For scenarios like the residential and school zone scenario, one would suggest a data rate of between 384kbps and 0.5Mbps.

As mentioned earlier, it is important to note that these design guidelines need to be customized for each scenario and for each application for best performance.

Chapter 7

Conclusion

With the initial work done in this work, there is a lot of room to improve and explore new grounds in this model. This section will present the conclusion of this work and also discuss suggested future enhancements.

In this work, we were able to create an effective video VANET simulation platform with which other researchers can develop and test various VANET applications. Even though OPNET does not use the RTP/RTCP protocol for video streaming, we have found a way to model our video using this protocol. This is done by designing our video model to work as individual streams – mini Pareto model. The platform was built using the OPNET simulation tool which allowed for the integration of our video model – developed from statistically analysing a live video trace; real world maps/ trajectory simulations and provided a complete tier of communication layers for proper performance analysis.

Integrating a VANET mobility model into our platform created challenges for us. So far, due to the limitation of the OPNET licence available (we did not have the ACE licence that allows High Level Architecture functionality [OPNE10]), we have to run mobility model first before integrating the results into our communication model. It would have been best to run the simulation model and the mobility model concurrently to allow the wireless communication affect the mobility of vehicles so that more viable results can be obtained.

From our simulation results, it is observed that designing a congestion control algorithm for a wireless real- time video application is more delicate as the timing and quality of service requirements might interfere with each other. We observed that it is important to develop a traffic controller that will keep the end-to-end delay constant in order to reduce the quality impact on the viewers. It is also observed that the scenario in which the application is deployed will affect the performance of the applications.

In summary, we were able to design and implement a theoretical video model, integrate the video model together with a VANET model into a communication tool and implement a practical traffic controller for video over RTP applications.

7.1 Future Work

There are various ways to improve the work done in this thesis because there is always room for improvement. In this work, due to the complicated theory behind the model, the correlation was calculated manually, using a time consuming and tedious route. This was done as test case and prototype to verify the effectiveness of our method. However, automation means should be found to calculate the correlation from the trace. An algorithm that will input the trace and output the mean off-time, mean on-time, frame duration and packet size for each bin will both save manual computation time and reduce error. On the other hand, as opposed to creating a video model, the live video trace can be made an input into OPNET – this will produce a more accurate result.

Having created the video model that handles the application layer, we used WiMAX technology as our MAC and physical layer protocols. Recently, other 4G technologies have been explored by various researchers e.g. LTE and this should be integrated into our model and compared with the WiMAX technology in order to evaluate the limitations and strengths of these new technologies in VANET applications. One could also go further to implement the WiMAX technology in pure adhoc networks. This could be useful when conventional WiMAX towers are down. Hence, the vehicle could have two modes: BS mode and adhoc mode.

From the performance curves shown in Chapter 4, it can be seen that the traffic controller used for this work was made simple for easy deployment. However, due to its relative simplicity, some packets go by uncontrolled, hence the need for a more detailed and thorough controller. While creating this controller, the number of iterations and mathematical analysis needs to be kept in mind as the implementation is at the end user side. For a mobile device, the number of computations needs to be kept at a minimal point.

As a step in this direction, the API-RCP developed at the CCNR lab could be adapted and tested for this application. Although, API-RCP has only be used for TCP connections, its implementation for UDP/RTP could be explored bearing in mind that reducing the sending rate will mean reducing the compression rate as opposed to reducing the sending-window. Furthermore, the implementation of API-RCP, which uses the queue-length as the congestion metric, will have to be adapted to use the end-to-end delay. The key in this case will be a fast adaptation mechanism in order to make the user oblivious of these changes.

For real-time video streaming, users are more concerned with receiving the video image

in record time as opposed to receiving a high definition image. Hence, during congestion periods, we can afford to trade video quality for prompt arrival. In this regard, a congestion control algorithm that drops packets could be implemented, however, bearing in mind that the pattern of drop should be considered as well as the percentage of drop.

Building a transparent simulator that allows users to follow through the intricacies of the design can also be an approach to consider when building a VANET platform. Simplifying the communication model can be an initial step to allow for proper design. It will also be effective to have different specialities come together integrate different VANET details into the model.

As oppose to the video model, it will also be productive if one can use different live traffic streams to represent each application type. This will produce an exact replica of the application and give a more accurate result.

References

- [Ahma06] Dr. S. Ahmadi, "Introduction to Mobile Radio Access Technology: PHY and MAC Architecture." http://vivonets.ece.ucsb.edu/ahmadiUCSB_slides_Dec7.pdf, Accessed in Dec. 2009
- [BaMa03] A. Balk, D. Maggiorini, M. Gerla and M.Y. Sanadidi 'Adaptive MPEG-4 Video streaming with bandwidth estimation', *Proceed. Quality of Service in Multiservice IP Networks: 2nd International Workshop*, Milano, Italy, 2003. pp 525- 538.
- [BeSh95] J. Beran, R. Sherman and et al "Long-Range Dependence in Variable-Bit-rate Video Traffic" *IEEE Transaction on Communications*, vol. 43, no.234, Feb. 1995, pp. 1566-1579.
- [Brit10] "WiMax." *Encyclopædia Britannica*. <<http://www.britannica.com/EBchecked/topic/1017801/WiMax>>, accessed on 27 Jul. 2010
- [Comb08] G. Combs, "Ethereal". Available at <https://www.wireshark.org>, accessed in 2008
- [Easy09] Easyfit, www.mathwave.com/products/easyfit.html, accessed in 2009
- [ErGr99] V. Erceg L.J. Greenstein, et al., "An empirically based path loss model for wireless channels in suburban environments", *IEEE JSAC*, vol.17, no.7, July 1999, pp. 1205-1222.
- [Erti10] Ertico, "GDF - Geographic Data Files", <http://www.eritco.com/en/links/links/gdf_-_geographic_data_files.htm> accessed in July 2010
- [FCC04] "Dedicated Short Range Communications (DSRC) Service" <http://wireless.fcc.gov/services/index.htm?job=about&id=dedicated_src>, accessed in January 201
- [FiHa07] M. Fiore, J. Harri, F. Filali, C, Bonnet, "Vehicular Mobility Simulation for VANETs," *Simulation Symposium, 2007. ANSS '07. 40th Annual*, vol., no., 26-28 March 2007, pp.301-309,
- [FlJa93] S. Floyd and V. Jacobson, "Random Early Detection Gateways for Congestion Avoidance", *IEEE/ACM transaction on Networking*, Vol. 1, No. 4, August 1993, pp. 397-413.
- [GhGh07] A. Ghosh and M. Ghosh, "Fundamentals of WiMAX: Understanding Broadband Wireless Networking." Prentice Hall, 2007
- [Glas08] M. Glaskin, "Could smart traffic lights stop motorists fuming?" Feb. 2008. <http://www.newscientist.com/article/dn13306>.
- [GuJi04] H. Gu and Q. Ji, "An automated face reader for fatigue detection," *Automatic Face and Gesture Recognition, 2004. Proceedings. Sixth IEEE International Conference*, 2004, pp. 111-116.
- [Hac99] A. Hac, "Congestion Control in a Wireless Network" *International Journal of Network Management*, Vol.9, 1999, pp. 185-192,
- [HaBr07] M.M. Hassani, R. Berangi and H. Tavakolaie, "An analytical model for evaluating utilization of TCP TAHOE using markovian model", *International Conference on Networking, Architecture, and Storage*, NAS 2007, pp. 257-258.
- [HaFl03] M. Hanley, S. Floyd, J. padhye and J. Widmer, "TCP Friendly Rate Control (TFRC_ : Protocol Specification", *IETF RFC 3448*, January 2003.
- [HeLa96] D. Heyman and T. Lakshman, "What are the implications of long-range dependence for VBR-video traffic engineering?" *IEEE/ACM Transactions on Networking (TON)*,

- vol. 4, issue 3, June 1996, pp 301-317,
- [HoBo01] S. P. Hoogendoorn, P. H. Bovy, "State-of-the-art of vehicular traffic Flow Modelling" *Proceedings of the Institution of Mechanical Engineers, Part I: Journal of Systems and Control Engineering*, Vol. 215, No. 4, 2001, pp 283-303.
- [HoPa01] S. H. Hong, R. Park and C. B. lee "Hurst parameter estimation of long-range dependent VBR MPEG Video traffic in ATM Networks" *Journal of Visual Communication and Image Representation*, Vol. 12, issue 1, March 2001, pp 44-65.
- [HoYa07] Y. Hong and O. Yang "Design of Adaptive PI Rate Controller for Best-Effort in the Internet Based on Phase Margin" *IEEE transaction on Parallel and Distributed Systems*, vol. 18, issue 4, 2007, pp. 550-561.
- [Huan01] J. Huang. "Presentation for Generalizing 4IPP Traffic Model for IEEE 802.16.3" http://www.ieee802.org/16/tg3/contrib/802163p-00_58.pdf
- [HuDe95] C. Huang, M. Devetsikiotis, I. Lambadaris and A.R. Kaye, "Modelling and simulation of self-similar variable bit rate compressed video: A unified approach," *Proceeding ACM SIGCOMM'95*, pp. 114-125.
- [HuXu03] C. Huang and L. Xu, "SRC: Stable rate Control for Streaming Media," *IEEE Globecom*, San Francisco, U.S.A, December 2003, pp. 4016-4021.
- [IEEE04] IEEE P802.16-REVd/D4 "Air interface for fixed broadband wireless access system", March 2004. http://hunter.hosted.pl/tts/Strony_www_TTS_2004.2005/LMDS_Marcin.Gilewski_Lukasz.Waksmanski/airInterface.pdf
- [InDr10] Intellidrive, "Use of Dedicated Short Range Communications (DSRC) Technology", accessed in January 2010, <http://www.intellidriveusa.org/about/dsrc-faqs.php>
- [Inte10] Intel, "Intel CTO Rattner Outlines Research Challenges in Home, Car and Network Energy Consumption", accessed in April 2010, <http://www.intel.com/pressroom/archive/releases/2010/20100413comp.htm>
- [ITUR97] ITU-R "Guideline for Evaluation of Radio Transmission Technologies for IMT-2000" 1997, http://www.itu.int/dms_pubrec/itu-r/rec/m/R-REC-M.1225-0-199702-I!!PDF-E.pdf
- [JaBr92] V. Jacobson, R. Braden, D. Borman 'TCP Extensions for High Performance' May 1992: <http://www.ietf.org/rfc/rfc1323.txt>.
- [JaKa88] V. Jacobson and M.J. Karels, "Congestion avoidance and control", *SIGCOMM '88 Workshop*, 1988, pp. 314-329.
- [Ledg01] E. Ledger, "Injuries Declining, But Know Your Accident Claim Options": accessed in January 2010, <http://www.caraccidentattorneys.com/resources/auto-accident/car-accident-claims/injuries-decline-claim-options.htm>.
- [Li06] K. Li, "IEEE 802.16e- 2005 Air Interface Overview", WiMAX Solutions Division Intel Mobility Group, June 05, 2006.
- [LiHu09] X. Li, H.Huang and W. Shu, "VStore: Towards Cooperative Storage in Vehicular Sensor Networks for Mobile Surveillance", *IEEE Wireless Communication and Networking Conference (WCNC)*, Budapest, Hungary, April 2009, pp. 1-6. 5-8.
- [LiKh09] B. Liu, B. Khorashadi, H. Du, D. Ghosal. C. Chuah, and M. Zhang, "VGSim: An integrated Networking and Microscopic vehicular Mobility Simulation Platform" *IEEE Communication Magazine*, vol.47, no.5, May 2009, pp.134-141,
- [MaJi98] S. Ma and C. Ji, "Modeling Video Traffic Using Wavelets" *IEEE Communications letters*, vol.2, no. 4 April 1998, pp. 100-103.
- [Malk98] G. Malkin, "RIP version 2", November 1998 <http://tools.ietf.org/html/rfc2453>

- [MeJa05] M.A. Mehmood, T.M. Jadoon, N.M. Sheikh, "Assessment of VoIP quality over access networks," *Internet, 2005. The First IEEE and IFIP International Conference in Central Asia on*, vol., no., Sept. 2005, pp., 26-29
- [MeLe96] H. Mehrvar, T. Le-Ngove and J. Huang "Performance Evaluation of Bursty Traffic Using Neural Networks" *Canadian Conference Electrical and Computer Engineers*, Vol. 2, 1996, pp. 995-958,
- [Morg10] Y.L. Morgan, "Managing DSRC & Wave Standards Suite Operations: In a V2V Scenario" *International Journal of Vehicular Technology*, Volume 2010 (2010), <http://downloads.mts.hindawi.com/MTS-Files/IJVT/papers/regular/797405.v2.pdf?AWSAccessKeyId=0CX53QQSTHRYZZQRKA02&Expires=1276817481&Signature=Fh39G7cn9D3ZE66DvCCYnLiZQ%2Bg%3D> .
- [OPNE10] OPNET, "Analyze and Troubleshoot Application Performance from a Network Perspective" accessed date, April 2010, http://www.opnet.com/solutions/brochures/ACE_Analyst.pdf
- [Post80] J. Postel "User Datagram Protocol" 28 August 1980,: <http://www.ietf.org/rfc/rfc768.txt>.
- [RaSa10] H.K. Rath, A. Sahoo, "Cross Layer based congestion control in wireless networks" accessed by January 2010, <http://www.it.iitb.ac.in/research/techreport/reports/8.pdf>.
- [Rama04] P. L. Ramage-Morin, "Motor vehicle accident deaths, 1979 to 2004" Component of Statistics Canada Catalogue no. 82-003-X Health Reports. July, 2008: <http://www.statcan.gc.ca/pub/82-003-x/2008003/article/10648-eng.pdf> .
- [Reed01] W.J. Reed, "The Pareto, Zipf and other power laws" *Economics Letters.*, vol. 74, issues 1, 20 Dec. 2001, pp. 14-19,
- [RyEl96] B. Ryu and A. Elwalid, "The importance of long-range dependence of VBR video traffic in ATM traffic engineering: myths and realities", *ACM SIGCOMM Computer Communication Review*, vol.26, no.4, Oct. 1996, pp.3-14.
- [ScCa03] H. Schulzrinne, S. Casner and et al" RTP: A Transport Protocol for Real-Time Applications" July 2003, <http://www.ietf.org/rfc/rfc3550.txt>
- [SoDr08] C. Sommer, F. Dressler, "Progressing toward Realistic Mobility Models in VANET Simulations" *IEEE Communication magazine*, vol. 46, no. 11, Nov. 2008, pp. 132-137.
- [Tane96] A. Tanenbaum, *Computer networks*, Prentice hall New Jersey 1996.
- [Tran10] Transport Canada, "Canadian Motor Vehicle Traffic Collision Statistics: 2007", August 2010, <http://www.tc.gc.ca/eng/roadsafety/tp-tp3322-2007-1039.htm>
- [TuKn96] D. R. Tufano, H. E. Knee, P. F. Spelt, "In-Vehicle Signing Functions of an In=Vehicle Information System", http://www.osti.gov/bridge/product.biblio.jsp?query_id=3&page=0&osti_id=219502
- [USCe10] U.S. Census Bureau – Topologically Integrated Geographic Encoding and Referencing (TIGER) system, accessed in Feb. 2010,: <http://www.census.gov/geo/www/tiger>.
- [VaMo07] D1.3.1 – VanetMobiSim: The vehicular mobility model generator tool for CARLINK, Nov. 15 2007. <http://carlink.lcc.uma.es/doc/provis/D1.3.1-VanetMobiSim%20The%20vehicular%20mobility%20model%20generator%20tool%20for%20CARLINK.pdf>
- [WaDu04] P. Wan, Z. Du, W. Wu, "A simple and efficient MPEG-4 video traffic model for wireless network performance evaluation," *Wireless Communications and*

- Networking Conference, 2004. WCNC. 2004 IEEE Vol.3, 21-25 March 2004, pp. 1738- 1742.*
- [WeHe08] A. Wegener, H. Hellbruck, and C. Wewetzer, "VANET Simulation Environment with Feedback Loop and its Application to Traffic Light Assistance" *IEEE Globecom workshop, 2008 IEEE* , vol. 3, Nov. 30 2008-Dec. 4 2008., pp.1-7,.
- [WiMa09] IEEE WirelessMan 802.16, "The 802.16 WirelessMAN MAC: It's Done, but What Is It?" http://ieee802.org/16/docs/01/80216-01_58rl/pdf, Accessed in 2009
- [WiRo05] L. Wischhof, H. Rohling, "Congestion control in vehicular ad hoc networks," *Vehicular Electronics and Safety, 2005. IEEE International Conference on*, 14-16 Oct. 2005, pp. 58- 63.
- [ZhHe07] W. Zhang, J. He "Modeling End-to-End Delay Using Pareto Distribution" *IEEE Second Internnatioal Conference on Internet Monitoring and Protection (ICIMP 2007)*, July 2007, pp. 21-21.

APPENDIX A: Processing Delay Curves

This Appendix shows the processing delay curves for the Downtown Scenario and the Highway Scenario. The processing delay consists of the addition of the encoding delay, decoding delay, compression delay and decompression delay. It can be seen that the controller reduces the processing delay (which is a part of the end-to-end delay) by about 42%. Note that this is shown for just two of the four Scenarios because the average value is the same in the four Scenarios.

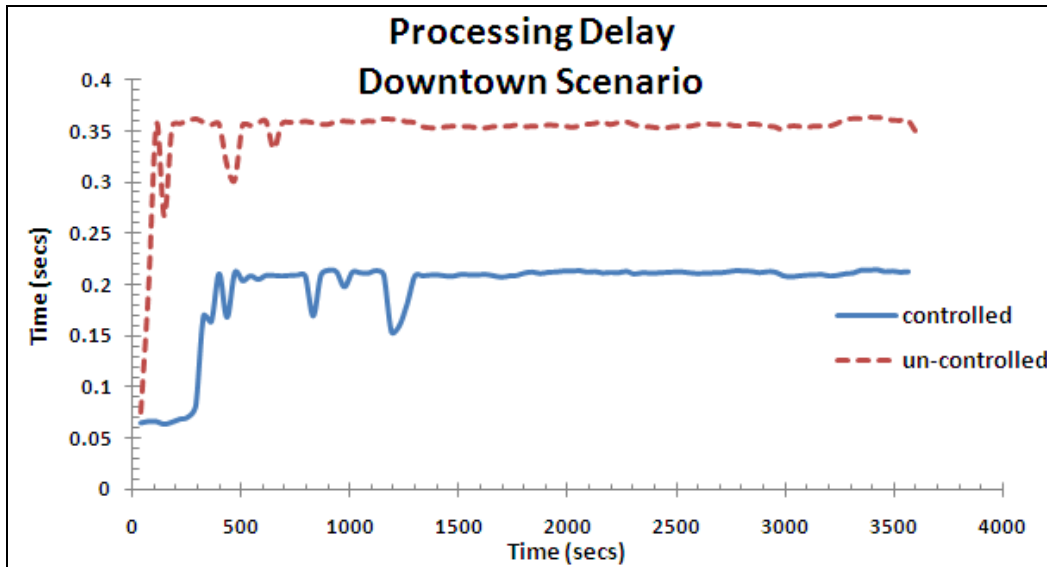


Fig. A1: Processing Delay for Downtown Scenario

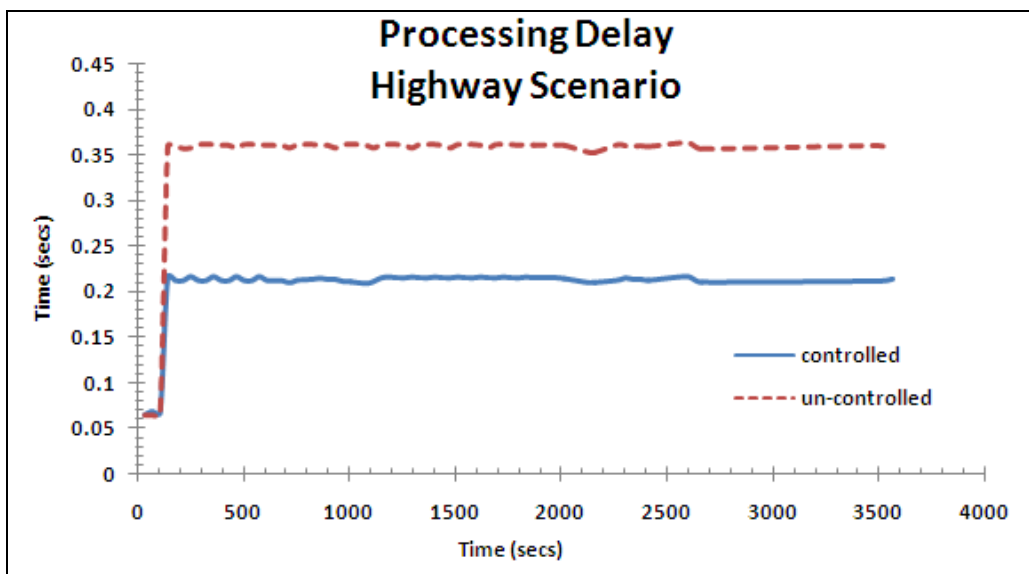


Fig. A2: Processing Delay for Highway Scenario